UNIVERSIDAD DE LA FRONTERA
Facultad de Ingeniería y Ciencias
Programa de Doctorado en Ciencias de Recursos Naturales

"POTENTIAL OF RAPESEED (*BRASSICA NAPUS*) PHOSPHOLIPIDS FOR THE DEVELOPMENT OF LIPOSOMES AS A SYSTEM FOR DELIVERY OF LACTOFERRIN A PREBIOTIC PROTEIN"

DOCTORAL THESIS IN FULFILLMENT OF THE REQUERIMENTS FOR THE DEGREE DOCTOR OF SCIENCES IN NATURAL RESOURCES

DANIELA BELÉN VERGARA GODOY
TEMUCO – CHILE
2020

“POTENTIAL OF RAPESEED (*BRASSICA NAPUS*) PHOSPHOLIPIDS FOR THE DEVELOPMENT OF LIPOSOMES AS A SYSTEM FOR DELIVERY OF LACTOFERRIN A PREBIOTIC PROTEIN”

Esta tesis fue realizada bajo la supervisión del director de Tesis, Dra. CAROLINA MARÍA SHENE DE VIDTS, perteneciente al Departamento de Ingeniería Química de la Universidad de La Frontera y es presentada para su revisión por los miembros de la comisión examinadora.

DANIELA BELÉN VERGARA GODOY

Dra. Carolina Shene de V.
(Advisor)

DR. ANDRÉS QUIROZ C.
DIRECTOR PROGRAMA
DOCTORADO EN CIENCIAS DE RECURSOS NATURALES

Dra. Mónica Rubilar D.

Dra. Maria Elena Lienqueo C.

DRA. MÓNICA RUBILAR D.
DIRECTORA ACADEMICA DE POSTGRADO
UNIVERSIDAD DE LA FRONTERA

Dra. María Elvira Zúñiga H.

Dr. Edgar Uquiche C.

A mis padres

Por su amor, preocupación y apoyo a lo largo de mi vida

Agradecimientos

Con este escrito finalizo un etapa y me siento muy feliz, porque durante el proceso aprendí muchísimo, conocí otras realidades y se abrió ante mí un mundo de cosas nuevas. Agradezco a mi familia padres y hermano que me apoyan y se preocupan de cada uno de mis pasos, sin duda ellos son el mejor soporte y me han entregado a través de su amor las herramientas necesarias para perseverar, lograr mis metas y dedicarme a lo que me gusta.

Quiero agradecer a la Dra. Carolina Shene por la confianza y la libertad de poder llevar a cabo esta Tesis Doctoral por el camino que yo deseé. Agradezco de igual forma a todo su equipo de trabajo en el Laboratorio de Bioprocesos, a Mariela, Paris, Liset, Allison, Diego, Sra. Yeicy y a cada una de las personas que conocí en el laboratorio durante los 9 años que allí estuve. Viví muchos momentos importantes de mi vida y pase por todos los estados de ánimo y situaciones que una persona pueda tener, pero siempre había momentos para compartir, comer, reír de las tragedias y pensar que todo pasa y tiene solución.

De igual forma agradezco a todas las personas que formaron parte del camino del Doctorado, a Marcelo por su ayuda, consejos, apoyo y por decirme siempre "tú puedes", te estaré siempre agradecida. A los amigos que hice Jony y Erik que son fuente de inspiración, superación, lealtad y vibra positiva, a Claudia porque su amistad fue uno de los grandes regalos que me entregó todo este proceso, por todo lo que compartimos, por su ánimo, apoyo y buenas energías. A Jana, Cami y Nico por ser la familia que yo escogí esas amigas que en 15 años de amistad han sido parte importante de mi formación tanto personal como profesional. Para todos ellos deseo que cada una de las cosas buenas que desean para mí, se les multipliquen y logren sus sueños y todo lo que se propongan con creces.

Al Laboratorio de Biofísica de Lípidos e Interfaces del Instituto de Química Avanzada de Cataluña (IQAC–CSIC) a la Dra. Olga López por recibirme con los brazos abiertos y a todo su equipo de trabajo, a Merce, Kirian, Gelen, Ana, Laia, Estitxu y Jeremy por su acogida en el laboratorio, por soportarme durante el tiempo que estuve ahí, por su buen humor, los almuerzos y hacerme reír tanto. A ti José porque nuestras largas conversaciones hicieron mis días mucho mejores de lo que ya eran, por tu apoyo y ayuda en todos los obstáculos que se presentaron en Barcelona, gracias por confiar en mi, por repetirme hasta el dia de hoy "ten fe" y permitirme conocer un poquito mas de ti. Definitivamente la vida cambia en otros lugares.

Agradezco a la comisión evaluadora por sus comentarios y sugerencias que me permitieron llevar de mejor manera esta investigación, a las secretarias del Doctorado Gladys y Mariela por su trabajo, paciencia y buena disposición. Finalmente agradezco a la Beca de Doctorado Conicyt 21161448 por el financiamiento para cumplir parte de mis sueños y a todos aquellos que han colaborado de alguna u otra forma en esta enriquecedora etapa. Mil gracias.

ABBREVIATIONS

AG	Arabic gum
ANOVA	Variance analysis
BSA	Bovine serum albumin
CCD	Central composite design
CDs	Cyclodextrins
CLSM	Confocal laser scanning microscopy
Cryo–TEM	Cryogenic transmission electron microscopy
DG	Gastric digestion
DHPG	3,4–dihydroxyphenylglycol
DSC	Differential scanning calorimetry
EE	Encapsulation efficiency
EFSA	European Food Safety Authority
ELSD	Evaporative light scattering detector
FAMEs	Fatty acid methyl esters
FDA	Food and Drug Administration
FFA	Free fatty acid
FTIR	Fourier transform infrared spectroscopic
GC	Gas chromatography
GF	Gastric fluid
GRAS	Generally recognized as safe
HPC	Hydrogenated phosphatidylcholine
HT	Hydroxytyrosol

ID	Intestinal digestion
IF	Intestinal fluid
LC	Low concentration
LF	Lactoferrin
LPC	Lyso–phosphatidylcholine
LUVs	Large unilamellar vesicles
MDA	Malondialdehyde
MLV	Multilamellar vesicles
NLC	Nanostructured lipid carriers
n–OSA	Octenyl succinic acid anhydride
O/G	Oil–in–gel
O/W	Oil–in–water
O/W/O	Oil–in–water–in–oil
PA	Phosphatidic acid
PC	Phosphatidylcholine
PCL	Poly(ε–caprolactone)
PDI	Polydispersity index
PE	Phosphatidylethanolamine
PEG	Polyethylene glycol
PEO	Poly(ethylene glycol)
PLA	Poly(lactic acid)
PLGA	Poly(lactic–coglycolic acid)
PPI	Pea protein isolate

PVA	Poly(vinyl alcohol)
RP	Rapeseed phospholipids
RSM	Response surface methodology
SAXS	Small angle X–ray scattering
SDS–PAGE	Sodium dodecyl sulfate polyacrylamide gel electrophoresis
SLN	Solid lipid nanoparticles
SP	Soy phospholipids
SPI	Soy protein isolate
ST	Stigmasterol
SUVs	Small unilamellar vesicles
TAG	Triacylglycerol
TBA	Thiobarbituric acid
TBARS	Thiobarbituric acid reactive substances
TCA	Trichloroacetic acid
TEP	1,1,3,3–tetraethoxypropane
TGA	Thermogravimetric analysis
T_m	Gel to liquid main transition temperature
W/O	Water–in–oil
W/O/W	Water–in–oil–in–water
WAXS	Wide angle X–ray scattering

SUMMARY AND THESIS OUTLINE

Current technological development of encapsulation techniques demands the use of new coating materials for the food industry in order to create new products, to improve the stability, efficiency, and useful life of bioactive compounds of interest. In this context, the encapsulation of bioactive compounds in liposomes is considered relevant and promising because it allows preserving the biological properties of different compounds during passage through the gastrointestinal tract. Liposomes are spherical vesicles formed by a phospholipid bilayer enclosing an aqueous core, creating a physical barrier to unfavorable environmental conditions and enhancing the bioavailability of bioactive compounds (proteins, vitamins, carotenoids, among others). Traditionally, liposomes have been made with phospholipids from soybeans, egg yolk, and milk; or with synthetic phospholipids. In this context, **rapeseed phospholipids (RP)**, extracted from a residue of the oil processing, are presented as a new source for the production of liposomes. In addition, researchers highlights the importance of using cost–effective naturally–occurring phospholipids in making liposomes for the delivery of food ingredients. Today, there is no information related to the use of rapeseed phospholipids as a delivery system for bioactive compounds. To apply the proposed encapsulation system, **lactoferrin (LF)** was used as a bioactive compound. LF is a protein present in biological fluids such as milk, tears and saliva; it has been suggested as an enhancer of the intestinal microflora because it promotes the growth of probiotic bacteria and inhibits the development of pathogenic bacteria. In addition, LF presents anti–inflammatory, antioxidant and immunomodulatory activities. Oral administration of non–encapsulated LF is susceptible to proteolysis in the gastrointestinal tract, reducing its therapeutic efficacy. This study contributes to increase knowledge about the use of rapeseed phospholipids for developing liposomes, and offers a novel and

effective delivery system for the prebiotic protein LF that maintain protein integrity throughout the gastrointestinal tract, ensuring a higher absorption degree per consumed dose. This study also offers a novel application to the by–product originating from the refining of rapeseed oil, which could diversify its use in the food industry.

In **Chapter I,** general introduction, hypotheses, general, and specific objectives are presented. The general objective of this Doctoral Thesis was **to establish *in vitro* the potential of liposomes based on rapeseed phospholipids (*Brassica napus*) as a delivery system for lactoferrin (LF), a prebiotic protein**.

Chapter II entitled **"Microencapsulation of bioactive compounds: an overview of methods and wall materials used in food and pharmaceutical industry"** is focused on exposing main technologies for microenapsulation, wall materials and bioactive compounds that has been used during the last five years, as well as its application in the food industry. Today, research is focused on identifying, isolating and using new bioactive compounds and wall materials extracted from natural sources, following the strong tendency of the market to introduce products that are more natural, sustainable and friendly to the environment. As well as preserve the biological properties of different compounds during passage through the gastrointestinal tract.

Chapter III corresponds to the published manuscript entitled **"Encapsulation of lactoferrin into rapeseed phospholipids based liposomes: optimization and physicochemical characterization"** conditions of RP liposomes preparation using response surface methodology (RSM) was carried out. Results were compared to those obtained with liposomes elaborated with soy phospholipids (SP). In addition, physicochemical properties and physical stability of LF–loaded liposomes using RP were evaluated. Results showed that compared to SP, RP allows to elaborate liposomes with a

higher encapsulation efficiency and a smaller size particle. On the other hand, the effect of storage temperature on the stability of RP liposomes was studied.

Chapter IV corresponds to the published manuscript entitled "**An *in vitro* digestion study of encapsulated lactoferrin in rapeseed phospholipid–based liposomes**". In this chapter, lipid membrane of rapeseed phospholipids liposomes was characterized and the protection offered to LF encapsulated in different formulations of RP liposomes during *in vitro* gastrointestinal digestion was determined. Lipid organization in terms of chain conformational order, lateral packing, and lipid phase transitions are among the factors that explains the stability performance of RP liposomes on LF encapsulation. RP liposomes can be used to encapsulate LF and improve its stability delaying its hydrolysis during gastric and intestinal digestion.

Chapter V corresponds to the manuscript entitled "**Lactoferrin loaded in liposomes prepared from rapeseed phospholipids and hydrogenated phosphatidylcholine: Behaviour under gastrointestinal digestion *in vitro* and antibacterial and prebiotic bioactivity".** In this chapter protein hydrolysis during sequential gastrointestinal *in vitro* digestion of LF–loaded liposomes elaborated with RP and hydrogenated phosphatidylcholine (HPC) was evaluated. Also studies on antibacterial and prebiotic activity of LF–loaded RP liposomes through *in vitro* tests were carried out. Our results suggest that liposomes elaborated with RP and HPC, can be a useful oral delivery system of molecules sensitive to digestive enzymes such as LF. Encapsulation of LF into RP+HPC liposomes did not compromise its antimicrobial bioactivity on *Staphylococcus aureus*, and prebiotic bioactivity on *Bifidobacterium infantis*, *Bifidobacterium longum*, and *Lactobacillus plantarum.*

Finally, **Chapter VI** presents a general discussion, conclusions, and suggest future directions for the encapsulation of LF into RP based liposomes researches.

TABLE OF CONTENTS

TABLE INDEX

FIGURE INDEX

CHAPTER I

General introduction, hypothesis, and objectives

1.1 GENERAL INTRODUCTION

Nowadays, consumers not only demand foods that provide nutrients for a healthy life, but also prefer those that provide health benefits such as bioactive compounds, vitamins, probiotics, prebiotics, essential fatty acids, carotenoids, among others. As a result of these strong trend, the use of lactoferrin (LF) as a bioactive compound has been considered. LF is known for its selective antibacterial activity; inhibits the growth of pathogenic bacteria in the intestine (Tian et al., 2010) and promotes the growth of specific probiotics (*Bifidobacteria* and *Lactobacillus*) (denominated as a prebiotic protein). However, the main problem for the oral consumption of LF is the proteolytic degradation through the gastrointestinal tract (Onishi, 2011). This degradation, leads to the development of more effective forms for LF protection through the use of natural materials.

Encapsulation creates a physical barrier that improves the stability and functionality of the required compound. Encapsulation requires the search for new encapsulating materials that can be used to encapsulate, protect, extend half–life and release bioactive compounds (Garti and McClements, 2012). Several encapsulation methods have been developed, such as spray drying, freeze drying, ionic gelation, emulsion, among others (Ribeiro et al., 2017). However, some of these methods have disadvantages, such as the use of temperatures that causes the loss of activity in thermolabile compounds, high operating costs due to the energy levels used as well as the involved equipment restrict their use. The lack of uniformity in the size and shape of the particles limits the bioavailability. On the other hand, there is a restricted number of food grade emulsifiers (Dordevic et al., 2014).

According to the above mentioned, the use of liposomes as a method of encapsulation has considerably increased in the food industry. Liposomes are spherical vesicles formed by the interaction of phospholipids and water molecules (Emami et al., 2016). Among their

advantages, liposomes are presented as non–toxic, flexible, biocompatible, fully biodegradable, and non–immunogenic for systemic and non–systemic administration (Akbarzadeh et al., 2013). In addition, elaborated formulations are easily obtained with uniform and small particle size. Liposomes can be manufactured using phospholipids extracted from plant raw materials, for example rapeseed (*Brassica napus*), which allows an easy and fast implementation in food systems, surpassing the established regulatory barriers (Da Silva Malheiros et al., 2010). Rapeseed is the second most important oilseed crop after soy, representing 20% of the world's supply. During the oil refining process, phospholipids are removed as a by–product. In addition, they are naturally biodegradable and non–toxic (Szentmihalyi et al., 2002). The ability of rapeseed phospholipids (RP) to develop a delivery system has not been investigated yet. Therefore, it is an interesting approach from the point of view of research and development of innovative products for the food industry.

Thus, the use of RP is proposed to develop liposomes in order to stabilize and increase the bioavailability of LF, taking into account the growing demand for food products based on natural formulations, and to impair the degradation of bioactive compounds with health benefits. RP based liposomes can offer a new and effective delivery system to improve stability of LF in the gastrointestinal tract, maximizing its antibacterial and prebiotic therapeutic efficiency and also contributing to the current trends of natural and functional food products by consumers.

1.2 HYPOTHESIS

From the Introduction presented above, the key findings can be summarized as follows:

- LF is considered a crucial element of the immune system. Nevertheless, its oral administration is susceptible to enzymatic hydrolysis in the gastrointestinal tract, leading to important reductions in therapeutic efficacy.
- Liposomal encapsulation technology is often employed to stabilize and to increase the bioavailability of bioactive compounds.
- Rapeseed phospholipids (*Brassica napus*) can be used to develop LF–loaded liposomes.
- Stability and bioactivity after digestion of LF loaded into liposomes have not been addressed in detail.

"Liposomes based on Rapeseed (*Brassica napus*) phospholipids can be used to encapsulate lactoferrin (LF) with a high encapsulation efficiency (>90%). LF encapsulated under these conditions (a) is protected from hydrolysis during in vitro gastrointestinal digestion, and (b) retains the antimicrobial and prebiotic activity".

1.2 OBJECTIVES

1.3.1 General Objective

To establish *in vitro* the potential of liposomes based on rapeseed (*Brassica napus*) phospholipids as a delivery system for lactoferrin (LF).

1.3.2 Specific Objectives

1. To define conditions for LF encapsulation into RP liposomes to improve encapsulation efficiency.

2. To evaluate the protection offered by RP liposomes to the encapsulated LF during *in vitro* digestion.

3. To establish the antibacterial and prebiotic activity of LF–loaded RP liposomes through *in vitro* tests.

CHAPTER II

Microencapsulation of bioactive compounds: an overview of methods and wall materials used in food industry

Daniela Vergara[a,b]*, Carolina Shene[b]

[a]Doctoral Program in Sciences of Natural Resources, Universidad de La Frontera, Temuco, Chile.

[b]Department of Chemical Engineering, Center of Food Biotechnology and Bioseparations, Scientific and Technological Bioresource Nucleus (BIOREN), Centre for Biotechnology and Bioengineering (CeBiB). Universidad de La Frontera, Temuco, Chile.

Review corresponding to the qualification exam

Microencapsulation of bioactive compounds: an overview of methods and wall materials used in food industry

2.1 Abstract

Currently, the importance of microencapsulation protect substances that are susceptible to decomposition or degradation reactions which may occur during process, storage or consumption (digestion process in the case of oral consumption) is a focus of research in the food industry. Many factors influence the quality of the microparticles, including preparation method, types of wall material and microencapsulated bioactive compounds. The encapsulation methods used vary according to the desired type of microcapsule (size and morphology), the chemical and physical properties of the bioactive compound and of the wall material, the type of controlled delivery and the scale of production. This review provides an overview of the past five years of scientific research on methods, wall materials, and bioactive compounds that have been used to develop delivery systems of microparticles. Currently, the research is directed on identifying, isolating and using new bioactive compounds susceptible for encapsulation, and wall materials extracted from natural sources, following the strong tendency of the market to develop natural, and sustainable products, produced with technologies friendly to the environment.

Keywords: Encapsulation, bioactive compounds, wall material, food applications, delivery system.

2.2 Introduction

In recent years, scientific knowledge is being used in the development of innovative products. For the succeful introduction of a product into the market products must be differentiated using emergent technologies, such as microencapsulation. Microencapsulation is a technique in which solid, liquid or gaseous molecule (referred to as the core, internal phase or fill) are surrounded by a coating material (referred to as wall material, shell, coating or membrane) creating a microparticle (Agnihotri et al., 2012). The microparticles can be distinguished in microspheres or microcapsules having different sizes and forms depending on the materials and the methods used in their preparation. The typical morphology of these microparticles varies between simple or irregular shape, with one or more layers of encapsulating agents, and with mono or multi–cores (Estevinho et al., 2013). Success of microencapsulation depends mainly on the selection of wall material that determines the stability of microparticles, the encapsulation efficiency, and the degree of protection core (Bakry et al., 2016a) against environmental factors (oxygen, light, humidity etc.), thus improving stability, handling and overall acceptability of the encapsulated substance.

In the 21st century, food industries are the main driving forces in microencapsulation advances. The different fields of application of microencapsulation are: pharmaceutical (68%), food (13%), cosmetics (8%), textile (5%), biomedical (3%), agriculture (2%) and electronics (1%) industries (Martins et al., 2014). Microencapsulation provides a physical barrier to protect the bioactive compounds which are liable to the conditions of the external environment, such as acidity, alkalinity, evaporation, heat, oxidization, light or moisture before the encapsulated compound is released (Bansode et al., 2010). In addition, microencapsulation has been used for the incorporation of ingredients, such as polyphenols,

volatile additives, colors, enzymes, and bacteria into foods in order to stabilize, protect, and preserve nutritional and health properties (Garti & McClements, 2012), as well as masking unpleasant taste and odors (Nesterenko et al., 2013).

Microencapsulation methods can be divided into two main categories: chemical and physical; being the latter subdivided into physico–chemical and physico–mechanical methods (Jyothi et al., 2010). The most commonly used microencapsulation methods for drug entrapment involve: chemical processes (interfacial and free radical polymerization methods), physico–chemical processes (coacervation (phase separation), ionotropic gelation methods), and physico–mechanical processes (fluid bed coating, solvent evaporation/extraction, spray drying, electrospinning, and electrospraying methods) (Lam & Gambari, 2014). Spray drying (physico–mechanical processes) is the oldest and the most widely used encapsulation method in the food industry (Ray et al., 2016). The encapsulation agents and the microencapsulation method determine the functional properties and the potential application of the encapsulated components (Bakry et al., 2016a).

Wall materials used for encapsulation can be selected from a wide variety of polymers, both synthetic and natural, depending on the material to be encapsulated, the encapsulation process and the desired characteristics in the end–product (Sánchez et al., 2016). Polysaccharides (starch, maltodextrins, and dextrose), gums (Arabic gum, acacia gum, alginates, and carrageenans), proteins (milk or whey proteins, and gelatin), lipids (short, medium, and long–chain fatty acids), and other lipid compounds are utilized as encapsulating agents (Aghbashlo et al., 2012; Flores & Kong, 2017).

Given the importance of microencapsulation, the objective of this review is to revise the main microencapsulation methods and wall materials used to develop products of interest

for the food industry in the last years. The information collected to prepare this revision follows the description of main published experimental studies in the last five years.

2.3 Microencapsulation of bioactive compounds

Bioactive compounds vary in their molecular characteristics (e.g. molecular weight, polarity, structure, physical state, charge, density and rheology), and functional attributes (Garti & McClements, 2012). Bioactive compounds for food applications are generally prone to degradation, both during storage and processing, as many of them are physically, chemically, and/or enzymatically unstable leading to their degradation or transformation with the consequent loss of bioactivity (Dias et al., 2015). The microencapsulation of bioactive compounds should prevent inactivation and degradation caused by low pH and enzymes of the gastrointestinal tract. In addition, many bioactive compounds are liable to chemical and physical degradation during processing due to the fragility of their molecular structure. Chemical degradation (pH, moisture, and oxidation) and physical degradation (temperature, light), lead to a reduced therapeutic efficiency and/or toxicological consequences (Lam & Gambari, 2014).

Microencapsulation helps a bioactive compound to reach its target site, through the choice of wall material (structure, composition) and microencapsulation method. Both factors influence the stability, functionality, delivery system efficiency and bioavailability (the fraction of a bioactive compound that is solubilized in the intestinal fluids in a suitable form for absorption) of the bioactive compounds. A microencapsulated bioactive compound can be released from the surrounding material by different physico–chemical mechanisms such as: diffusion, fragmentation, erosion, or inflammation (Garti & McClements, 2012)

Exist a variety of encapsulated compounds with different degrees of solubility in water, ranging from lipophilic carotenoids and slightly soluble catechins to water–soluble anthocyanins can be encapsulated using carbohydrate and protein biopolymers, and lipids (Flores & Kong, 2017). The most important microencapsulated bioactive compounds are: lipids (flavors, antimicrobials, fatty acids, carotenoids, vitamins A, and D), proteins (peptides), carbohydrates (prebiotics, dietary fibers), probiotics, minerals, and drugs. Table 2.1 shows the most frequently microencapsulated bioactive compounds for food applications. Reasons for their microencapsulation are also shown in Table 2.1.

2.4 Microencapsulation methods of bioactive compounds

The selection of a microencapsulation method depends on the nature of the bioactive compounds (hydrophilic/hydrophobic, size, physical state), on the intended release rate, release profile (Andersson–Trojer et al., 2013), the final application of the product, considering physical and chemical, stability, concentration, release mechanism, and manufacturing costs (Martins et al., 2014). Moreover, the method used determines the particle size macrocapsules (> 5,000 μm), microcapsules (0.2 to 5,000 μm), and nanocapsules (< 0.2 μm) (Mahdavi et al., 2014). The cost of microparticle production rises as: particle size decreases, encapsulation efficiency decreases, or morphology complexity increases (Gaonkar et al., 2014). Fig. 2.1 shows approximate size ranges and costs of several encapsulation methods.

Final characteristics of microencapsulated products are affected by: properties of wall material, bioactive compounds, formulation parameters (viscosity, type of solvent, emulsifiers, composition wall material, bioactive composite/wall material ratio), and operating conditions agitation, sonication and temperature. The main properties affected

are: microparticle morphology, product yield, and encapsulation efficiency (Paulo & Santos, 2017).

In general, first step in microencapsulation process is the mixing of the dispersed phase (core) that contains the bioactive compounds with the aqueous dispersion of wall material, to obtain a dispersion, a solution, or an emulsion (Rodríguez et al., 2016). The second step involves the actual production of the microcapsules by chemical or mechanical processes (Sagis, 2015). There are multiple encapsulation processes available to combine the wall material and core materials into microcapsules. The four general categories are atomization, spray coating, coextrusion, and emulsion–based processes. Each method produce the range of particle sizes and morphologies (Gaonkar et al., 2014). Scanning electron micrographs (SEM) can be used to observe differences in morphology and size of the microparticules (Fig. 2.2).

According to Ribeiro et al. (2017) the main methods for the encapsulation of bioactive compounds are: spray drying, coacervation, ionic gelation, liposome, freeze drying, electrospinning/electrospraying, inclusion complex. Fig. 2.3 shows a general schematic sequence, from the choice of bioactive compounds, wall materials and microencapsulation method to final industry applications.

2.4.1 *Spray drying and freeze drying*

Spray drying consists of the atomization of a liquid with a high content of soluble solids in a hot gas stream, generating a powdered product. For thermally sensitive materials, spray drying is the preferred method and the most common industrial encapsulation method (Verma & Singh, 2013). Inlet liquid feed rate, gas flow rate, and inlet and outlet gas temperature are controlled to reduce thermal degradation; in addition, the content of soluble

solids and viscosity of the fed solution can also affect the retention of biological activity and encapsulation efficiency (content of core material effectively encapsulated). Spray drying is a relatively inexpensive, easily scalable, fast, and efficient system for the microencapsulation of active components such as essential oils, natural colorants, vitamins, and probiotics (Garti & McClements, 2012). The most commonly used encapsulanting materials are dairy proteins and plant protein isolates, and polysaccharides/gums, such as Arabic gum, maltodextrin, modified starch, inulin, and cashew gum (Ribeiro et al., 2017). Compared with other drying methods, freeze drying or dehydration by sublimation of a frozen product, can yield high quality products. Due to the low temperature, absence of liquid water and oxygen under vacuum, most deterioration reactions are slowed down or practically stopped. The porous structure of the powdered product facilitates rapid and almost complete rehydratation (Ishwarya et al., 2014). Nevertheless, the high operational cost associated with freeze drying restricts it is us to high–value products (Ratti, 2013).

2.4.2 *Electrospinning/electrospraying*

Electrospinning and electrospraying are electrohydrodynamic atomization methods used for encapsulation (Cheng et al., 2017). Both methods use electrostatic forces to produce electrically charged jets from viscoelastic polymer solutions which are dried by evaporation of the solvent, producing ultrathin structures (Drosou et al., 2017). The typical configuration for electrospinning and electrospraying consists of four main components: 1) a high voltage source (1–30 kV) usually operated in direct current mode, although alternating current mode is also possible, 2) a blunt tip stainless steel needle or capillary, 3) a syringe pump, and 4) a manifold affixed to a ground, a flat plate or a rotating drum (Bhushani & Anandharamakrishnan, 2014).

The basic difference between these two processes lies in the concentration of the solutions (Husain et al., 2016). More viscous solutions with high polymer concentration are used in electrospinning whereas low viscosity solutions are used in electrospraying. Quality and characteristics of the final product are determined by the elasticity, viscosity, temperature, humidity, conductivity and surface tension of the polymer, strength of the electric field, the distance to the collector, and flow rate (Nezarati et al., 2013).

The basic materials for electrospinning are polymers and solvents. Many biocompatible and biodegradable synthetic polymers, such as poly(ε–caprolactone) (PCL), poly(lactic acid) (PLA), Poly(lactic–coglycolic acid) (PLGA), Poly(vinyl alcohol) (PVA), and Poly(ethylene glycol) (PEO) have been directly electrospun into nanofibers. For the same applications several natural polymers including natural proteins (e.g., collagen, gelatin, zein, fibrinogen, elastin, and silk) and natural carbohydrates (e.g., chitosan, dextran, alginate, hyaluronic acid, chondroitin sulfate, and chitin) (Cheng et al., 2017). This method has been used for encapsulation and delivery of polyphenolic (Gómez–Estaca et al., 2015), antioxidants (Aceituno–Medina et al., 2015), fish oils (Moomand & Lim, 2014), and antibiotics (Macocinschi et al., 2015).

2.4.3 *Ionic gelation*

Ionic gelation is a microencapsulating method based on the capability of polyelectrolytes to form cross links in the presence of ions; ionic gelation produces hydrogel beads termed as gelispheres. Gelispheres can be defined as spherical cross linked hydrophilic polymeric entities showing extensive gelation and swelling in simulated bio–fluids (Katouzian & Jafari, 2016). Microencapsulation by ionic gelation is simple, versatile, low cost, and does not involve the use of organic solvents or extreme pH and temperature. The most common

ionic gelation material is sodium alginate, which is converted into a water–insoluble gel with salts like calcium chloride (Garti & McClements, 2012). Gelispheres can be prepared by external or internal ionic gelation. In external ionic gelation the Ca^{2+} ions are externally introduced into the interstitial spaces between the alginate polymer chains to initiate crosslinking. This results in the initial formation of a semi–solid membrane encasing the droplet with a liquid core. On the contrary, in internal gelation an insoluble calcium salt is added to the alginate solution and the mixture extruded into oil. This mixture is acidified to bring about the release of Ca^{2+} from the insoluble salt for cross–linking with the alginate (Leong et al., 2016). The ionic gelation has been used for the encapsulation and delivery of antioxidants (Bermudez–Oria et al., 2017), oils (Morales et al., 2017), polyunsaturated fatty acids (Piornos et al., 2017), and bacteria (Sathyabama et al., 2014).

2.4.4 *Inclusion complex*

Microencapsulation in inclusion complexation is usually performed to overcome problems due to loss solubility of cyclodextrins (CDs) (Devasari et al., 2015). CDs are non–toxic, macrocyclic oligosaccharides, consisting of six or more α–1,4–linked D–glucopyranose units, characterized by a hydrophobic interior suitable to receive slightly polar compounds. The hydrophilic exterior is responsible for the aqueous solubility of CDs and their complexes. The most common CDs are formed from six (α–CD), seven (β–CD) or eight (γ–CD) glucopyranose units, with cavity sizes of approximately 0.5, 0.6, and 0.8 nm, respectively (Gharib et al., 2015).

The inclusion of hydrophobic compounds takes place mainly by hydrophobic interactions between guest molecules and the walls of CD cavity. The driving forces to form inclusion complexes are electrostatic and van der Waals interactions as well as

hydrogen bonding (Szente et al., 2016). Despite the number of factors and different forces involved in the complexation with CDs, the production of complexes is a rather simple process. There are several methods (in the solid state, in the semi–solid state, in solution) to obtain CD–bioactive compounds complexes depending on the properties of the guest and the nature of the chosen CD (Mura, 2015).

The ability of CDs to form an inclusion complex with bioactive compounds depends on the relative size of CD, and both the size and functional groups of the bioactive compounds or drug. If the bioactive compound is too large in size, it will not fit properly into the CD cavity (Jambhekar & Breen, 2016). CDs are often used to form complexes with fairly hydrophobic bioactive compounds (oil–soluble vitamins, carotenoids, and fatty acids), but they can also be used for more hydrophilic bioactive compounds (such as polyphenols), provided they fit into the cavity (McClements, 2015b). Moreover, inclusion complexes have been used for the encapsulation of volatile organic molecules, for masking odors, flavors, or aromas retention (Ciobanu et al., 2013).

2.4.5 *Emulsion systems*

Emulsion is a class of disperse systems consisting of two immiscible liquids. The liquid droplets are dispersed in a liquid medium (continuous phase). Depending on which is the dispersed and continuous phase the emulsions are classified in: oil–in–water (O/W), water–in–oil (W/O), and multiple phase emulsions, such as oil–in–water–in–oil (O/W/O) or water–in–oil–in–water (W/O/W). Emulsifiers play two key roles in the development of successful emulsion based products. In the O/W emulsions emulsifiers facilitate the initial formation of small lipid droplets (McClements, 2015a). Currently, emulsifiers used industrially to stabilize O/W emulsions are synthetic surfactants, such as tweens and spans

and animal–based emulsifiers such as gelatin, egg protein, whey protein, and caseinate. In the search for more natural products plant proteins, saponins and phospholipids, such as lecithins are used as biosurfactants (McClements & Gumus, 2016). Emulsion systems are essential components of food, cosmetics, and drugs for enhancing the bioavailability of poorly water–soluble active compounds. This encapsulation method is sometimes coupled with spray or freeze drying to produce a powder (Tonon et al., 2011).

2.4.6 *Liposomes*

Liposomes are nano/micro–sized spherical vesicles, having an aqueous core enclosed by one or more phospholipid bilayers. Due to the presence of both lipid and aqueous phases in the structure, they can be used for the entrapment and delivery of either amphiphilic, water–soluble, or lipid–soluble materials (Imran et al., 2015). There is a wide variety of conventional methods to prepare liposomes, including thin film hydration, reverse–phase evaporation, solvent injection, and detergent dialysis. In order to alter particle size and minimize the polydispersity, post–formation steps such as sonication, extrusion, and high–pressure homogenization are needed (Grimaldi et al., 2016). The main advantage about these micro/nano structures is the capability to control release at the target site (Fang & Bhandari, 2010). As colloid carriers, liposomes have many advantages, including biocompatibility, bioavailability, solubilization of insoluble compounds, and a sustained–release performance (Cui et al., 2016). Liposomes are generally classified according to their size and number of bilayers. Liposomes that contain only a single bilayer membrane are called small unilamellar vesicles (SUVs) or large unilamellar vesicles (LUVs). The SUVs have diameters between 0.02 and 0.05 μm whereas LUVs diameters

range from 0.05 to 0.1 μm, whereas, multilamellar vesicles (MLV) are large vesicles having size between 0.05 and 10 μm (Gharib et al., 2015).

The main materials of conventional liposomes are natural and safe constituents such as lecithin from egg yolk or soy beans, and cholesterol. Cholesterol has various effects on the capacity of the liposomes to encapsulate and deliver a bioactive compounds (Liu et al., 2017). Because cholesterol reduces the rotational freedom of the phospholipid hydrocarbon chains in a bilayer, it helps to decrease the loss of hydrophilic materials and also stabilizes the lipid bilayer (Oliveira et al., 2014). The encapsulation efficiency of liposomes is a function of the amount of phospholipids present in the dispersion; the higher the number of phospholipid vesicles, the larger the volume of hydrophilic encapsulated compound. For highly hydrophobic compounds, the encapsulation efficiency is usually close 100% regardless of the liposome type and composition (Singh & Thompson, 2012). Bioactive hydrophobic compounds vitamin E, resveratrol, and epigallocatechin gallate (EGCG) (Chen et al., 2017a), and bioactive hydrophilic compounds vitamin C (Marsanasco et al., 2015), and bovine serum albumin (BSA) (Espirito et al., 2014) have been incorporated into liposome–based delivery systems.

The manufacture of liposome presents challenges in the elaboration processes commonly used. This limits their wider application and challenge their general applicability as it complicates the development of a robust, scalable and affordable process (Shah et al., 2020). With the development of new manufacturing processes, microfluidization emerfes as a relatively new area of liposome synthesis, where the small dimensions in a micro mixer allow for fast mixing, dominated by diffusion or convection. Microfluidics refers to fluid handling methods in a controlled volume, typically below millimeter scales, which allows for implementation of the mixing process into planar chips which offer leane manufacturing

and scale-independent manufacture, the application of liposomes and other lipid-based nanoparticles can be more readily translated from the research through to production and use (Kastner et al., 2015).

2.4.7 *Coacervation*

Coacervation has been studied extensively for encapsulating reactive, sensitive, or volatile additives or nutrients, with the purposes of increasing their shelf–life. Proteins and polysaccharides are the most widely used wall materials for (micro) encapsulation via coacervation in the food industry (Yan & Zang, 2014). Generally, coacervation is divided into three steps: 1) formation of an O/W emulsion, 2) particle formation, where the wall material surrounds the core material creating a membrane, and 3) consolidation of microcapsules by adding a hardening agent (Martins, 2012).

The coacervation process can be categorized into: simple (one polymer) or complex coacervation. Complex coacervation is a type of associative phase separation which is driven by strong electrostatic interactions between two opposite charged polymers. Under specific pH, polymers mixing ratio, and ion strength, insoluble complexes between the polymers are formed and concentrate into coacervate droplets to form a coacervate phase (Ach et al., 2015). This method is widely used for encapsulating lipophilic compounds, such as essential (Peng et al., 2014), vegetable (Yang et al., 2015), fish (Wang et al., 2014), and palm (Marfil et al., 2015) oils.

2.5 Wall materials for microencapsulation of bioactive compounds

Microencapsulation of compounds for food applications uses wall materials with resistance to stomach and small intestine conditions. Additional properties should include

low flavor and reduced color, high emulsifying capacity, biodegradability, homogeneity in shape and size, low hygroscopicity and relatively low in cost. Wall materials used for encapsulation of food ingredients must have GRAS (generally recognized as safe) status; should be biodegradable and efficient as the protective barrier during processing or storage under various conditions (Alexe & Dima, 2014). Both EU through the EFSA (European Food Safety Authority) and the USA through the FDA (Food and Drug Administration) have many strict rules about material usage for food applications (Dias et al., 2015). Table 2.2 summarizes the microencapsulation methods for food applications, wall materials, bioactive compounds, particle size, and encapsulation efficiency of the resulted microcapsules regarding all treatments used.

2.5.1 *Polysaccharides used as wall material*

Among the class of wall material used in the field of microencapsulation, carbohydrates are the most commonly used. Polysaccharides are ideal for use as delivery agents because they are structurally stable, abundant in nature and inexpensive. The colossal molecular structure of polysaccharides contributes to their stability as carriers during production and processing of microencapsulated products (Mohan et al., 2015).

Among the most used polysaccharides in microencapsulation are: starch, pectin (Dafe et al., 2017), maltodrextrin, Arabic gum (Gupta et al., 2015), cliclodextrins (Desai et al., 2016), inulin (de Barros et al., 2016), octenyl–succinate starch (Gonçalves et al., 2016), cellulose (Chen et al., 2015), alginate (Wu et al., 2017), carrageenan and chitosan (Dima et al., 2014). Polysaccharides can be used alone or in combination with other polysaccharides, or proteins (complex coacervation). The use of mixtures is an alternative to further increase of the efficiency of the encapsulation process (Kuck & Zapata, 2016).

Arabic gum (AG) also known as acacia gum, is a natural gum collected from acacia tree. It consists of a mixture of arabinogalactan (90–99%) and glycoprotein (Klein et al., 2010). It is an anionic polysaccharide frequently used in industries due to its highly emulsifying and good encapsulating properties as well as its high solubility and low viscosity (Gulao et al., 2014). Gupta et al. (2015) have shown the encapsulation efficiency of the mixture of AG, maltodrextrin, and modified starch for iron encapsulation (91.58%). These iron microcapsules were added to milk and showed significant difference in total sensory scores from iron salt fortified milk during storage. AG has some disadvantages; it is produced in few countries (such as Senegal and Sudan), and the quality and composition are highly variable (Comunian et al., 2016). Maltodextrin and modified starch have become viable alternatives to AG because they are abundant and low–cost materials (Peng et al., 2013). Maltodextrin is obtained by the acid hydrolysis of different starch sources (corn, potato or others). Maltodextrin is the most used biopolymer for encapsulating by spray drying because it has high solubility in water, low viscosity, low cost, neutral taste and aroma, and offers good protection of flavours against oxidation (de Barros et al., 2016). However, due to its low emulsifying activity and marginal retention of volatiles, it is generally used in mixtures with other biopolymers such as, soy protein, and pectin (Pereira et al., 2016). A mixture of maltodextrin and inulin was studied for encapsulating blueberry juice by spray drying. The effect of these encapsulating polymers was determined by characterizing the physicochemical properties and retention of antioxidants. Inulin and maltodextrin, were successfully used for the spray drying of blueberry juice, preserving the physicochemical properties. However, maltodextrin presented a higher ability than inulin to encapsulate and conserve the content of antioxidants such as resveratrol and quercetin 3–D–galactoside (Araujo–Díaz et al., 2017).

Pectin is a naturally–occurring anionic polysaccharide consisting of linear chains of α–(1,4) linked D–galactopyranosyluronic acid units (with varying degrees of carboxyl methyl esterification) and rhamnogalacturonan units. Pectins, from citrus peel and apple pomace, are widely used in the food industry as gelling or thickening agents (Liu et al., 2015). Since pectin is not degraded in the upper gastrointestinal tract, but it is degraded by colonic microflora, pectin–derived delivery system have a promising potential for colon–specific bioactive delivery (Auriemma et al., 2013). Bermúdez–Oria et al. (2017) demostred that hydroxytyrosol (HT) and 3,4–dihydroxyphenylglycol (DHPG), two phenolic antioxidants naturally found in olive, can be encapsulated into a pectin–based formulation in high amounts (around 50%). The hydrogel beads showed a particular release pattern of the bioactive compounds in spite of the apparently intact appearance of the beads after 2 h immersion in the simulated gastric environment. For the three examined types of beads, an important amount of HT (20–30%) and DHPG (70–80%) arrived intact at the colon. Pectin has also been suggested as an interesting carrier for oral administration of antioxidants to prevent or improve chronic inflammatory bowel disease *in situ*.

Starch and cellulose are renewable biopolymers widely distributed in nature with a huge diversity of industrial applications. Starch is a cheap, abundant and edible polysaccharide with fantastic properties such as biodegradability, biocompatibility and cost–effectiveness having a long history as an excipient in drug formulations (Hong et al., 2014). Starch is applied in the food industry as a colloidal emulsifiers and thickening agent (Zhu, 2017). Native starch can be modified by chemical, physical or enzymatic methods. Modifications are aimed at increasing or changing functional properties of starch granules, such as swelling capacity, viscosity, solubility, and gelatinization extent. Maltodextrins, CD and octenylsuccinate–starch are starch derivatives that have been used as wall materials in

different encapsulation methods (Hoyos–Leyva et al., 2016). Dafe et al. (2017) developed a novel pectin/starch hydrogel through ionic gelation to improve the survival of *Lactobacillus plantarum* ATCC:13643 in a simulated gastrointestinal–bile salt solution, and during storage. Incorporation of starch with pectin provided significant cell protection against the harsh conditions of simulated gastric tract, and increased the tolerance to strongly acidic media and bile solutions.

Esterification using octenyl succinic acid anhydride (n–OSA) is one of the chemical methods for starch modification. The incorporation of the bulky octenyl–succinic groups into starch molecules imparts amphiphilic and surface–active properties. The so–called OSA starch has been successfully used as a stabilizer and a thickening agent of emulsions in beverages, encapsulated flavors, and mayonnaises (Chivero et al., 2016). Moreover, OSA starches have been used to make solid microcapsules that contain hydrophobic compounds: essential, fish, fruit, and dietary oils. Compared with Arabic gum and gelatin, OSA starch is an inexpensive and abundant material resource (Wang et al., 2017). Chiu et al. (2017) encapsulated sodium (salt) within the inner water phase of W1/O/W2 emulsions externally stabilized by OSA starch (0–3%) with the aim of enhancing saltiness perception. In the mouth amylase hydrolyzed the starch and destabilized the O/W emulsion releasing the inside W/O phase and, subsequently sodium, resulting in a salty taste.

The CDs refer to a group of cyclical natural molecules that consist of α–(1,4)–linked glucopyranose units (described above). These oligosaccharides are obtained through the action of glycosyltransferase. The most commonly CDs are α–CD, β–CD, and γ–CD, which consist of cyclic arrangements of 6, 7, or 8 glucopyranose units, respectively. These non–toxic starch derivatives are not absorbed in the gastrointestinal tract but are completely metabolized by colonic microflora. The CDs are used in the food industry because they

confer protection to lipophilic food components sensitive to oxygen, light and temperature actions, they are able to encapsulate food pigments and vitamins, stabilize vitamins and essential oils, and control the release of some food components (Dima et al., 2015). The CDs have been extensively tested for masking or removing the unpleasant smell and taste of some components.

Chitosan (β–(1,4)–poly–D–glucosamine) is a copolymer of N–acetyl–D–glucosamine and D–glucosamine with different degrees of N–acetylation (40–98%) and molecular weight ranging between 50–2000 kDa. The linear cationic polysaccharide, water insoluble chitosan, derived from chitin via deacetylation has a wide range of bioactivities such as antioxidant, antimicrobial, antifungal, antitumor, antiallergic, immune system activating, anti–hypertensive and cholesterol lowering properties, besides being from a natural source, biologically reproducible, almost non–toxic, biocompatible, and biodegradable (Kumar et al., 2017). Due to mucoadhesive nature, chitosan it is a good candidate for prolonging the residence time and increasing encapsulate release time in the gastrointestinal tract (Fathi et al., 2014). Chitosan has a great potential for the microencapsulation of probiotics and prebiotics (Varankovich et al., 2017), aromatic compounds (Yang et al., 2017), enzymes (Koyani & Vazquez–Duhalt, 2016), and antioxidants (Casanova et al., 2016). The complex coacervate between chitosan and soy protein isolate (SPI) markedly improves the oxidative stability of algal oil (polyunsaturated fatty acids) (Yuan et al., 2017). The chitosan–SPI coacervated microcapsules showed higher encapsulation efficiency, lower polydispersity, and improved oxidative stability compared with the SPI microcapsules. This improvement was attributed to the antioxidant properties of chitosan as well as the increased protection against oxidation due to the barrier formed after complex coacervation and cross–linking (Yuan et al., 2017).

Carrageenan is an anionic linear polysaccharide extracted from red seaweed (Rhodophyceae), consisting of alternating α–(1,4) and β–(1,3) linked anhydrogalactose residues that contain a variable number of sulphate groups (Elsabee & Abdou, 2013). Depending on the number of sulphate groups in the galactose dimers, three major fractions, are found: k (kappa)–carrageenan, ι (iota)–carrageenan, and λ (lambda)–carrageenan. Variation of these fractions affects gel strength, texture, solubility, synergism, and melting temperature of carrageenan. Soukoulis et al. (2017) evaluated the feasibility of oil–in–gel (O/G) emulsions, produced via IG of k–carrageenan, as a delivery systems for β–carotene. I*n situ* IG was induced by Na^+, K^+ or Ca^{2+} added at 0.2–0.6% (w/w) level. The O/G emulsions containing monovalent ions exerted the highest β–carotene retention storage particularly at high (37 and 55 ºC) temperatures.

Alginate, which contains two monomeric units of β–D–mannuronic acid and α–L–guluronic acid, is a natural anionic polysaccharide extracted from brown algae (Liu et al., 2013a). Sodium alginate is a water–soluble biopolymer that forms a gel structure in the presence of divalent cations such as calcium and zinc. The α–L–guluronic acid provides gel–forming capacity, whereas β–D–mannuronic acid determines the flexibility. Due to its hydrophilic properties, this biopolymer has considerable potential for entrapment of hydrophilic food bioactives. However, the two major limitations are low the encapsulation efficiency due to encapsulant leaching and the rapid dissolution (burst release) at the intestinal pH or in the presence of sodium ions (Fathi et al., 2014). The encapsulation of oil fish (eicosapentaenoic and docosahexaenoic acid) in alginate core–shell beads with different α–L–guluronic acid contents (70.4, 79.4, and 88%) were investigated (Wu et al., 2017). The wall materials of beads with low α–L–guluronic acid content (70.4%) could be

a suitable material for improving the oxidation stability of fish oil in an acidic medium, based on the obtained peroxide and p–anisidine values.

2.5.2 *Proteins used as wall material*

Proteins extracted from animal derived products (whey proteins, gelatin, and casein) and plants (soy, pea, and cereal) are widely used for encapsulation of bioactive compounds. Proteins are commonly used in the food industry as emulsifiers in the stabilization of O/W emulsion. Emulsifying property of wall materials is especially important for microencapsulation of oil–soluble ingredients, such as flavor oil, oil–soluble vitamins, and fish oil. Since proteins are of amphiphilic, they can distribute onto the oil–water interface with the hydrophilic groups guided toward the water phase and the hydrophobic groups oriented toward oil phase lowering the interfacial tension required to form the emulsion (Gaonkar et al., 2014).

2.5.2.1 *Plant proteins used for microencapsulation purposes*

The use of plant proteins as wall–forming materials in microencapsulation, reflects the present “green” trend in the food industries. In food applications, plant proteins are known to be less allergenic compared with animal derived proteins (Li et al., 2012). Moreover, plant proteins are renewable and biodegradable, and they own good functional properties, such as emulsifying capacity, filmogenic properties, and water solubility (Nesterenko et al., 2013). Nevertheless, due to the large globular nature of plant proteins, they have impediments for deposition at the interface; these is not the case of the smaller and more flexible proteins, such as casein (Karaca et al., 2015).

Soy proteins are the most important representatives of legume protein, whose major components are 11S (glycinin) and 7S (β–conglycinin) globulins. The soy proteins have been used alone or in combination with anionic polysaccharides depending on the application. Soy protein isolates have remarkable biological values and functional properties. Xiao et al. (2014) reported that coacervate microencapsulation increased the stability of capsanthin against moisture, heat, and light using SPI–chitosan.

Pea (*Pisum sativum*) protein isolate (PPI) is the most widely studied protein for complex coacervation. Pea proteins have interesting gel forming, emulsifying properties, and additionally hypoallergenic attributes (Nesterenko et al., 2013). For complex coacervation, pea protein (or isolate) is associated with polysaccharides, for example, ι–carrageenan, gellan gum, and alginate (Varankovich et al., 2015; Varankovich et al., 2017). On the other hand, a study performed by Tamnak et al. (2016) revealed that the pectine–PPI conjugate induced higher emulsion stability and ζ–potential, smaller droplet size and stronger encapsulation properties than the native pectin and Tween 80.

Piornos et al. (2017) use the protein isolate from a novel yellow lupin (*Lupinus luteus*) variety AluProt–CGNA® as emulsifying agent and optimize the formulation of the emulsion containing linseed oil in alginate/lupin protein macroscopic beads. The results show that the stability of encapsulated oil against heat treatments (50–75 °C, 24 h) was higher than free linseed oil used as control, demonstrating the effectiveness of the encapsulating system.

On the other hand, Linseed (*Linum usitatissimum*) is a rich source of proteins and polysaccharides which could be obtained as by–products from the linseed oil industry. Burgos–Diaz et al. (2016) they showed that a linseed fraction composed of 47.20% w/w protein and 37.88% w/w polysaccharide, can be considered as potential natural emulsifier

for improving stability of O/W (oil linseed/water) emulsions against variations of pH, ionic strength, and temperature. The bioemulsifier stability against physical and chemical treatments is very important for the design and manufacture of delivery systems of bioactive lipids. Kuhn et al. (2014) found that flaxseed protein isolate (FPI) based emulsions are more stable than mixed FPI–whey protein isolate stabilized emulsions. A higher FPI content (0.7% w/v) led to a greater creaming stability of the FPI systems as consequence of the gel network formation in the continuous phase and partly also to decreased interfacial tension between aqueous and oil phases, whereas the mixed FPI–whey protein isolate (3.0–0.7% w/v) was more unstable, which could be attributed to depletion effects. Bustamante et al. (2017) established that soluble protein fractions from chia seed and flaxseed as components of the encapsulation solution with maltodextrin improved probiotic survival (*Lactobacillus plantarum* and *Bifidobacterium infantis*) during spray drying and viability during storage at 4 °C in comparison with the control treatment (only with maltodextrin).

2.5.2.2 *Animal proteins used for microencapsulation purposes*

Animal proteins tend to be more soluble than plant proteins at wider pH range. Because they tend to be of smaller and more flexible, diffuse rapidly to the interface, stabilizing the oil droplets within a coarse emulsion (Karaca et al., 2015).

Traditionally, gelatin is the most common animal protein used as wall material in combination with polysaccharides. Gelatin from collagen isolated from the boiled connective tissues, tendons, bones and skins of animals (Lam & Gambari, 2014) The use of gelatin generates a safety problem due to the emergence of the prion diseases. Gelatin has been used for the microencapsulation of omega–3 fatty acids and phytosterol, since it has

suitable properties for its use in various encapsulation methods such as spray drying and complex coacervation (Wang et al., 2014). Curcumin encapsulation in gelatin microparticles produced by electrospraying has been shown to be an effective means to increase its water solubility, improving dispersion, as well as bioaccessibility in comparison with the commercial curcumin (Gómez–Estaca et al., 2015).

Caseins (representing around 80% of milk proteins) are mainly used as a protein ingredient in various food products to enhance their physical and functional properties. Caseins are GRAS and have exceptional surface–active and stabilizing properties, excellent emulsification and gelation (Ranadheera et al., 2016). In O/W emulsion systems, sodium caseinate (Na–CN) acts as an emulsifier, which adsorbs on the oil–water interface during homogenization stabilizing oil droplets against coalescence via electrostatic and steric repulsions. A Na–CN–SP isolate mixed protein stabilized emulsion with a narrow droplet size distribution was successfully prepared with no other additive based on the combined stabilization effects of the mixed proteins. The emulsion presented physicochemical characteristics, microstructure, and long–term storage stability suitable for clinical application as a liposoluble nutrition delivery system (Ji et al., 2015). On the other hand, it has been reported recently that sodium caseinate–stabilized emulsions can be ideal carriers for tea polyphenols (Sabouri et al., 2017).

Whey protein is considered a by–product of cheese production. It is rich in proteins (β–lactoglobulin, α–lactoglobulin, immunoglobulin and serum albumin), and it is being widely used by the food industry due to its nutritional and functional properties (Comunian & Favaro–Trindade, 2016). Whey proteins are mostly used as hydrogels and in nanoparticle systems for encapsulation and controlled release of different active ingredients. It is also used in the formation of complex cocaervates with several polysaccharides under different

conditions (Ach et al., 2015). Bilek et al. (2017) encapsulated an anthocyanin rich black carrot concentrate (5%) with the emulsion method to make thermally induced whey protein–based microcapsules. The microcapsules presented 2.0 g/kg phenolics, 1.43 g/kg flavonoids, 0.86 g/kg anthocyanin. Later these microcapsules were used as a natural colorant in yogurt. The encapsulated concentrate in whey hydrogels showed homogenous distribution of the pink color in yogurts when was added at 5, 10, 15, and 20% w/w capsule concentrations.

2.5.3 *Biodegradable polymers used as wall material*

The biodegradable polymers have emerged as potential candidates for the development of carriers for targeting compounds to specific sites in the body. In recent years, numerous processes for bioactive compounds encapsulation have been developed using aliphatic polyesters, such us poly(lactic acid) (PLA) and copolymers of lactic and glycolic acids that are well known biodegradable polymers (Martins et al., 2014). The delivery of drugs to a human body can be achieved through different routes, including oral, transdermal, topical, and parenteral routes. The permanent applications require of biostable polymers able to conserve their properties during their life span in the human body. In contrast, temporary applications require biodegradable polymers for a limited period of time (Li, 2017).

The PLA is a linear hydrophobic aliphatic polyester synthesized from lactic acid monomers, which are obtained by the fermentation of biomass, such as corn or wheat, or waste products, such as whey or molasses (Rhim, 2013), making it affordable and available for biomedical applications (Sheikh et al., 2015). There are two optical forms of PLA: D–lactide and L–lactide Poly(lactic–coglycolic acid). The Poly(lactic–coglycolic acid) (PLGA) is a linear copolymer that can be prepared at different ratios between its constituent

monomers, lactic (LA) and glycolic acid (GA). Depending on the ratio of lactic to glycolic acid used for the polymerization, different forms of PLGA can be obtained with different molecular weight and physico–chemical properties, as water solubility (Gentile et al., 2014).

The PLA and PLGA are widely used for drug delivery due to their biocompatibility and biodegradability, being approved for human use by the FDA (Anderson & Shive, 2012). The PLA has poor hydrophilicity and in some applications may need to be blended with hydrophilic components. Polyethylene glycol (PEG) is the most popular hydrophilic polymer for surface modification of nanoparticulates, and has been used to modify hydrophobic PLA to form amphiphilic copolymer PEG–PLA (formed by addition polymerization) (Liang et al., 2016). In a study carried out by Thong et al. (2014) developed polymeric micelles composed by PLA–PEG copolymers at different ratios (3:1, 2:1, 1:1, 1:2, 1:3 w/w) were applied in order to improve curcumin solubility. Systematic investigation showed that PLA/PEG ratio has large impact on curcumin solubility, encapsulation efficiency, particle size obtained, and curcumin release behavior of curcumin/PLA–PEG particles prepared by emulsification/solvent evaporation/freezer drying. The ratio 3:1 w/w of PLA/PEG results in better curcumin solubility, encapsulation efficiency and larger particle size. On the contrary, the ratio 1:3 w/w of PLA/PEG decreases curcumin release rate.

The advantages of employing microparticles for bioactive compounds delivery have been widely demonstrated. Cook et al. (2014) developed a multiparticulate dosage form, consisting of poly (D,L lactic–co–glycolic acid) (PLGA) microcapsules containing prebiotic Bimuno^{TM} by solvent evaporation method. Subsequently, these microcapsules were incorporated into an alginate–chitosan matrix containing probiotic *Bifidobacterium*

breve through ionic gelation and fluid–bed drying. The results show that galactooligosaccharides were successfully encapsulated into hollow PLGA microcapsules. These microcapsules were able to control the release of galactooligosaccharides, giving a triphasic release profile under *in vitro* gastrointestinal conditions; around 25% of the galactooligosaccharides was released over a 6 h period and concluded after 288 h. Moreira et al. (2016) coated thyme oil with PLGA through a coacervation process; the produced microcapsules exhibited a sustained oil release that ensures a level of antimicrobial activity.

2.5.4 *Lipids used as wall material*

Lipids are often chosen as encapsulating agents because of their melt and moisture barrier properties. These properties are important in both microcapsule fabrication and the release mechanism of the encapsulated bioactive. The lipids most commonly used are: hydrocarbon–rich substances (saturated long–chain fatty acids and waxes), simple lipids (mono–/di– and triglycerides) and lipid–derived substances (polyol–esters, modified mono–/diglycerides, and phospholipids) (Gaonkar et al., 2014).

Some requirements that should be considered for choosing of suitable lipids are: the solubility of the bioactive compounds in lipid matrices, since this influences the loading capacity, encapsulation efficiency, and subsequent usefulness chemical stability (oxidation and lipolysis); they must be biodegradable, and acceptable toxicological profile and not lead to the production of toxic residues during processing (Tamjidi et al., 2013). Lipid based delivery systems include liposomes, solid lipid nanoparticles (SLN), nanostructured lipid carriers (NLC), emulsions, and micelles (Fathi et al., 2012).

Lecithin, an ionic phospholipid, is widely used in the preparation of single–layered and bi–layered microcapsules, because of non–toxicity, good compatibility and nutritional

effects (e.g., lowering the cholesterol level in the blood). Some of the most common lecithins used in the food industry are extracted from soybeans, eggs, milk, sunflower, rice, and rapeseed seed. It has been reported that the use of lecithin improves microcapsules properties, such as higher entrapment efficiency, better oxidative stability, and smaller particle size. Stable O/W emulsions can be produced using certain types of lecithin as emulsifiers, provided that level is optimized (Moran–Valero et al., 2017).

Paini et al. (2015) optimized the encapsulation of apigenin in liposomes elaborated with rapeseed lecithin to prevent the degradation of this active compound. The liposomes displayed remarkable encapsulation efficiencies more than 92% of apigenin without using organic solvents. Liu et al. (2013b) encapsulated lactoferrin in liposomes, prepared with milk fat globule membrane–derived phospholipids to protect the protein at low pH conditions and against pepsin action; the proteins encapsulated in the liposomes was hydrolyzed at a lower rate compared with the protein in aqueous solutions.

Acevedo et al. (2014) used oleosomes from *Brassica napus* to encapsulate astaxanthin with a 99% efficiency; oleosomes are oil bodies consisting of a triacylglycerol core sorounded by a phospholipid monolayer embedded with oleosins. Microencapsulated astaxanthin in oleosomes shows a higher oxidative stability under light and air exposure compared with free astaxanthin.

A means of controlling the oral bioaccessibility of lipophilic bioactive compounds is to incorporate them in emulsion–based delivery. Salvia–Trujillo et al. (2013) assessed the influence of initial fat droplet size large (23 μm); medium (0.4 μm); and small (0.2 μm) on the digestion of lipids and the bioaccessibility of encapsulated β–carotene in corn O/W emulsions. It was shown that the speed and extent of lipid digestion increased with decreasing mean droplet diameter (small ≈ medium > large); this behavior was attributed to

the increase of the surface area exposed to pancreatic lipase as the droplet size decreases. There was also an appreciable increase in β–carotene bioaccessibility with decreasing droplet diameter (small > medium > large).

Cho et al. (2014) studied the influence of droplet size (0.21, 0.70, or 2.20 μm) and oil digestibility (corn oil versus mineral oil) on the bioavailability of heptadecanoic acid and Coenzyme Q10 using a rat feeding study. The study showed that small droplets were digested more rapidly than large droplets using a simulated small intestinal model (pH stat), which was attributed to the greater surface area of lipid exposed to intestinal juices. The pH stat model also confirmed that emulsified corn oil was digestible, whereas emulsified mineral oil was indigestible. On the other hand, the rat feeding study showed that bioavailability of heptadecanoic acid and Coenzyme Q10 was the highest in small intestinal tissues, when they were encapsulated within digestible oil droplets with the smallest size.

Solid lipid nanoparticles (SLN) and nanostructured lipid carriers (NLC) are colloidal carriers, with particle sizes from about < 1 μm. These systems have been designed to combine the advantages of polymeric particles (different chemical modifications), liposomes (membrane permeability) and emulsions (bioavailability) to offer new carrier systems having good physical stability, protection of labile bioactive compounds from degradation, controlled release, and compatibility (Sagis, 2015). The SLN are produced by replacing the oil of an O/W emulsion with a solid lipid or a blend of solid lipids that remain in solid phase at room and body temperatures. The NLCs are composed of oily droplets that can solubilize the encapsulated substances and render them embedded in a solid lipid matrix. As a result, NLC have a higher loading capacity than SLN.

Finally, lipids have been used as wall material to reduce moisture exchange between the environment and the microencapsulated bioactive compounds. In this context, waxes are

esters of a long–chain aliphatic acid with a long–chain aliphatic alcohol; waxes have a very small or buried hydrophilic part, so they interact poorly with water. One of the main problems of food products is the short shelf life of fresh products. The effects of the emulsion coatings on the microbial safety and physicochemical storage qualities of plums during storage were investigated Kim et al. (2013). The carnauba wax–based coating with incorporated lemongrass oil did not impact negatively the perceived flavor, fracturability, or glossiness of coated plums. The emulsion coatings showed potential for improving the safety of the fruit against *Salmonella typhimurium* and *Escherichia coli* increasing microbial safety and shelf life of plums.

2.6 Conclusions and future perspectives

In this review, we have focused on exposing microencapsulation in terms of the main methods, wall materials and bioactive compounds used during the last five years of research, as well as its application in food products. The properties of the materials, formulation of parameters, and operating conditions are the most studied factors to define optimal conditions to increase the encapsulation efficiency and to protect sensitive and unstable bioactive compounds from various factors (light, temperature, pH, etc.), ensuring their bioavailability.

Today, research in food products focus on identify, isolate, and preserve functional properties of new bioactive compounds. For the later suitable microencapsulation methods and wall materials for each bioactive needs to be defined. In this context, the search for new sources of polymeric materials (GRAS) that are biocompatible, biodegradable and able to release the active compound at the desired site of action. In addition, the more regulated

food market make the industry demands natural functional ingredients, preservatives, colorings or flavorings.

Due to the great interest of the consumers, both industries follow the tendency to develop more natural products that are sustainable and friendly with the environment, developing economically viable methods for the future production in large scale that allow the uniformity in the size of the particles. Finally, in spite of the great amount of research on the microencapsulation of bioactive compounds, the studies related to their application in finished products are limited. This fact should draw the attention of researchers to direct their efforts to this aspect.

2.7 Acknowledgements

The author thanks CONICYT Doctoral Scholarship 21161448.

Table 2.1. Examples of microencapsulated bioactive compounds in food industry.

Bioactive compounds	Examples	Reason to microencapsulate
Lipids	Essential oils Vegetable oils Fish oils Fatty acids Pigments	– They tend to oxidize rapidly in the presence of air, light and heat. Microencapsulation improves delivery during digestion
Phenolic compounds	Catechins Resveratrol Naringenin	– These natural compounds are very sensitive to light and heat. Moreover, they often present a poor biodisponibility mainly due to low water solubility. Additionally many of these molecules possess a very astringent and bitter taste, which limits their use in food or in oral medications.
Vitamins	A C D E	– Sensible to degradation. During consumption, the bioavailability of these compounds might be limited due to structure break–down and low absorption.
Carotenoids	Curcumin B–Carotene	– Poor water–dispersibility, chemical stability, and bioavailability. Susceptible to isomerization and oxidation upon exposure to oxygen, light and heat, which can result in loss of color and antioxidant activity.
Proteins	Bovine serum albumin Lactoferrin	– Microencapsulation protects proteins from degradation by enzymes, and can release them slowly to perform higher constant serum concentration for a prolonged time.
Probiotics	*Lactobacillus* *Bifidobacteria*	– The main problem is the low survival of these microorganisms in food products and in gastrointestinal tract.
Prebiotics	Galactooligosaccharides	– Microencapsulation avoids adverse interactions with others ingredients, improves the texture of the product and controls delivery in the gastrointestinal tract

Fig. 2.1. Comparison of different methods encapsulation with respect to particle size range and costs of production.

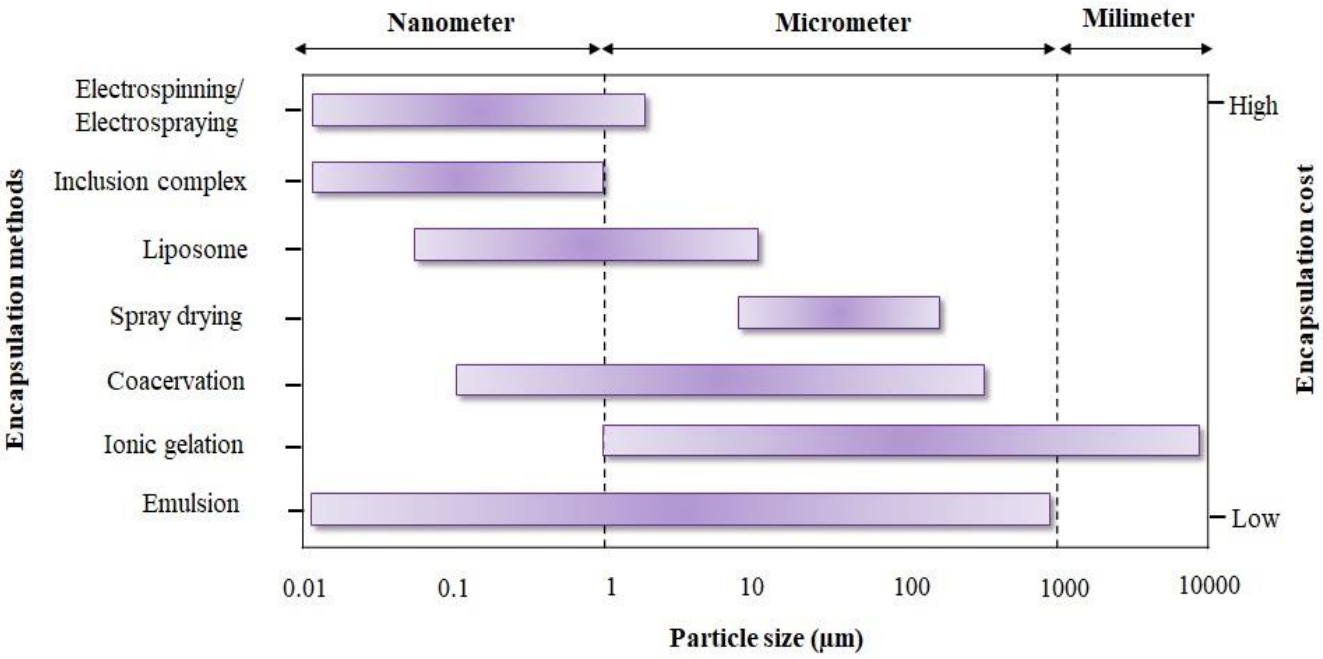

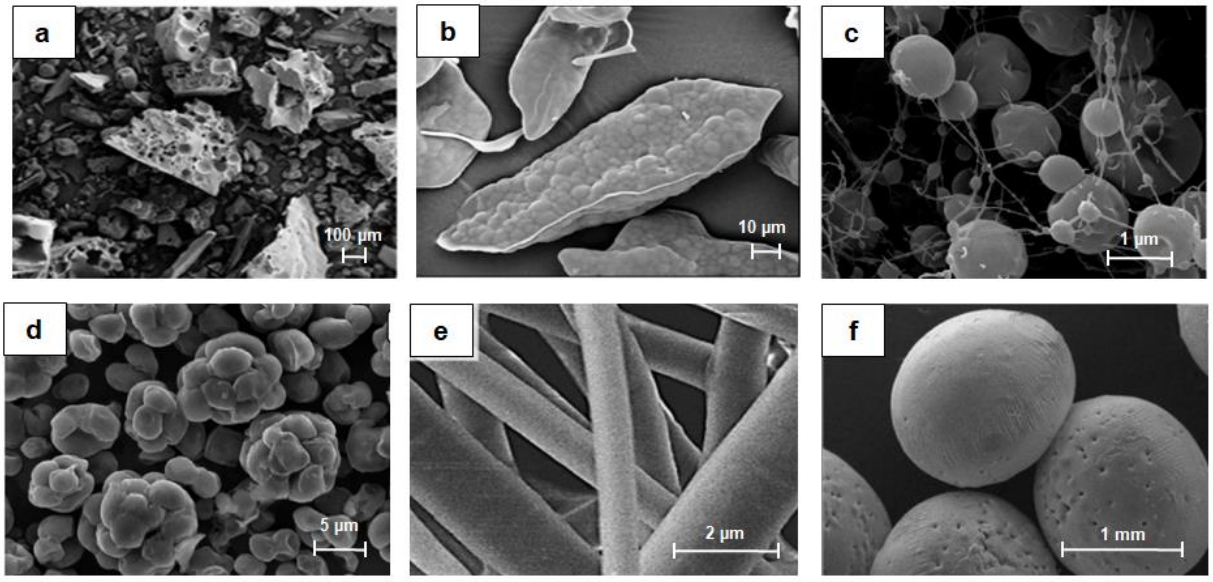

Fig. 2.2. Scanning electron micrographs (SEM) images. Morphology of microparticles performed with different methods, wall materials and bioactive compounds.

a. Powders of anthocyanins microencapsulated with maltodextrin and soy proteins isolate. (freeze drying method) (Pereira et al., 2016).

b. Microcapsules "multi–core" of tuna oil microencapsulated with gelatin and sodium hexametaphosphate (complex coacervation method) (Wang et al., 2014).

c. Microparticles of curcumin microencapsulated with gelatin. (electrospraying method) (Gómez–Estaca et al., 2015).

d. *d*–limonene microencapsulated in yeast *S. cerevisiae* (spray drying method). (Sultana et al., 2017).

e. Triclosan and curcumin microencapsulated in polyethylene glycol and poly(butylene succinate) solution, respectively. (electrospinning method) (Llorens et al., 2016).

f. Linseed oil microencapsulated with alginate and lupin protein (ionic gelation method) (Piornos et al., 2017).

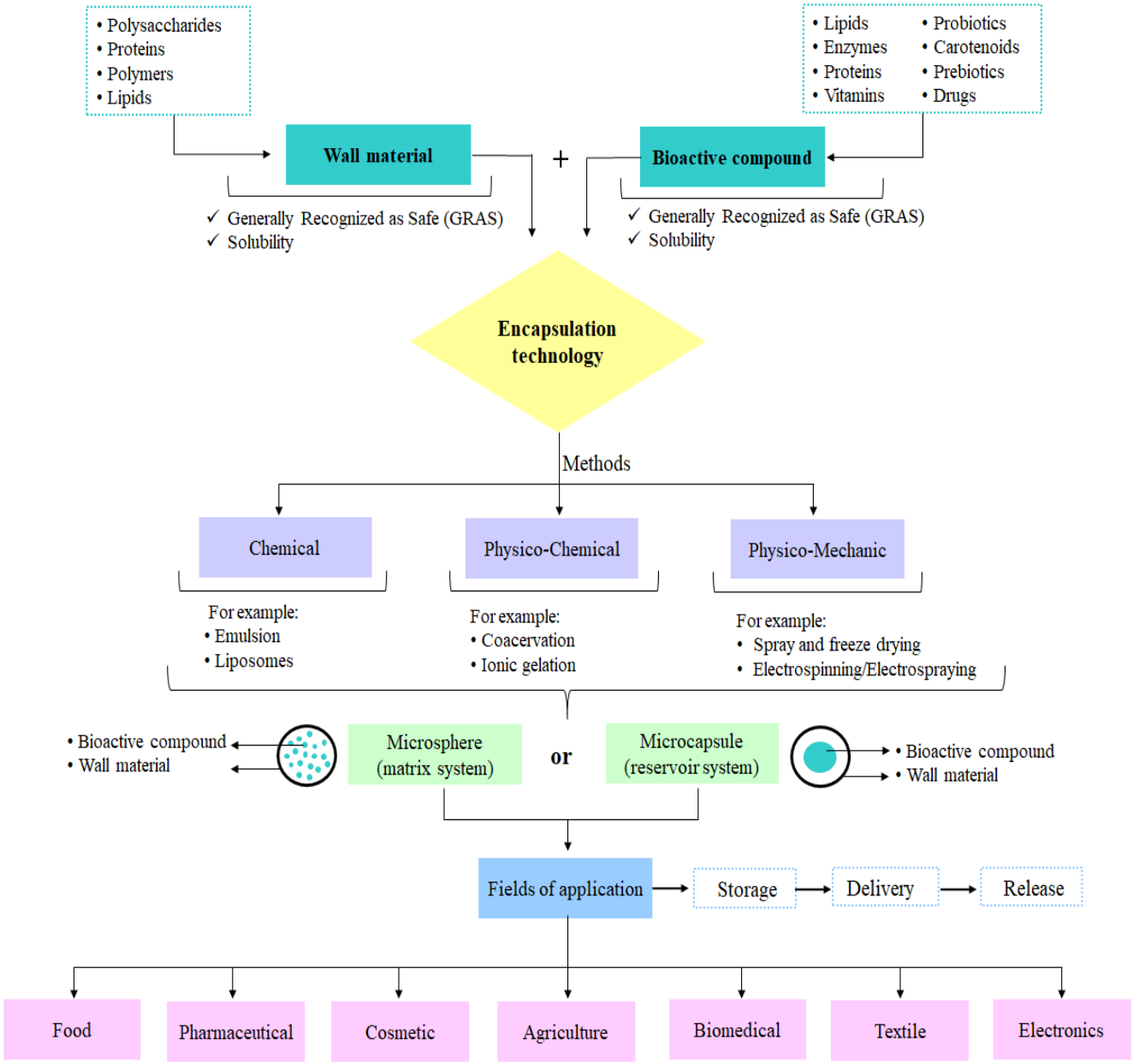

Fig. 2.3. Schematic procedures for the development of microencapsulation protocols.

Table 2. Summary of methods, bioactive compounds and wall materials used in microencapsulation.

Method	Bioactive compounds	Wall material	Treatment	Size microparticle	[1]EE (%)	Application	Authors
Spray drying	Ginger essential oil	Cashew gum and inulin	Cashew gum–inulin (3:1 w/w)	15.5 ± 0.2 µm	30.4 ± 1.0	Antimicrobial and antioxidant	(De Barros et al., 2016)
Spray drying	Tuna oil and mint oil	Whey protein isolate (WPI)	Tuna oil–Mint oil–WPI (3:3:24%)	Day 0 221.8 ± 6.2 nm Day 28 471.4 ± 16.7 nm	94.0 ± 0.1	Functional food	(Bakry et al., 2016b)
Spray drying	D–limonene and ethyl hexanoate	*S. cerevisiae*	*S. cerevisiae*–d–limonene (4:1 w/w) *S. cerevisiae*–ethyl hexanoate (4:1 w/w)	7.6 ± 0.9 µm 6.3 ± 0.3 µm	d–limonene 48.0 ± 3.0 Ethyl hexanoate 45.0 ± 2.7	Flavor	(Sultana et al., 2017)
Electrospraying	Curcumin	Gelatin	Curcumin–gelatin (1:10 w/w)	1.2 µm in diameter	100.0	Food colorant and functional ingredient	(Gómez–Estaca et al., 2015)
Ionic gelation	Linseed oil	Alginate and lupin protein	Alginate (47 g/L) Lupin protein (56 g/L) Oil–water (15:100 v/v)	1.8 ± 0.1 mm	Optimal 98.3 ± 1.3	Prevention of cardiovascular diseases, hypertension and inflammation	(Piornos et al., 2017)
External gelation	Sunflower oil	Alginate and shellac	Oil (30 % w/w) Alginate–Shellac (20–250 g/L) Ratio (50:50% v/v) Oil–wall material (20:80% v/v)	2.1 ± 0.1 mm	98.7 ± 0.1	Functional food	(Morales et al., 2017)
Extrusion	*L. plantarum*	Pectin and starch	Pectin–starch (0.5:1.5g/g)	1.3 ± 0.2 mm	94.8 ± 0.8	Probiotic	(Dafe et al., 2017)

Inclusion complex	Naringenin	β–cyclodextrin (β–CD)	Naringenin–β–CD (1:1 w/w) (1:2 w/w) (1:3 w/w)	—	69.5 83.2 84.4	Anti–inflammatory, anticarcinogenic, antitumour, anti–estrogenic, and antioxidant	(Semalty et al., 2014)
Inclusion complex	Astaxanthin	Oleosomes extracted from *B. napus*	Astaxanthin/oleosomes (0.01:0.30 w/w)	3.4 ± 0.5 µm	> 99.0	Preventative against cancer, immune response enhancer , anti–inflammatory and antioxidant	(Acevedo et al., 2014)
Solvent evaporation	Iron	Arabic gum, maltodextrin and modified starch	Arabic gum–maltodextrin–modified starch (4:1:1 w/w)	15.5 µm	91.6	Food fortification	(Gupta et al., 2015)
Complex Coacervation	Echium oil	Gelatin, arabic gum and cashew gum	Echium oil–gelatin (5% w/w) Arabic gum or cashew gum (5% w/w)	Arabic gum 45.5 µm Cashew gum 22.1 µm	—	Functional food	(Comunian et al., 2016)
Complex coacervation	Pimento oil	Chitosan and κ–carrageenan	Chitosan–κ–carrageenan (3:1w/w)	1211.0 ± 5.1 µm Diameter of dried microspheres	96.2 ± 2.1	Antioxidant and antimicrobial	(Dima et al., 2014)
Complex coacervation	Thyme oil (red and white)	Poly(lactic co–glycolic) Acid (PLGA)	PLGA: dimethylformamide DMF (0.1:7 w/v) Thyme oil (0.2 m/L)	Red: 44.8 µm White: 48.6 µm	Red: 70.0 White: 57.0	Antimicrobial	(Moreira et al., 2016)
Complex coacervation	Algal oil	Soy protein isolate (SPI) and chitosan	SPI–Chitosan (0.125 g g^{-1})	65.2 ± 0.7 µm	97.4 ± 1.2	Fortification of food product	(Yuan et al., 2017)
Complex coacervation Freeze drying	*B. adolescentis*	Pea protein isolate (PPI), alginate, iota–carrageenan and gellan gum	PPI–alginate PPI–ι–carrageenan PPI–gellan gum (2.0%:0.5% w/w)	~2.0 mm ~2.5 x 1.5 mm ~3.0 x 2.0 mm	—	Probiotic	(Varankovich et al., 2015)

Liposome	Cinnamon oil	Soy lecithin and cholesterol	Soy lecithin–cholesterol (5:1w/w)	144.3 ± 1.1 nm	29.2 ± 1.5	Antibacterial	(Cui et al., 2016)
Liposome	Nisin	Soy lecithin	Soy lecithin (5%)	181.0 ± 50.0 nm	47.0	Food preservative	(Imran et al., 2015)
Liposome/sonication	Apigenin	Rapeseed lecithin	Apigenin–lecithin (38:2 g/g)	260.3 ± 11.1 nm	98.3 ± 1.0	Antioxidant	(Paini et al., 2015)

[1]EE: Encapsulation efficiency

CHAPTER III

Journal of Food Engineering (2019), 26: 229–38
DOI: 10.1016/j.jfoodeng.2019.05.012

Encapsulation of lactoferrin into rapeseed phospholipids based liposomes: optimization and physicochemical characterization

Daniela Vergara[a,b]*, Carolina Shene[b]

[a]Doctoral Program in Sciences of Natural Resources, Universidad de La Frontera, Temuco, Chile.

[b]Department of Chemical Engineering, Center of Food Biotechnology and Bioseparations, Scientific and Technological Bioresource Nucleus (BIOREN), Centre for Biotechnology and Bioengineering (CeBiB). Universidad de La Frontera, Temuco, Chile.

Associated to specific objective 1.

Encapsulation of lactoferrin into rapeseed phospholipids based liposomes: optimization and physicochemical characterization

3.1 Abstract

Rapeseed phospholipids (RP), extracted from a residue of the oil processing, were used to elaborate liposomes for the encapsulation of lactoferrin (LF). Response Surface methodology was used to evaluate the effect of RP concentration (3–12 mg/mL), stigmasterol (ST) concentration (0–3 mg/mL), and sonication time (0–20 min) on the encapsulation efficiency (EE) and particle size. Commercial soy phospholipids (SP) were used to prepare liposomes under the same conditions. Results show that RP liposomes have a higher EE and a smaller particle size than those obtained using SP. Optimal conditions for the preparation of small LF–loaded RP liposomes (<200 nm) with the highest EE were: 10.18 mg/mL of RP, 0.61 mg/mL of ST and 4.06 min of sonication time. EE, particle size, polydispersity index, and ζ–potential of LF–loaded RP liposomes were 91.94 ± 0.61%, 148.57 ± 2.76 nm, 0.23 ± 0.01, and –31.03 ± 1.83 mV, respectively. Morphology confirmed the size, spherical shape and smooth surface of the LF–loaded RP liposomes. These results suggest that RP liposomes offer a novel option for stabilizing LF.

Keywords: Rapeseed phospholipids, liposomes, encapsulation, lactoferrin, delivery system.

3.2 Introduction

LF is a natural iron–binding glycoprotein present in milk but also in secreted fluids of mammals. LF has immunomodulatory, antioxidant, and antimicrobial activities (Onishi, 2011). Oral administration of LF is susceptible to proteolysis in the gastrointestinal tract, resulting in less than 1% absolute oral LF bioavailability levels (Troost et al., 2002). Encapsulation is a powerful tool for the development of food and pharmaceutical ingredients, since it enables the protection of a wide range of compounds by embedding them into a protective matrix. In general, delivery systems are able to protect bioactive compounds during their transit through digestive system and under adverse processing and/or storage conditions (light, temperature, moisture, oxygen), increasing their bioavailability.

Several encapsulation methods have been developed, such as spray drying, freeze drying, ionic gelation, and emulsion, among others. However, these methods have some disadvantages, among which are the effect of high temperatures on thermolabile compounds, high operating costs due to the high energy required for dispersion, and the lack of uniformity in the size and shape of the particles that limits the bioavailability.

The use of liposomes as a method of encapsulation is reported to be advantageous for the administration of various bioactive compounds due to their biocompatibility, biodegradability, lower toxicity and ability to entrap compounds, which increase their commercial use (Akbarzadeh et al., 2013). Liposomes may be used for a wide variety of applications, including the entrapment and controlled release of drugs, nutraceuticals, and unstable bioactives, such as peptides, enzymes, and polyphenols (Ma et al., 2014; Colletier et al., 2002; Hasan et al., 2014). Liposomes are small and spherical particles (20 nm to 2 μm in size), consisting of one or more phospholipid bilayers enclosing an aqueous core;

these structures are generally produced from highly purified phospholipids extracted from soy oil or egg yolk. Cholesterol addition is an important factor for liposomes preparation. Cholesterol reduces the rotational freedom of the phospholipid hydrocarbon chains, stabilizes the lipid bilayer, and helps to decrease the leakage of hydrophilic materials (Eloy et al., 2014). Previous studies have demonstrated that LF–loaded liposomes acts more effectively than free LF on the rat immune system via oral administration (Ishikado et al., 2005), and prevent LF gastric degradation under simulated gastrointestinal conditions (Liu et al., 2013).

To date, few works report properties of phospholipids from natural sources and their use for encapsulation of bioactives such as LF. Rapeseed (*Brassica napus)* is the second most important oilseed crop after soy, representing 20% of the world's supply (Wilson, 2008). During the rapeseed oil refining process, compounds such as proteins, pigments, free fatty acids, and phospholipids are removed. The valorization of these by–products for the production of high value products such as lecithin (mixture of phospholipids) has been investigated (Ceci et al., 2008). Some studies have reported that the cost of isolating and purifying phospholipids from natural sources would be lower than the cost of synthetic or semi–synthetic phospholipids (Singh et al., 2017). A recent review by Machado et al. (2014) highlights the importance of using cost–effective naturally–occurring phospholipids in making liposomes for the delivery of food ingredients.

The aims of the present study were to recover phospholipids from a waste generated in the rapeseed oil processing and to use them to elaborate LF–loaded liposomes. The combined influence of the concentrations of rapeseed phospholipids (RP) and stigmasterol (ST), and sonication time on the liposome encapsulation efficiency (EE) and particle size was studied by means of the Response Surface Methodology (RSM) using a Central

Composite Design (CCD) of experiments. For comparison the same experimental design was applied to study the effects of the factors on development of LF–loaded liposomes using commercial soy phospholipids (SP). Lipid oxidation and physical stability of LF–loaded RP liposomes during the storage at different temperatures were evaluated. The use of RP could be a novel strategy to stabilize and protect bioactive proteins such as LF into liposomes.

3.3 Materials and methods

3.3.1 Materials

Rapeseed oil was obtained from the residue left after cold pressing process was carried out by OleoTop S.A. (Freire, Araucania Region, Chile). Lactoferrin (LF) was purchased from Jarrow Formulas, (Los Angeles, California, USA). Commercial soy phospholipid (SP) was purchased from Prinal S.A (Santiago, Chile). Stigmasterol (ST) was purchased from Sigma–Aldrich (St. Louis, MO). All chemicals and solvents used were of analytical or HPLC grade.

3.3.2 Extraction of phospholipids from rapeseed oil

Rapeseed phospholipids were recovered through of water degumming process. Briefly, the oil was heated at 80 °C, mixed with water (3% w/v) and stirred for 15 min in a magnetic stirrer. The mixture was centrifuged at 8000×*g*, 4 ºC for 20 min. The degummed oil was removed and the gums were dried at 60 °C for 24 h. For the extraction of phospholipids, the dry gums were mixed with acetone (1:1.5% w/v) and stirred for 30 min. Subsequently, the mixture was centrifuged at 5000×*g*, 4 °C for 10 min; this procedure was repeated three

times under the same conditions. The solvent in the pooled fractions was removed at 40 °C in an air convection heat oven (Binder ED 400) to obtain the rapeseed phospholipids (RP).

3.3.3 RP characterization

3.3.3.1 Phosphorous analysis

The AOCS (2009) 12–55 ammonium molybdate method was used to determine the phosphorous content of RP and SP samples by ashing them, followed by the spectrophotometric measurement (660 nm) of phosphorus as a blue phosphomolybdic acid complex. Phosphorus content was determined by means of standard curve prepared using KH_2PO_4 as a standard. Results are reported as g phosphorous per kg.

3.3.3.2 Proximate analysis

The proximate analysis was performed by thermogravimetric analysis (TGA) (Perkin–Elmer STA–6000). Analyses of the samples (~20 mg) were done under nitrogen atmosphere (40 mL/min) from 25 to 800 °C with a heating rate of 50 °C/min. The fraction of moisture, volatile components, fixed carbon, and ash were determined.

3.3.3.3 Fourier transform infrared spectroscopic (FTIR) analysis

FTIR spectrum was used for determining phospholipid bands in RP and SP. A Cary 630 FTIR Spectrometer, (Agilent Technologies Inc., Danbury, CT, USA) was used for analysis. The infrared spectra were obtained as an average of 140 scans between 4000–600 cm^{-1}.

3.3.3.4 Phospholipids composition

Phospholipid content of the extracted RP and SP was determined by HPLC–ELSD. The HPLC system was an Alliance Waters e2695 Separation Module (Waters Inc., Mass, USA). The Evaporative Light Scattering Detector (ELSD) was NitroGen N118LA (Peak Scientific, UK). The conditions for ELSD were: nitrogen pressure of 50 psi, and drift tube temperature of 50 ºC. For the separation a RP–C18 column (5.0 µm × 4.6 mm × 250 µm Inertsil® ODS–3, GL sciences Inc., Japan) was used. The elution program comprised isocratic conditions with methanol/chloroform/acetonitrile/water (87.5:5:3.75:3.75 v/v/v/v). The column was kept at 35 ºC, and the mobile phase flow rate was 1 mL/min. The samples were dissolved in chloroform (~5 mg/mL), and filtered through a 0.22 mm syringe filter prior to injection. Sample injection volume was 20 µL. Phospholipids were identified and quantified comparing the retention time and area using a Soy Phospholipid Mixture standard (Avanti Polar Lipids Inc., AL, USA).

3.3.3.5 Fatty acid composition

Fatty acid methyl esters (FAMEs) were prepared as described by Shene et al. (2016). The separation of the FAMEs was carried out on a gas chromatography (GC–2010 Plus; Shimadzu, Kyoto, Japan), equipped with a flame–ionization detector, and a split injector. The capillary column was Rtx–2330 (60 m × 0.32 mm × 0.2 µm film thickness; Thames Restek, Saunderton, UK). Nitrogen was used as the carrier gas. The column temperature profile was as follows: 140 °C for 5 min, then increased to 240 °C at a rate of 3 °C/min and held at this temperature for 5 min. The injector and the detector were held at 210 °C. The FAMEs were identified with a 37–component standard FAME Mix (Supelco, Bellfonte, PA, USA).

3.3.3.6 Tocopherol composition

Samples were subjected to saponification and subsequent extracted with petroleum ether. Petroleum ether was evaporated and the samples were suspended in methanol. The analysis for identification and quantification of tocopherols was carried out in a Shimadzu high performance liquid chromatography (HPLC) system (Tokyo, Japan) equipped with a CTO–20AC oven and a SPD–M20A UV–VIS diode array detector. A Sunfire C18 column (4.6 mm × 150 mm × 3.5 μm, Waters) at 30 ºC was used. The mobile phase was methanol at a flow rate of 0.5 mL/min. The injection volume was 15 μL. Detection was made at 284 nm. Identification α–, δ–, and γ–tocopherol peaks were accomplished according to Edison (2009). Quantification was made comparing the corresponding area with that of α–tocopherol (Sigma–Aldrich St Louis, MO, USA) using a calibration curve built in the concentration range between 0.00 and 100 mg/L.

3.3.3.7 Amino acid composition

Samples were hydrolyzed and derivatized according to the AccQ–Tag method (Waters AccQ–Tag Solutions). The amino acid quantification was performed through HPLC Alliance Waters e2695 Separation Module (Waters Inc., Mass, USA) coupled with a UV detector (626 LC System, Waters Inc., Mass, USA). Amino acids were identified and quantified comparing the retention time and area using Amino Acid Standard H (Thermo Scientific Pierce, Rockford, IL, USA) and the Empower software (Waters, Milford, USA).

3.3.4 Preparation of LF–loaded liposomes

Liposomes were prepared by the thin–layer dispersion method. Briefly, into a round–bottom flask, phospholipids and ST were dissolved in a hexane:ethanol (1:0.25 v/v)

mixture. The solvent was removed in a rotary evaporator (DLAB RE100–Pro, Beijing, China) at 40 °C; a thin lipid film was formed on the flask walls. The dried lipid film was rehydrated with phosphate buffer (pH 7.4, 0.01 M), containing LF at 1 mg/mL, under orbital agitation (15 h, 150 rpm, at 25 °C) (Zhicheng ZHWY–211C, Shanghai, China). Disruption of the suspension was performed at 4 ºC by applying sonic energy (Sonicator® ultrasonic liquid processor XL2020, New York, USA); power was set at 40% for 4 min in a pulsed mode, and 1 min stop. The suspension was filtered through a 0.22 μm syringe filter.

3.3.5 Experimental design

RSM was used to optimize conditions for the LF–loaded RP liposomes elaboration. Five levels (determined in preliminary experiments) were studied for each of the three independent variables: RP concentration, ST concentration, and sonication time (Table 3.1). Details of the 17 design points are shown in Table 3.3. The same experimental design was applied replacing RP by SP. All the experiments were developed in triplicate. The experimental data were subjected to multiple regression analysis to obtain the adjusted polynomial equation. Analysis of variance (ANOVA) was done to identify the significant coefficients. The three–dimensional and contour graphs were built to identify the optimal combination of independent variables. For the analysis of the results the Design–Expert 10.0.6 software was used.

3.3.6 Characterization of LF–loaded liposomes

3.3.6.1 Determination of particle size, polydispersity index, and ζ–potential

The particle size, polydispersity index (PDI), and ζ–potential of LF–loaded liposomes were determined using a Zetasizer Nano ZS (series HT, Malvern Instrument, U.K.) at 25

°C. Conditions for measurement were defined according to Liu et al. (2013). The relative refractive index, i.e., the ratio of the refractive index of the phospholipids (1.490) to that of the dispersion medium (1.330), was 1.120. The absorption of the phospholipids was 0.001.

3.3.6.2 Determination of encapsulation efficiency

The encapsulation efficiency (EE) was determined according to the methodology described by Xu et al. (2012). Briefly, the sample of LF–loaded liposomes was diluted with phosphate buffer (pH 7.4, 0.01 M) (1:10) and transferred into an Amicon Ultra–0.5 centrifugal device (100 kDa MWCO, Merck Millipore, Darmstadt, Alemania) to separate the liposomes. The filter was centrifuged at 14000×g for 10 min (Hitachi Himac CT15E microcentrifuge). Protein concentration of the filtrate (C_{pf}) (Lowry et al., 1951) and filtrate volume (V_f) were determined. The EE (%) was calculated according to Eq. (1):

$$\boldsymbol{EE}\ (\%) = \frac{(C_{pt}\,V_t - C_{pf}\,V_f)}{Cpt\,V_t}\ x\ 100\% \qquad (1)$$

Where: C_{pt} is the protein concentration in the loaded sample, and V_t the sample loaded to Amicon Ultra–0.5 centrifugal device.

3.3.6.3 Morphology

The morphology of non–sonicated LF–loaded RP liposomes was observed using confocal laser scanning microscopy (CLSM, Zeiss LSM780, Jena, Germany) and scanning transmission electron microscopy (STEM, Hitachi SU–3500, Tokyo, Japan). The sample (1 mL) was mixed with 40 µL of BODIPY® (Thermo Fisher Scientific, Molecular Probes™) and 3 µL of SYPRO orange (Life Technologies, Eugene, OR, USA), to stain the phospholipids and the protein, respectively. The mixed solution was placed on a concave

confocal microscope slide, and 5 µL of agarose (0.5% w/v) were added to fix the sample. The sample was then covered with a coverslip and dried at room temperature in the dark. Images of the sample were acquired with a 100× magnification lens. For the image acquisition in STEM the LF–loaded RP liposomes formulation (1 mL) was incubated in 1% osmium tetroxide solution (Sigma–Aldrich) for 2 h at 4 °C. The excess of the solution was removed by centrifugation (5000×*g*, 10 min).

3.3.6.4 Stability of the LF–loaded RP liposomes during the storage

Physicochemical stability, particle size, PDI and ζ–potential of the LF–loaded RP liposomes was studied during storage at 4, 25, and 37 ºC. Aliquots of the stored samples (incubated at 4, 25 and 37 ºC) were collected after 7, 15, 30, 45, and 60 days. In addition, to the physical stability changes in the liposome solution: appearance, sedimentation, and color change were determined by visual inspection.

3.3.6.5 Lipid oxidation

The thiobarbituric acid (TBA) reactive substances (TBARS) method was used. Briefly, a solution of trichloroacetic acid (TCA)–TBA–HCl was prepared by mixing 15 g TCA, 375 mg TBA, 1.76 mL 12 N HCl, and 82.9 mL H_2O. One mL of the TCA–TBA–HCl solution was mixed with 200 µL of sample. The mixture was incubated at 95 °C (water bath) for 30 min; after cooled down to room temperature the mixture was centrifuged at 4000×*g* for 5 min, and the absorbance was measured at 532 nm. Results were expressed as µg of MDA equivalent per mg of sample, based on a 1,1,3,3–tetraethoxypropane (TEP) (Merck) standard curve, in a concentration range between 0.0 and 0.5 µg/mL.

3.3.7 Statistical analysis

All experimental data were collected from triplicate samples and expressed as the mean ± standard deviation. Statistically significant differences were examined using ANOVA and Tukey test. The significance of the factors was determined at a 5% confidence level.

3.4 Results and discussion

3.4.1 Extraction and RP characterization

The extraction yield of phospholipids from the rapeseed oil residue was 36.60 ± 0.08 g/kg (3.66%). Table 3.2 shows the chemical composition of RP and SP; the significant differences ($P<0.05$) between both materials are indicated.

The phosphorus content of the extracted RP was 1.88 ± 0.09 g/kg. The RP proximate composition was, moisture 1.07 ± 0.03% (w/w), volatile components 88.66 ± 0.13% (w/w) fixed carbon 1.41 ± 0.10% (w/w) and ash 8.74 ± 0.28% (w/w). SP had a similar proximate composition (Table 3.2).

Fig. 3.1 shows the FTIR spectra of RP and SP. Four bands were used to determine the presence of phospholipids, between 1765 and 1720 cm^{-1} (band 1) due to the C=O vibration; between 1200 and 1145 cm^{-1} (band 2) due to the PO_2 vibration; between 1145 and 970 cm^{-1} (band 3) due to P–O–C νsym vibration; and between 1200 and 970 cm^{-1} (band 4) due to both P–O–C and PO_2 vibrations. Characteristic bands were present in both RP as well as in SP, which confirms the effectiveness of the extraction method.

Phospholipid composition depends on the source, and its processing conditions, whilst the fatty acid composition is similar to that of the oil. Total content of phospholipids in RP and SP were 276.34 and 299.31 mg/g, respectively. The main phospholipids in RP and SP were phosphatidylcholine (PC), phosphatidylethanolamine (PE), phosphatidic acid (PA)

and lyso–phosphatidylcholine (LPC). In RP, PA + LPC (126.94 ± 18.71 mg/g) were the most abundant, followed by PE and PC (122.98 ± 3.78, and 26.42 ± 0.24 mg/g, respectively). In SP the most abundant phospholipid was PE (270.80 ± 32.39 mg/g), followed by PA + LPC and PC (15.63 ± 2.51, and 3.88 ± 1.10 mg/g, respectively). The total phospholipid content may vary depending on the amount of residual oil in the lecithin. According to Cui and Decker (2016) main phospholipids in rapeseed are PC, PE, and PA. The low PC content of the extract in contrast to the high LPC content could be due to the hydrolysis of PC whose fatty acid chain could be removed from either the sn–1 or sn–2 position as acetone washes are carried out during the extraction (Henna–Lu et al., 2012). Lysophospholipids are well known for their ability to destabilize phospholipid bilayers, resulting in the formation of micelles (Van Echteld et al., 1981); nevertheless, the addition of ST (used as membrane stabilizer) to liposomal formulations would reduce this effect.

About 90% of total fatty acids of RP are unsaturated. In SP, the level of unsaturated fatty acids is a little lower (76–77%). The RP contained mostly oleic (55.02 ± 0.06%) and linoleic (27.97 ± 0.07%) acids, with low levels of palmitic (7.84 ± 0.02%), α–linolenic (6.26 ± 0.01%), and stearic (1.27 ± 0.03%) acids. In contrast, the main fatty acid in SP was linoleic acid (52.45 ± 0.34%), with lower levels of oleic (17.39 ± 0.08%) and palmitic acids (19.80 ± 0.21%).

Total tocopherol content of RP (77.67 mg/100 g) was lower than the content of SP (161.27 mg/100 g). In RP, δ–tocopherol was the most abundant, followed by α– and γ–tocopherol (50.03 ± 3.32, 17.05 ± 2.93, and 10.59 ± 0.71 mg/100 g, respectively). In SP, α–tocopherol (96.99 ± 6.08 mg/100 g) was the most abundant, followed by γ– and δ–tocopherol (62.08 ± 4.25 and 2.20 ± 0.23 mg/100 g, respectively). Differences in the composition of tocopherols in RP and SP could be due to the source of the samples

(rapeseed or soy), and the extraction method. In this context, Taladrid et al. (2017) reported that the acetone, used in the process of phospholipid purification, contributes to the removal of tocopherols. It is necessary to consider that the presence of tocopherols in the raw materials could provide protection against the oxidation of polyunsaturated fatty acids present in phospholipids due to their antioxidant activity.

The most abundant amino acid in RP was proline (119.93 ± 9.87 mg/100 g), followed by histidine (79.53 ± 3.56 mg/100 g), and arginine (14.97 ± 2.56 mg/100 g). SP was relatively rich in histidine (83.06 ± 3.33 mg/100 g) and proline (82.53 ± 2.81 mg/100 g) followed by arginine (45.05 ± 0.95 mg/100 g), whereas the less abundant amino acids were threonine, alanine and cysteine with 26.27 ± 1.26, 20.63 ± 0.93, and 9.07 ± 0.53 mg/100 g, respectively. The heat treatment in the degummed process may reduce and destroy amino acids because the of Maillard reaction. In addition, differences in rapeseed cultivation conditions and oilseed crushing influence the content of protein. The content of essential amino acids such as histidine and arginine in RP is favorably for food purposes.

During the process of extraction of phospholipids by degumming in hot water at 80 ° C, it can be assumed that possible enzymes present in the oil and/or phospholipids are denatured by the effect of heat, not influencing the final composition.

3.4.2 Experimental design and data analysis

The effect of the independent variables: concentration of RP phospholipid (mg/mL), ST concentration (mg/mL), and sonication time (min), and their interactions on the responses EE and particle size of the liposomes were determined. The condition of the 17 experimental runs in the design of experiments and the obtained responses are presented in Table 3.3. To show the type of interactions between the independent variables and the

relationship between responses and levels of each variable, the response surface plots for EE and particle size are presented in Fig. 3.2 (a–d).

3.4.3. Effect of the independent variables on the encapsulation efficiency

The EE of RP liposomes ranged from 61.36 ± 1.62% (run 17) to 91.79 ± 1.09% (run 4) (Table 3.3). The ANOVA for the coefficients in the quadratic model is shown in Table 3.4. The determination coefficient (R^2 = 0.971) of the quadratic regression model for EE, indicated that the model was highly significant and adequate for prediction within the range of experimental variables. The linear coefficient of sonication time, all quadratic term coefficients, and two of the interaction coefficients (RP concentration–ST concentration and ST concentration–sonication time) were significant ($P<0.05$).

EE of the SP liposomes ranged from 56.47 ± 2.15% (run 13) to 87.56 ± 1.40% (run 9) (Table 3.3), values lower than those of the RP liposomes. The determination coefficient (R^2 = 0.994) of the quadratic regression, indicated that the model was highly significant and adequate for prediction within the range of experimental variables. All the coefficients in the quadratic model were significant ($P<0.05$).

Previous studies on LF–loaded liposomes prepared using milk fat globule membrane derived phospholipids, and L–α–phosphatidylcholine from egg yolk have reported EE of 46.40 ± 8.70% and 58.14 ± 1.37%, respectively (Liu et al., 2013; Yao et al., 2014) values that are lower than those obtained by RP and SP liposomes.

Factors affecting the EE and particle size of liposomes can be broadly divided in two categories: (1) the formulation, and (2) process variables. In the first category are found phospholipid concentration, and ST concentration. In the present work, the effect of only one process condition, sonication time, was evaluated.

It is known that the concentration of phospholipids affects EE of most bioactive compounds; this property is determined by the particle size. The total internal volume of liposomes is determined by two factors: (1) the entrapment volume of individual particle (determined by particle size, size distribution, and lamellarity), and (2) the total particle number (Xu et al., 2012). The increase in EE of LF due to the increase in phospholipid concentration is principally attributed to the increase in the total particle number (both for RP and SP). Similar results have been reported for the encapsulation of different proteins and peptides, such as beta–lactoglobulin (β–Lg) (Ma et al., 2014), nisin (Imran et al., 2015), and acetylcholinesterase (Colletier et al., 2002) in liposomes. However, our results showed a saturation of this effect and even a decrease of EE was observed with the highest concentration of phospholipids (12 mg/mL both to RP and SP) (Fig. 3.2 a–b). This could be ascribed to impediments of the thin layer methodology at a high concentration of phospholipids.

LF has net positive charge at physiological pH (isoelectric point (pI) LF > pH formulation buffer 7.4) which generates a strong electrostatic interaction with the negatively charged groups of phospholipids favoring the EE. These interactions would increase as the concentration of phospholipids increases. In addition, other factors, such as the charge of the phospholipids, buffer composition, and buffer ionic strength can influence the EE of proteins in liposomes

The significance of the interactions ST concentration – RP (or SP) concentration, and ST concentration – sonication time on EE was explained because ST acts as a membrane stabilizer (Eloy et al., 2014) reducing the leakage of LF from inside the liposomes whereas elevated sonication time would promote the leak of the protein.

3.4.4 Effect of the independent variables on the particle size

The results showed that the average particle size of the different LF–loaded RP liposomes formulations was in the range of 97.56 ± 2.13 to 203.62 ± 0.90 nm. Minimum and maximum sizes were obtained under the conditions of runs 14 and 13, respectively (Table 3.3), which only differ in the sonication time; in run 14 sonication time was 20 min and in run 13, the sample was not sonicated.

The statistical significance of the regression model (Table 3.4) was checked by F–test and P–value. Linear and quadratic coefficients for sonication time were highly significant ($P<0.05$). The low P–value and the relatively large determination coefficient ($R^2 = 0.841$), showed that the model was highly significant and adequate for prediction within the range of experimental variables.

Particle size of LF–loaded SP liposomes was found in the range 93.92 ± 9.69 to 172.43 ± 13.53 nm (Table 3.3); the minimum and maximum sizes were obtained under the conditions provided for runs 12 and 17, respectively. The low P–value and the large determination coefficient ($R^2 = 0.952$) indicated that the model was highly significant and adequate for prediction within the range of experimental variables. Linear coefficient for sonication time and the quadratic coefficients for SP concentration and ST concentration were found to be significant ($P<0.05$) (Table 3.4).

According to the obtained results, particle size was reduced as sonication time increased. RP concentration, ST concentration, and their interaction had no impact on the average particle size of RP liposomes. However, SP concentration and ST concentration had a significant impact on the liposome particle size. Another source of information on the quality of a liposome formulation is the PDI. The higher PDI values of the SP liposomes

compared to RP liposomes (Table 3.3) could indicate a broader size distribution or the development of a bimodal particle size distribution.

Particle size is an important property of liposomes for oral delivery of bioactive compounds. It was demonstrated that liposomes with smaller particle size increases their absorption efficiency in the gastrointestinal tract, their biodistribution and pharmacokinetic profiles (Tahara et al., 2018). In this context, the sonication process plays a significant role in reducing particle size. Sonication generates ultrasonic vibrations, which increases collisions among liposomes particles, while ultrasonic waves can break down large–sized liposomes. However, it is also necessary to consider that sonication could promote hydrolysis and oxidation of phospholipids if used for prolonged periods (>20 min) (Silva et al., 2010). Additionally, the incorporation of ST or cholesterol into the lipid composition enhances the liposome membrane stability against ultrasonic stress and could reduce the leakage of LF from inside the liposomes. If not controlled, a prolonged sonication increases the temperature altering fluid properties and the integrity of bioactives. In this study, the temperature was controlled throughout the experiment using a thermo–stated bath, and the sonication was carried out within 4 min intervals, as a way to control the hydrolysis and lipid peroxidation.

On the other hand, the type of fatty acid in a lipid membrane influences particle size. For example, in a liposomal formulation using phospholipids with unsaturated or polyunsaturated fatty acids, such as oleic, linoleic or α–linolenic acid, an increase on the particle size and liposome membrane fluidity was observed (Maherani et al., 2012). On average, LF–loaded liposomes with smaller particle size were obtained using RP, which is explained due to the higher content of polyunsaturated fatty acids (linoleic + α–linolenic acid) of SP (56.78%) compared to RP (34.23%) (Table 3.2).

The purpose of carrying out the statistical test with RP and SP is based on the need to compare the extracted material (RP) of this study with another having a proven encapsulation capacity, under the same conditions. Results show that compared to SP, the use of RP allowed obtaining liposomes with a higher EE and a smaller particle size. The differences are ascribed to the different phospholipid, and fatty acid composition, and the purity of both materials

3.4.5 Validation of the optimized model

To validate the adequacy of the quadratic model equations, three confirmation experiments were conducted to generate LF–loaded RP liposomes with the highest EE and a particle size in the obtained range (from 97.56 ± 2.13 to 203.62 ± 0.90 nm). These conditions were: RP concentration 10.18 mg/mL, ST concentration 2.23 mg/mL and sonication time 4.05 min. With these conditions the experimental values of EE and particle size were: 91.94 ± 0.61% and 148.57 ± 2.76 nm, respectively (Table 3.5). The values predicted by the models are close to the experimental values (differences less than 2.00%) indicating that the RSM was effective for optimizing the preparation conditions of LF–loaded RP liposomes.

3.4.6 Characterization of LF–loaded RP liposomes

3.4.6.1 Particle size, polydispersity, and ζ–potential of LF–loaded RP liposome

The particle size, polydispersity index (PDI), and ζ–potential were measured for the formulation that maximizes the EE; the values were 148.57 ± 2.76 nm, 0.23 ± 0.01, and –31.03 ± 1.83 mV, respectively. Liposomes that contain only a lipid bilayer membrane are called small unilamellar vesicles (SUV's) and have diameters between 20 nm and 100 nm.

Large unilamellar vesicles (LUV's) have diameters larger than 100 nm. According to this classification, LF–loaded RP liposomes corresponded to LUV`s. PDI is a measure of the size distribution of the particles. A PDI value around 0.1 represents monodispersity, values between 0.10 and 0.25 indicate a narrow particle size distribution, and values near to 1 indicate polydispersity (Tantra et al., 2010). The PDI value (0.23 ± 0.01) suggests that LF–loaded RP liposomes have a narrow particle size distribution. Previous studies using RP for liposome elaboration have reported that: unloaded RP liposomes had an average particle size of 125.50 nm with a PDI of 0.52 (Tehrany et al., 2012); apigenine–loaded RP liposomes had an average particle size of 158.90 ± 6.10 nm with a PDI of 0.21 ± 0.02 (Paini et al., 2015); and curcumin–loaded RP liposomes had an average particle size of 133.10 nm ± 0.80 with a PDI of 0.19 ± 0.01 (Hasan et al., 2014). Although in these studies different conditions were used in the particle preparation (sonication, power, phospholipids concentration), and the composition of RP and type of liposomes formed (number of layers, and volume trapped) were also different, the values of particle size and PDI are very similar to those obtained in this work. On the other hand, the ζ–potential, a measure of the strength of mutual repulsion or attraction among particles, correlates with the stability of colloidal dispersions. A high ζ–potential (in absolute value) means more stable systems. The negative ζ–potential (–31.03 ± 1.83 mV) is due to the phosphate groups (PO_4^{3-}) present in phospholipids and indicated that LF–loaded RP liposomes were electrically and physically stable. A wide range of ζ–potential values for food peptide–loaded liposomes ranging from –5.50 mV (da Rosa–Zavareze et al., 2014), to –40.80 mV (Mosquera et al., 2014) has been reported. This broad range can be explained due to differences in the source and composition of the phospholipid material, such as free fatty acids and amino acids, the encapsulating agent, and pH, viscosity, and ionic strength of the solution. The reported ζ–

potential values of liposomes and also the values found in this work suggest that liposomes are more stable than sodium alginate particles loaded with LF (–3.50 ± 0.20 mV to –18.10 ± 0.40 mV) (Li et al., 2019).

3.4.6.2 Morphology

The microstructure of the LF–loaded RP liposomes not submitted to sonication was observed using CLSM (Fig. 3). Fig. 3.3a shows the phospholipid bilayer (green color, see arrow) whereas Fig. 3.3b shows the spherical shape of the liposomes and indicates that the LF (red color) is within phospholipid bilayer. Morphology of LF–loaded RP liposomes observed under STEM (Fig. 3.3c–d) appeared spherical and homogenous with no sign of coalescence. The STEM analysis revealed nano–sized droplets (~200 nm), which is highly consistent with the average particle size measured by the dynamic light scattering system (Malvern zeta–size Nano ZS). The LF–loaded RP liposomes exhibited characteristic suggested for ideal liposomes: small and spherical with uniform size distribution, and no roughness or rupture on the surface.

3.4.6.3 Stability of LF–loaded RP liposomes

In general, liposome formulations are thermodynamically unstable; the particles have a high tendency to degrade, flocculate, fusion or aggregate, thus leading to the leakage of entrapped bioactive compounds during storage or after administration, and changes in particle size and charge. To evaluate the stability and shelf life of LF–loaded RP liposomes, particle size, PDI, and ζ–potential, during a 60 days storage at 4, 25, and 37 °C, were determined; the results are shown in Fig. 3.4 (a–c). It was found that during the 60 days storage at 4 °C the LF–loaded RP liposomes exhibited a 1.48–fold increase in particle size

(from 148.57 ± 2.76 nm to 219.30 ± 15.96 nm), and a 1.57–fold increase in PDI (from 0.23 ± 0.01 to 0.36 ± 0.03). The ζ–potential decreased 39% (from –31.03 ± 1.83 mV to –19.58 ± 1.10 mV). In contrast to these results, during the storage at 25 and 37 °C, a significant increase in particle size was observed (334 ± 21.21 nm and 465.94 ± 15.45 nm, respectively). On the other hand, at 37 ºC the ζ–potential increased significantly reaching –6.88 ± 0.70 mV. In addition, minimal differences were observed in the changes of PDI and ζ–potential when the LF–loaded RP liposomes were stored at 4 and 25 °C.

It was reported that after a 30 days storage of SP liposomes loaded with casein hydrolysates at 4 and 25 °C the particle size increased 7–9 and 40 times, respectively (Sarabandi et al., 2019). In addition, Marín et al. (2018) reported that SP liposomes loaded with collagen hydrolysate stored at 4 °C for 2 weeks showed no significant changes in size (102.30 ± 0.80 nm to 104.70 ± 0.40 nm) and PDI (0.24 ± 0.02 to 0.25 ± 0.06), whereas the ζ–potential increased from –43.40 ± 0.70 mV to –31.70 ± 0.60 mV. Our findings can be compared with those of Guner et al. (2017) that reported increases in particle size from 164.00 ± 9.46 nm to 175.10 ± 2.86 nm and 166.60 ± 18.31 nm to 185.90 ± 9.89 nm when SP liposomes were stored at 4 and 25 °C, respectively, during 30 days.

Physical and chemical stability of liposome systems are closely related and changes in any one of the two will affect the other. Temperature is a key factor that promotes aggregation and fusion of liposomes. A high temperature promotes the reorientation of lipid molecules, since positively charged ammoniums in choline groups may move to the membrane surface. Consequently, a decrease in ζ–potential is generated because of the loss of electrostatic repulsion that favors aggregation, increasing particle size and PDI in LF–loaded RP liposomes. In addition, in the already agglomerated particles the surface charge (ζ–potential) increased and bridges between the adjacent particles are formed (Sarabandi et

al., 2019). Finally, the higher stability of the RP liposomes at the lowest temperature (4 °C) can be attributed to the lower permeability of the liposome membrane, the low molecular mobility, and a delayed oxidative process of the unsaturated fatty acids in phospholipids. Our results demonstrate that LF–loaded RP liposomes stored at 4 °C were stable during short–term storage (less than 60 days) and could serve as a delivery system for LF.

Changes in the visual appearance of the liposome suspensions during the storage are shown in Fig. 3.5. LF–loaded RP liposomal optimized formulation stored at 4 ºC showed no change in color after 60 days. On the contrary, the liposomal formulation stored at 25 and 37 ºC showed a yellow coloration after 60 days. In addition, no precipitation or phase separation were observed in the optimized formulation stored at the different temperatures. From these results, it is suggested to keep liposomal formulations refrigerated in order to reduce negative effects on the stability.

3.4.6.4 Lipid oxidation

TBARS method measures the level of malondialdehyde (MDA) formed by the breakdown of unsaturated fatty acids. It is necessary to consider that hydroperoxides can decompose to secondary products such as aldehydes, ketones, acids, and alcohol; these secondary products can be decomposed (tertiary oxidation) in parallel to the secondary oxidation registered through TBARS method (Henna–Lu et al., 2012). Fig. 3.6 compares the evolution of MDA equivalent content due to accelerated thermal autoxidation of LF–loaded and unloaded RP liposomes at 60 ºC during 60 days. The initial accumulation of secondary products of lipid oxidation could be attributed to the liposome preparation methodology or RP extraction process. After 3 days, the MDA value of the LF–loaded RP liposomes increased approximately four times reaching 2.69 ± 0.09 µg MDA/mg RP,

whereas unloaded RP liposomes registered a slightly lower value (2.02 ± 0.07 µg MDA/mg RP). Subsequently, the MDA values began to decrease and remained around the initial value. The decrease in MDA values after reaching the maximum value could be due to the depletion of fatty acids for MDA formation or could be related to the positive correlation that exists between lipid oxidation and the development of yellow pigmentation in phospholipids. Aldehydes, products of lipid hydroperoxides degradation, can form bonds with the amine groups of phospholipids, which participate in browning reactions (Thanonkaew et al., 2007). Pigmentation developed after the aldehydes production could interfere in the measurement of RP liposomes oxidation hindering the correct measure of MDA, which forms pink–colored species.

The relatively low lipid peroxidation, compared to values reported by Marín et al. (2018), especially considering the high percentage of unsaturated fatty acids of RP, might be a consequence of endogenous antioxidants such as, α– γ– and δ–tocopherols (Table 3.2). Previous studies have reported benefits on the oxidative stability of lipid formulations due to phospholipid–tocopherol interaction (Taladrid et al., 2017). In addition, cholesterol (or ST) present in liposome formulations might retard peroxidation because of its effect on the biophysical properties of the phospholipid bilayer (Eloy et al., 2014).

LF–loaded RP liposomes showed MDA values higher than those of unloaded RP liposomes; this could be caused by an effect of lipid–protein interaction on the progress of oxidative reactions. Therefore, oxidative stability is a function of both the inherent stability of empty liposomes and the encapsulated compound. The amino acid composition of the encapsulated protein would also influence the stability; amino acids more prone to oxidation are tryptophan, histidine, proline, lysine, cysteine, and tyrosine.

3.5 Conclusions

In the present study, RP from a residue of rapeseed oil processing were extracted and characterized. The RP were used for developing liposomes to encapsulate the bioactive LF. It was shown that compared to SP, RP allows to elaborate liposomes with a higher EE and a smaller size particle. CLSM images demonstrated the effective encapsulation of LF in RP liposomes. STEM clearly showed the spherical shape of LF–loaded RP liposomes. Temperature had a significant effect on the stability of RP liposomes during storage; the lowest temperature (4 ºC) was the most desirable storage condition. Although the results are promising and suggest that RP liposomes could be a natural delivery system for LF, studies aimed at checking the stability of the loaded RP liposomes in the gastrointestinal system are needed.

3.6 Acknowledgements

This research was supported by funds from CONICYT through CONICYT Doctoral Scholarship 21161448 and the Center of Biothecnology and Bioengineering (CeBiB) FB–0001. In addition acknowledgement must be granted to the Scientific and Technological Bioresource Nucleus (BIOREN) at Universidad de La Frontera, Temuco.

Table 3.1. Independent variables and working levels used in the surface response methodology to optimize conditions for elaboration of LF–loaded liposomes and to examine their effects.

Independent variables	Code	Level and value				
		–α	**–1**	**0**	**+1**	**+α**
RP or SP concentration (mg/mL)	X_1	3.0	4.8	7.5	10.2	12.0
ST concentration (mg/mL)	X_2	0.0	0.6	1.5	2.4	3.0
Sonication time (min)	X_3	0.0	4.0	10.0	16.0	20.0

RP = rapeseed phospholipids
SP = soy phospholipids
ST = stigmasterol

Table 3.2. Composition of rapeseed phospholipids (RP) and a soy phospholipids (SP) used in liposome production.

	RP	SP
Phosphorus content (g/kg)	1.88 ± 0.09[a]	1.96 ± 0.01[a]
Proximate analysis (%)		
Moisture	1.07 ± 0.03[a]	0.92 ± 0.01[b]
Volatile components	88.66 ± 0.13[a]	88.48 ± 0.01[a]
Fixed carbon	1.41 ± 0.10[b]	2.43 ± 0.04[a]
Ash	8.74 ± 0.28[a]	8.04 ± 0.04[a]
Phospholipids mg/g		
Phosphatidylcholine (PC)	26.42 ± 0.24[a]	3.88 ± 1.10[b]
Phosphatidylethanolamine (PE)	122.98 ± 3.78[b]	279.80 ± 32.39[a]
Phosphatidylinositol (PI)	ND	ND
Phosphatidic acid (PA) + Lysophosphatidylcholine (LPC)	126.94 ± 18.71[a]	15.63 ± 2.51[b]
Fatty acid (%)		
Palmitic acid (C16:0)	7.84 ± 0.02[b]	19.80 ± 0.21[a]
Stearic acid (C18:0)	1.27 ± 0.03[b]	4.42 ± 0.02[a]
Oleic acid (C18:1)	55.02 ± 0.06[a]	17.39 ± 0.08[b]
Linoleic acid (C18:2)	27.97 ± 0.07[b]	52.45 ± 0.34[a]
α–Linolenic acid (C18:3)	6.26 ± 0.01[a]	4.33 ± 0.09[b]
Others	1.64 ± 0.00[a]	1.62 ± 0.12[a]
Tocopherols (mg/100 g)		
α–tocopherol	17.05 ± 2.93[b]	96.99 ± 6.08[a]
δ–tocopherol	50.03 ± 3.32[a]	2.20 ± 0.23[b]
γ–tocopherol	10.59 ± 0.71[b]	62.08 ± 4.25[a]
Amino acids (mg/100 g)		
Alanine	ND	20.63 ± 0.93
Arginine	14.97 ± 2.56[b]	45.05 ± 0.95[a]
Cysteine	ND	9.07 ± 0.53
Histidine	79.53 ± 3.56[a]	83.06 ± 3.33[a]
Proline	119.93 ± 9.87[a]	82.53 ± 2.81[b]
Threonine	ND	26.27 ± 1.26

ND = Not Detected; Different superscript letters indicate significant differences ($P<0.05$) for composition in the different phospholipid (RP or SP) in the row (n=3).

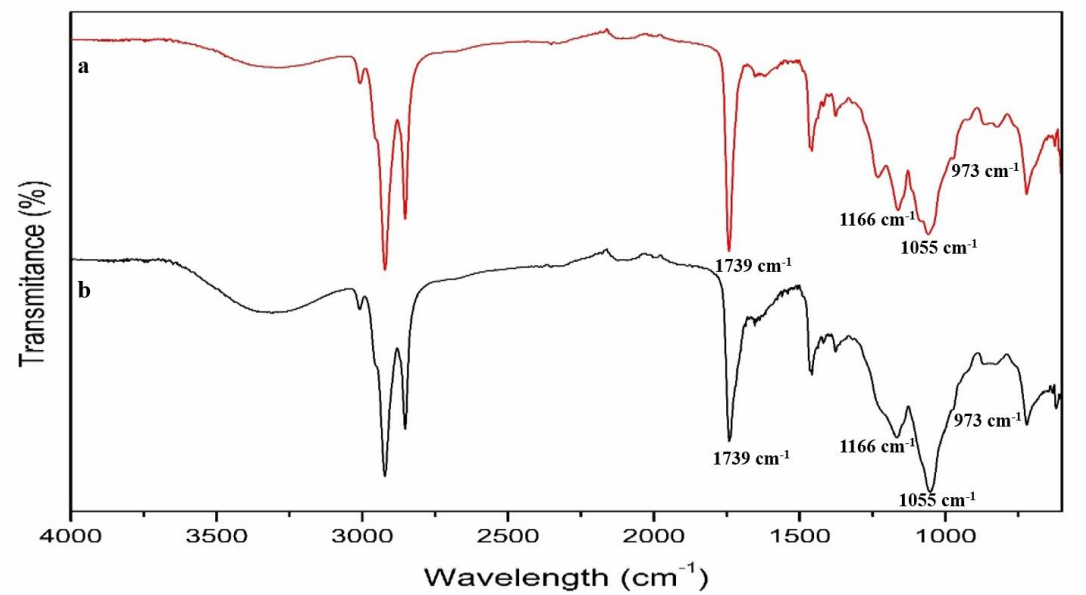

Fig. 3.1. Fourier transform infrared (FTIR) spectrum of (a) rapeseed phospholipids (RP) (red curve), (b) soy phospholipids (SP) (black curve).

Table 3.3. Central composite design with the actual and predicted values for encapsulation efficiency (EE) and particle size, as well as polydispersity index (PDI) and ζ–potential of the liposomes elaborated with rapeseed phospholipid (RP) and soy phospholipid (SP).

	Run	X_1	X_2	X_3	EE (%)		Particle size (nm)		PDI	ζ–potential (mV)
					Actual value	Predicted value	Actual value	Predicted value		
LF–loaded RP liposomes	**1**	4.80	0.60	4.00	86.48 ± 0.68	87.29	118.98 ± 3.01	130.65	0.22 ± 0.01	–23.67 ± 1.78
	2	10.20	0.60	4.00	82.05 ± 1.77	80.46	132.51 ± 3.66	144.94	0.21 ± 0.01	–28.09 ± 1.06
	3	4.80	2.40	4.00	86.75 ± 1.88	88.33	128.48 ± 8.21	136.46	0.25 ± 0.00	–25.09 ± 1.70
	4	10.20	2.40	4.00	91.79 ± 1.09	94.90	140.63 ± 1.93	151.85	0.25 ± 0.02	–29.21 ± 1.00
	5	4.80	0.60	16.00	81.22 ± 2.18	79.76	107.29 ± 6.56	100.68	0.27 ± 0.02	–23.31 ± 2.21
	6	10.20	0.60	16.00	74.47 ± 1.36	74.53	115.64 ± 6.39	112.28	0.21 ± 0.02	–24.09 ± 0.78
	7	4.80	2.40	16.00	66.88 ± 0.55	70.11	98.97 ± 6.21	91.16	0.33 ± 0.01	–25.95 ± 1.11
	8	10.20	2.40	16.00	77.44 ± 1.66	78.27	110.92 ± 1.50	103.87	0.23 ± 0.03	–26.46 ± 1.24
	9	3.00	1.50	10.00	91.57 ± 0.41	89.86	99.15 ± 2.14	98.27	0.21 ± 0.05	–19.54 ± 0.34
	10	12.00	1.50	10.00	91.63 ± 0.28	90.97	126.62 ± 5.51	120.97	0.22 ± 0.01	–29.96 ± 1.44
	11	7.50	0.00	10.00	72.22 ± 0.14	74.32	112.79 ± 7.45	106.61	0.23 ± 0.01	–30.30 ± 0.66
	12	7.50	3.00	10.00	82.77 ± 1.37	78.31	104.77 ± 1.41	104.42	0.22 ± 0.01	–24.27 ± 0.09
	13	7.50	1.50	0.00	85.65 ± 0.29	84.09	203.62 ± 0.90	180.10	0.39 ±.0.01	–29.27 ± 2.23
	14	7.50	1.50	20.00	64.76 ± 2.43	63.96	97.56 ± 2.13	114.55	0.27 ± 0.07	–24.60 ± 2.71
	15	7.50	1.50	10.00	62.31 ± 1.62	62.08	112.60 ± 4.20	109.83	0.23 ± 0.01	–27.17 ± 1.28
	16	7.50	1.50	10.00	62.03 ± 1.49	62.08	105.99 ± 2.54	109.83	0.23 ± 0.00	–25.54 ± 1.45
	17	7.50	1.50	10.00	61.36 ± 1.62	62.08	109.78 ± 4.07	109.83	0.23 ± 0.01	–26.12 ± 1.25

LF–loaded SP liposomes	**1**	4.80	0.60	4.00	74.10 ± 1.48	73.90	144.92 ± 7.00	133.25	0.37 ± 0.03	–42.02 ± 1.55
	2	10.20	0.60	4.00	73.06 ± 1.62	72.11	115.85 ± 0.40	121.21	0.36 ± 0.02	–44.88 ± 0.45
	3	4.80	2.40	4.00	73.06 ± 0.54	72.15	121.28 ± 2.71	123.52	0.27 ± 0.01	–39.47 ± 0.92
	4	10.20	2.40	4.00	75.21 ± 0.13	74.96	126.18 ± 0.40	117.09	0.26 ± 0.02	–45.06 ± 1.83
	5	4.80	0.60	16.00	77.44 ± 0.27	77.05	98.74 ± 22.24	106.95	0.23 ± 0.00	–41.52 ± 2.90
	6	10.20	0.60	16.00	70.01 ± 1.08	70.27	114.77 ± 1.32	111.66	0.44 ± 0.02	–49.99 ± 0.89
	7	4.80	2.40	16.00	84.22 ± 2.81	84.52	112.00 ± 2.04	105.76	0.28 ± 0.03	–43.48 ± 2.01
	8	10.20	2.40	16.00	82.79 ± 1.97	82.34	105.29 ± 1.58	116.08	0.27 ± 0.02	–49.73 ± 0.88
	9	3.00	1.50	10.00	87.56 ± 1.40	87.97	100.46 ± 12.72	104.51	0.28 ± 0.04	–42.98 ± 2.58
	10	12.00	1.50	10.00	84.14 ± 2.28	84.66	105.86 ± 9.30	103.07	0.34 ± 0.00	–52.40 ± 0.09
	11	7.50	0.00	10.00	74.81 ± 1.40	75.27	99.00 ± 4.68	99.30	0.27 ± 0.00	–42.88 ± 2.46
	12	7.50	3.00	10.00	83.39 ± 0.56	83.86	93.92 ± 9.69	94.88	0.23 ± 0.01	–41.45 ± 2.76
	13	7.50	1.50	0.00	56.47 ± 2.15	57.54	165.46 ± 44.39	172.93	0.35 ± 0.03	–42.73 ± 0.02
	14	7.50	1.50	20.00	66.45 ± 2.29	66.31	156.39 ± 13.09	150.18	0.36 ± 0.02	–48.08 ± 2.07
	15	7.50	1.50	10.00	76.79 ± 1.40	76.20	168.47 ± 40.35	169.21	0.41 ± 0.04	–49.70 ± 2.09
	16	7.50	1.50	10.00	75.41 ± 2.89	76.20	167.76 ± 37.49	169.21	0.39 ± 0.05	–48.75 ± 1.63
	17	7.50	1.50	10.00	76.61 ± 2.29	76.20	172.43 ± 13.53	169.21	0.39 ± 0.00	–49.06 ± 0.33

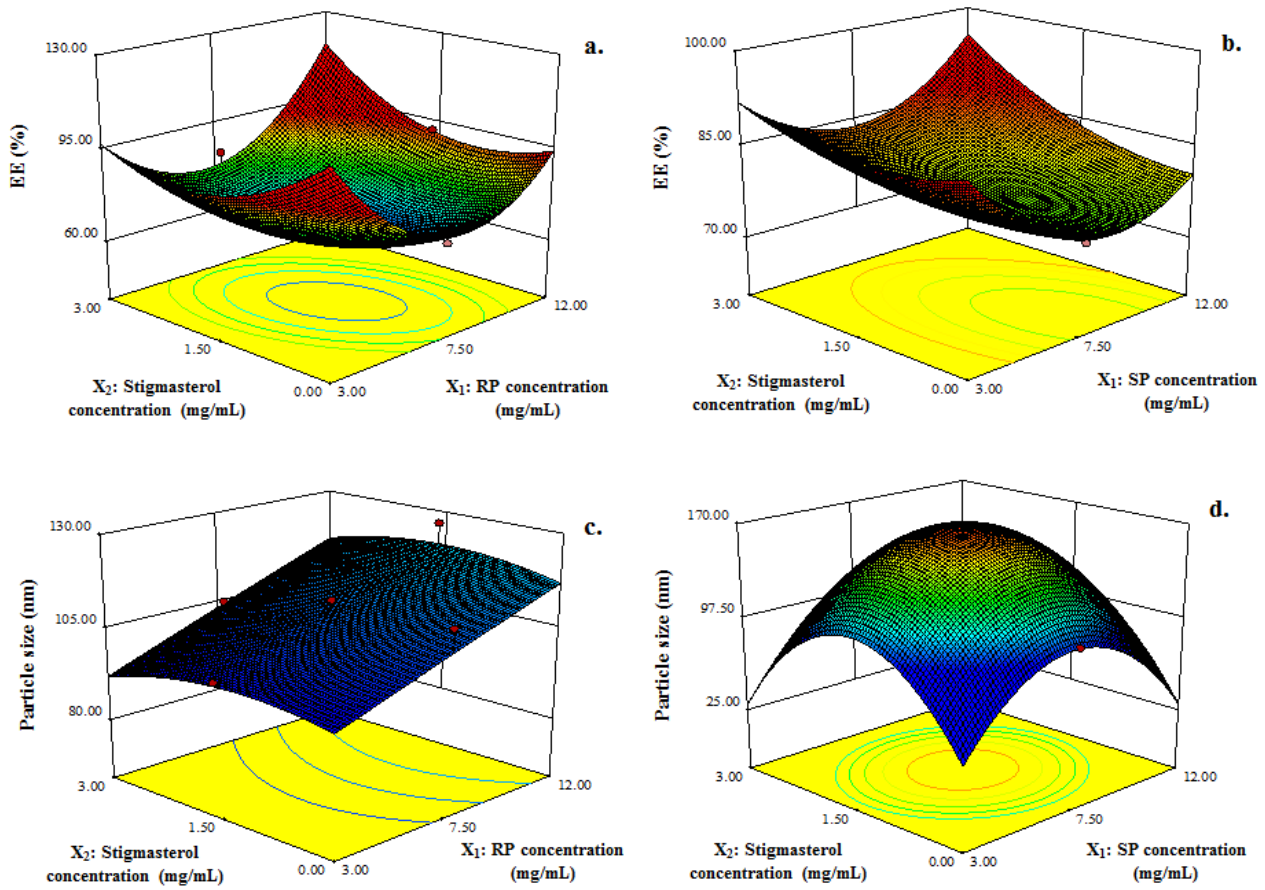

Fig. 3.2. Response surface and contour plots for the graphical analysis of the effect of the independent variables on the responses. (a) Effect of RP concentration and ST concentration on EE, (b) effect of SP concentration and ST concentration on EE, (c) effect of RP concentration and ST concentration on particle size, and (d) effect of SP concentration and ST concentration on particle size (sonication time was 10 min).

Table 3.4. Analysis of variance (ANOVA) and regression coefficients between response variables encapsulation efficiency (EE) and particle size, and the independent variables: X_1, phospholipids concentration (mg/mL) X_2, ST concentration (mg/mL), and X_3, sonication time (min) used for elaboration of LF–loaded liposomes. Rapeseed phospholipid (RP) and soy phospholipid (SP).

	Source	DF	EE (%)			Particle size (nm)		
			Coefficient	Sum of squares	P value	Coefficient	Sum of squares	P value
LF–loaded RP liposomes	**Model**	9	62.01	1883.32	0.0001	109.83	8381.93	0.0376
	X_1	1	0.33	1.50	0.6764	6.75	622.17	0.1409
	X_2	1	1.20	19.65	0.1586	–0.65	5.81	0.8771
	X_3	1	–6.02	494.67	< 0.0001	– 19.49	5186.87	0.0020
	X_1^2	1	10.12	1153.59	< 0.0001	–0.074	0.062	0.9872
	X_2^2	1	5.13	296.55	0.0005	–1.53	26.24	0.7432
	X_3^2	1	4.32	210.32	0.0013	13.26	1981.08	0.0211
	X_1X_2	1	3.35	89.65	0.0119	0.28	0.62	0.9598
	X_1X_3	1	0.40	1.28	0.6992	–0.67	3.62	0.9028
	X_2X_3	1	–2.67	57.14	0.0311	–3.83	117.50	0.4941
	Residual	7		55.27			1581.17	
	Lack of fit	5		54.79			1559.166	
	Pure error	2		0.48			22.00	
	Total	16		1938.59			9963.10	
	R^2		0.9715			0.8413		

	Adj–R^2		0.9348			0.6373		
	CV		3.62			12.61		
LF–loaded SP liposomes	**Model**	9	76.22	897.64	< 0.0001	169.54	12318.88	0.0008
	X_1	1	0.99	13.35	0.0042	0.42	2.44	0.8726
	X_2	1	2.57	90.21	< 0.0001	–1.32	23.92	0.6183
	X_3	1	2.62	93.92	< 0.0001	–6.76	629.01	0.0319
	X_1^2	1	3.57	143.51	< 0.0001	–23.43	6189.22	< 0.0001
	X_2^2	1	1.18	15.74	0.0027	–25.80	7503.91	< 0.0001
	X_3^2	1	–5.06	288.10	< 0.0001	–3.10	102.00	0.3175
	X_1X_2	1	1.15	10.56	0.0076	1.40	15.76	0.6848
	X_1X_3	1	–1.25	12.43	0.0051	4.19	140.20	0.2474
	X_2X_3	1	2.31	42.55	0.0001	2.14	36.51	0.5402
	Residual	7		5.39			616.38	
	Lack of fit	5		4.26			603.71	
	Pure error	2		1.13			12.66	
	Total	16		903.02			12935.26	
	R^2		0.9940			0.9523		
	Adj–R^2		0.9864			0.8911		
	CV		1.15			7.36		

Table 3.5. Predicted and experimental values of encapsulation efficiency (EE) and particle size of the liposomes elaborated with RP phospholipids under optimum conditions.

Response	Predicted value	Experimental value	Deviation (%)
EE (%)	93.64	91.94 ± 0.61	1.84
Particle size (nm)	147.98	148.57 ± 2.76	0.40

Note: Deviation (%) = (predicted value – experimental value) / predicted value × 100

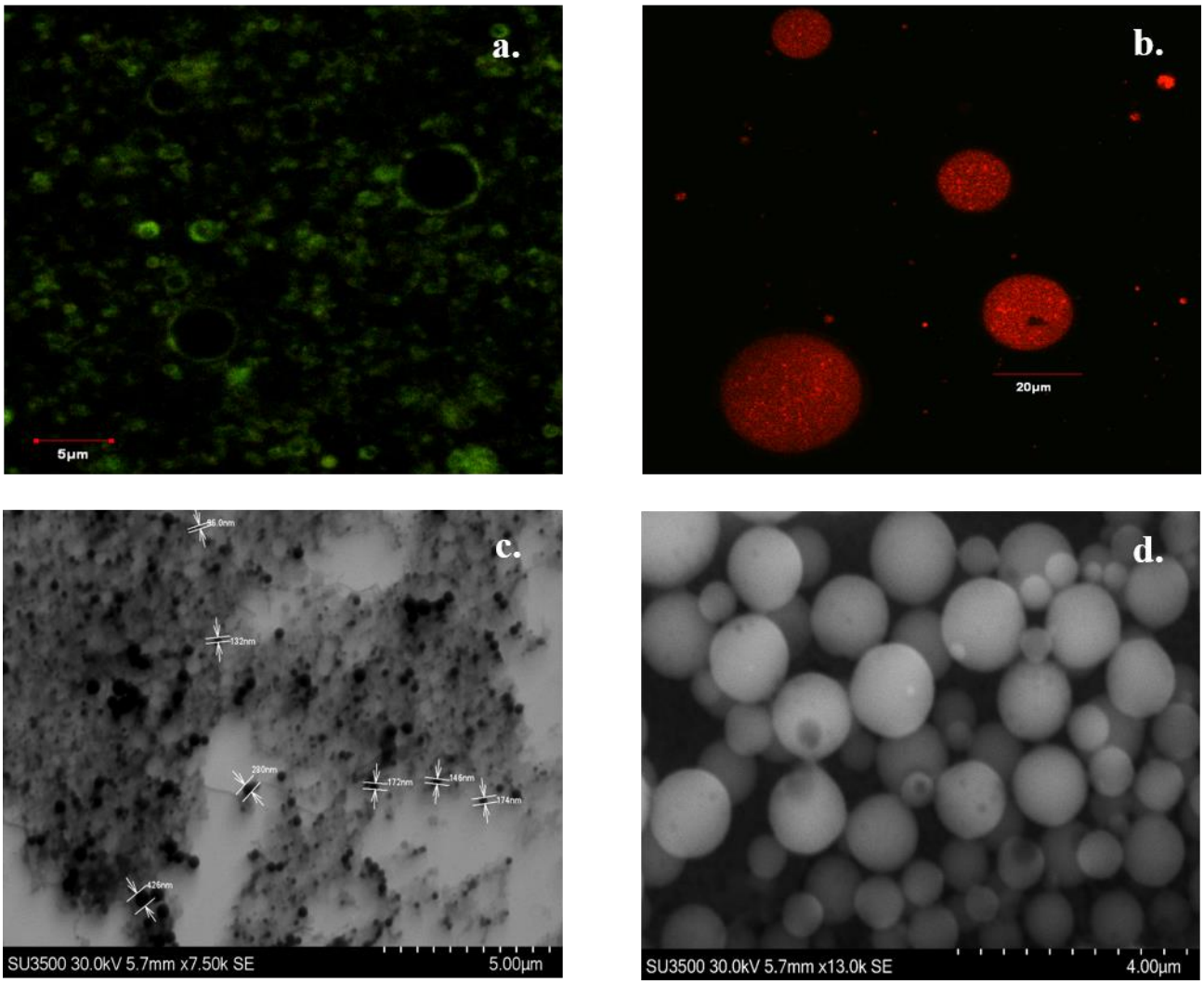

Fig. 3.3. Morphology of LF–loaded RP liposomes. (a–b) Confocal laser scanning microscopy images. (c–d) Scanning transmission electron microscopy images.

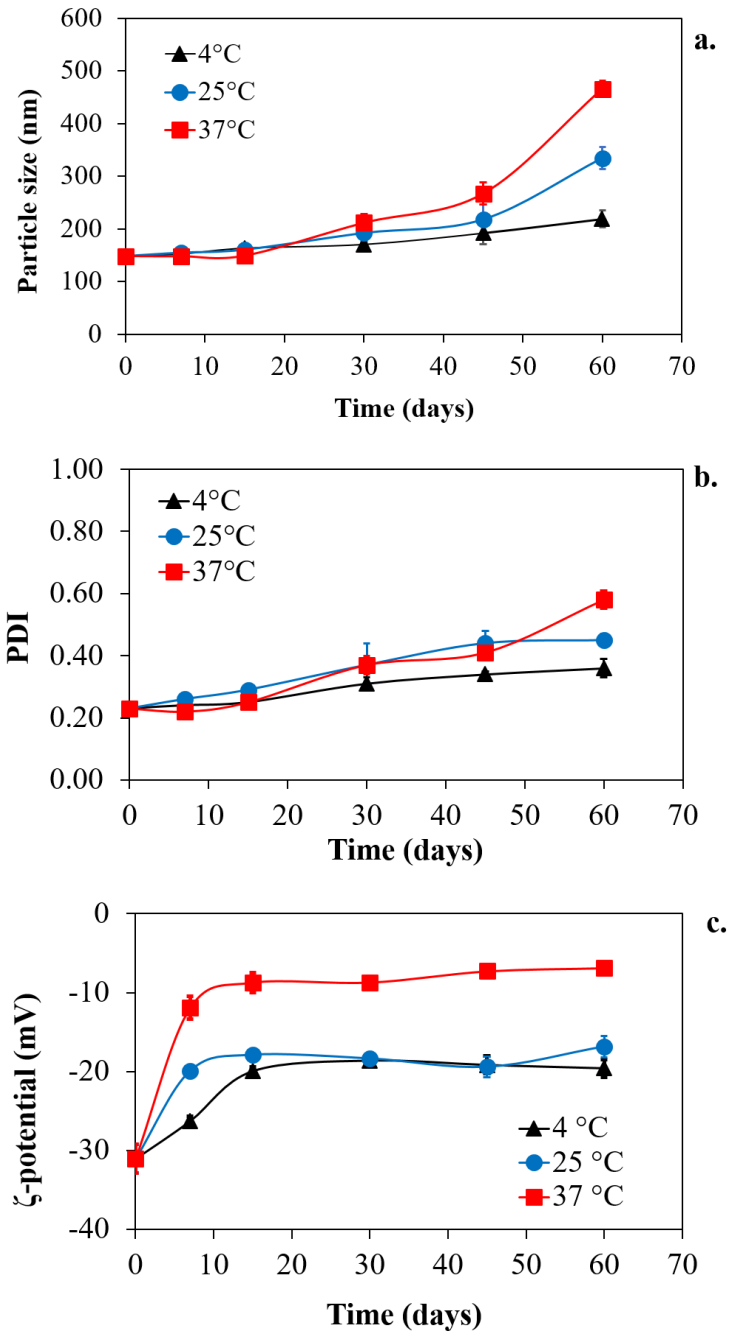

Fig. 3.4. Physical stability of LF–loaded RP liposomes under different storage temperatures (4, 25, and 37 °C). (a) Particle size, (b) polydispersity index (PDI), and (c) ζ–potential.

Fig. 3.5. Visual appearance of LF–loaded RP liposome stored under different temperatures (4, 25 and 37 °C). (a) Initial, (b) after 30 days, and (c) after 60 days.

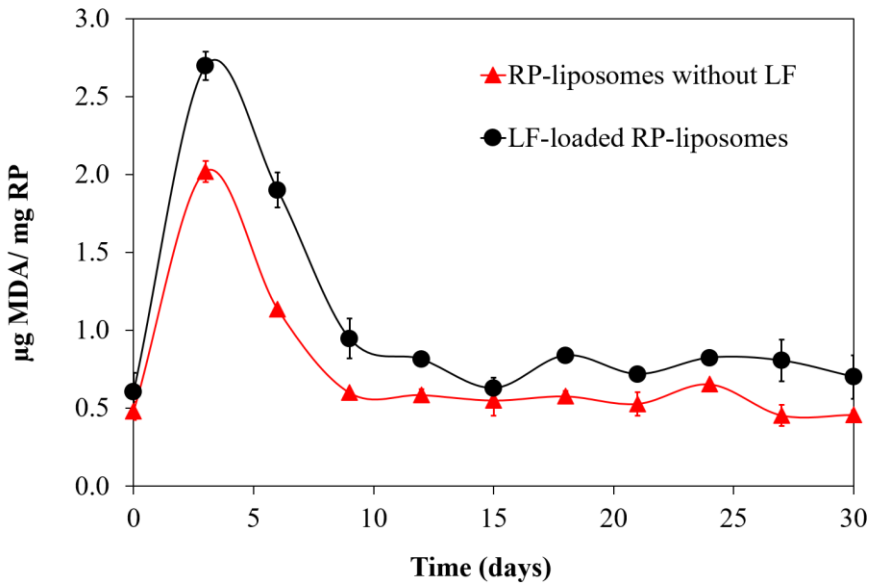

Fig. 3.6. Comparison of the content of secondary oxidation products, TBARS, during storage at 60 °C of RP liposomes with or without LF.

CHAPTER IV

Food Chemistry
DOI: 10.1016/j.foodchem.2020.126717

An in vitro digestion study of encapsulated lactoferrin in rapeseed phospholipid–based liposomes

Daniela Vergara[a,b*], Olga López[d], Mariela Bustamante[b], Carolina Shene[b,c]

[a] Doctoral Program in Sciences of Natural Resources, Universidad de La Frontera, Ave. Francisco Salazar 01145, Box 54–D, Temuco, Chile.

[b] Center of Food Biotechnology and Bioseparations, Scientific and Technological Bioresource Nucleus (BIOREN), Centre for Biotechnology and Bioengineering (CeBiB). Universidad de La Frontera, Ave. Francisco Salazar 01145, Box 54–D, Temuco, Chile.

[c] Department of Chemical Engineering, Universidad de La Frontera, Ave. Francisco Salazar 01145, Box 54–D, Temuco, Chile.

[d] Department of Chemical and Surfactant Technology, Institute of Advanced Chemistry of Catalonia (IQAC–CSIC), C/Jordi Girona 18–26, 08034, Barcelona, Spain.

Associated to specific objective 2.

An *in vitro* digestion study of encapsulated lactoferrin in rapeseed phospholipid–based liposomes

4.1 Abstract

Effectiveness of liposomes elaborated with rapeseed phospholipid (RP) extracted from a residue of oil processing, stigmasterol (ST) and/or hydrogenated phosphatidylcholine (HPC) for the encapsulation lactoferrin (LF) was studied; lipid membrane of liposomes was characterized (bilayer size, chain conformational order, lateral packing, lipid phase, and morphology) and the protection offered to the encapsulated LF during *in vitro* digestion was determined. Liposomes composed of RP+ST$^{LC\ (low\ concentration)}$ showed spherical and irregular vesicles without perforations. Lamellar structure was organized in a liquid–ordered phase with a potential orthorhombic packing. Stability and size of the liposomes were more affected by gastric digestion than intestinal digestion; 67–80% of the initially encapsulated LF remained intact after gastric digestion whereas the percentage was reduced to 16–35% after intestinal digestion. Our results shows that liposomes elaborated with RP, properly combined with other lipids, can be a useful oral delivery system of molecules sensitive to digestive enzymes.

Keywords: Rapeseed phospholipids, liposomes, lactoferrin, digestion, delivery system.

4.2 Introduction

Lactoferrin (LF) is a natural iron–binding glycoprotein (molecular weight ~78–80 kDa, ~700 amino acids), mainly present in milk and also secreted through fluids of mammals. LF not only participates in the transport of iron but is also a prebiotic protein with a wide range of physiological functions; it is considered an important defense molecule because of its antibacterial and antifungal activity (Iglesias–Figueroa et al., 2019). However, oral delivery of LF decreases most of its functions due to enzymatic degradation in the gastrointestinal tract, resulting in less than 1% absolute oral LF bioavailability levels (Troost et al., 2002), hindering its potential benefits. LF degradation has led the research of new forms of protection, with the aim of decreasing its hydrolysis after oral administration (Yao et al., 2015).

Encapsulation is a powerful tool for overcoming the aforementioned drawbacks. Encapsulation offers immobilization, protection against environmental factors (light, temperature, pH, moisture, and oxygen), controlled release, structure, and functionalization for sensitive compounds, increasing their bioavailability (Jafari & McClements, 2017). Recent studies in the food and nutrition have considered the utilization of liposomes to encapsulate and control the release of bioactive components, such as antioxidants, fatty acids, and proteins (Gibis et al., 2016; Vélez et al., 2017; Liu et al., 2013). Liposomes are small and spherical vesicles (20 nm to 2 µm in size), formed by hydrophilic–hydrophobic interactions that occur between phospholipids, cholesterol, and water molecules (Zhang et al., 2019a). Cholesterol is an important component of liposome membranes; in cell membranes cholesterol reduces the rotational freedom of the phospholipid hydrocarbon chains, stabilizes the lipid bilayer, and helps to decrease the loss of hydrophilic materials (Kaddaha et al., 2018) especially in fluid lipid membranes. Jovanović et al. (2018)

established that plant cholesterol or phytosterols (β–sitosterol, stigmasterol, and campesterol) not only act as stabilizers in liposomal membranes, but also as antioxidants, enhancing the protection role of liposomes

Liposomes can be manufactured using phospholipids extracted from plant raw materials, which allows an easy and fast implementation in food systems, surpassing the established regulatory barriers (Sun et al., 2018). Phospholipids from plant sources, for example of rapeseed, can be found as a by–product of the oil refining process. Recently, we showed that RP can be used for developing LF–loaded liposomes with a high encapsulation efficiency (EE, ~90 %) in small particles (<200 nm) (Vergara & Shene, 2019).

For the successful use of LF–loaded into RP based liposomes as a food ingredient, not only optimal processing conditions need to be determined but evidence of the protection offered to LF after its consumption has to be demonstrated. It has been shown that LF–loaded liposomes prepared with milk derived phospholipids, may prevent gastric degradation of LF and reduce the rate of hydrolysis of LF under intestinal conditions (Liu et al., 2013). Niu et al. (2019) reported that encapsulation of LF does not compromise its antimicrobial bioactivity. To our knowledge, the fate of LF encapsulated in RP liposomes during *in vitro* gastrointestinal digestion, which is important for the effective use of liposomes, has not been determined.

Recently, we have carried out a detailed characterization of RP and RP liposomes (chemical composition, physical stability, appearance, and storage effects among other); in addition, conditions that maximize LF encapsulation efficiency (EE) were determined (Vergara & Shene, 2019). Thus, to extend our previous work the aims of the present study were (1) to characterize the lipid membrane of RP liposomes, (2) to evaluate the protection offered to LF encapsulate in different formulations of RP liposomes during *in vitro*

digestion, and (3) to determinate the lipid composition of RP liposomes to achieve the best protection of LF during *in vitro* digestion. These results could contribute for the development of an effective system for the oral delivery of LF that could be used in nutraceutical and functional products.

4.3 Materials and methods

4.3.1 Materials

Rapeseed oil was obtained from the residue left after cold pressing process carried out by OleoTop S.A. (Freire, Araucania Region, Chile). Rapeseed phospholipids (RP) were extracted following the methodology described in our previous study (Vergara & Shene 2019). Stigmasterol (ST) was purchased from Sigma–Aldrich (St. Louis, MO, USA). Hydrogenated soy phosphatidylcholine (HPC) (Phospholipon® 90H) was supplied from Lipoid GmbH (Ludwigshafen, Germany). Lactoferrin was purchased from Jarrow Formulas, (Los Angeles, California, USA). Pepsin from porcine gastric mucosa (enzymatic activity of 3,200–4,500 U/mg protein) pancreatin from porcine pancreas (4 × United States Pharmacopeial (USP) specifications) and bile bovine were purchased from Sigma–Aldrich (St. Louis, MO, USA). All chemicals and solvents used were of analytical or HPLC grade.

4.3.3 Preparation of liposomes

Liposomes with the different compositions defined in Table 4.1 were prepared by the thin–layer dispersion method. The optimal formulation, based on the desirable quality attributes (high EE and small particle size) described previously (Vergara & Shene, 2019) was used as a starting point. Briefly, RP (10.20 mg/mL) and ST (2.20 mg/L, cholesterol of plant origin) dissolved in chloroform (2 mL) were placed into a round–bottom flask. The

solvent was removed in a rotary evaporator (Buchi R–100, Flawil, Switzerland) at 40 °C; a thin lipid film was formed on the flask walls. To ensure the complete removal of the dissolvent from the film, the round–bottom flask was left overnight inside a vacuum desiccator. Then, the dried lipid film was rehydrated with phosphate buffer (pH 7.4, 0.01 M), containing LF at 1 mg/mL and subjected to sonication using a bath sonicator Ultrasons H–D (P–Selecta, Barcelona, Spain) during 4 min. For liposomal membrane characterization liposomes were prepared without LF. Finally, liposomal formulations were maintained 24 h at room temperature to ensure hydration. This formulation was named RP+ST$^{low\ concentration\ (LC)}$.

4.3.3 Characterization of the structure of RP+ST^{LC} liposomes

To evaluate the physicochemical characteristics of the RP+ST^{LC} liposomes and the effect of enzymatic digestion on the vesicular structure, several techniques were used.

4.3.3.1 Small angle X–ray scattering (SAXS)

SAXS measurements of the RP+ST^{LC} liposomes were carried out using a S3–MICRO (Hecus X–ray systems GMBH Graz, Austria) coupled to a GeniX Cu high flux source (Xenocs, Grenoble). X–ray radiation with a wavelength corresponding to a Cu–Kα source (1.542 Å) was used. Transmitted scattering was detected using a PSD 50 (Hecus; Graz, Austria), and the temperature was controlled by means of a Peltier TCCS–3 (Hecus GmbH; Graz, Austria). The sample was inserted in a flow–through glass capillary (Hilgenberg GmbH; Malsfeld, Germany) with a 1 mm diameter and 10 mm wall thickness. The scattering intensity I (in arbitrary units) was measured as a function of the scattering vector Q (in reciprocal Å) defined through:

$$Q = (4\pi \sin\theta)/\lambda \quad \text{(Eq. 1)}$$

Where θ is the scattering angle and λ is the wavelength of the radiation (1.542 Å). The position of the scattering peaks is directly related to repeat distance of the molecular structure, as described by Bragg's law (Bragg, 1913):

$$2d \sin\theta = n\lambda \quad \text{(Eq. 2)}$$

Where *n* and *d* represent the order of the diffraction peak and repeat distance, respectively. In a lamellar structure, the various peaks are located at equidistant positions; the position of the n^{th} order reflection, Qn is given by:

$$Qn = 2\pi n/d \quad \text{(Eq. 3)}$$

4.3.3.2 Differential scanning calorimetry (DSC)

DSC measurements were performed using a calorimeter (Mettler Toledo 821E, Greifensee, Switzerland). Samples were concentrated by centrifugation at 9,000 × g for 10 min to increase the signal intensity. Aliquots of ~10 µL were placed inside aluminum DSC pans and sealed hermetically. The scan rates for heating and cooling were 5 °C/min and −5 °C/min, respectively, over a temperature range from –60 to +60 °C. The DSC curves were analyzed by the STARe SW 9.30 Software (Mettler Toledo, Greifensee, Switzerland). The curve shown in result section correspond to the second heating scan.

4.3.3.3 Cryogenic transmission electron microscopy (cryo–TEM)

The morphology of the RP+ST^{LC} liposomes was evaluated by cryo–TEM. Samples (~3 µL) were applied on a holey carbon grid. The blotted grids were plunged into liquid ethane cooled with liquid nitrogen using a Vitrobot (FEI Company, Eindhoven, The Netherlands).

The vitreous sample film was transferred to a Tecnai F20 TEM (FEI Company, Eindhoven, The Netherlands) microscope using a cryotransfer holder (Gatan, Pleasanton, USA). Images were acquired at 200 kV at a temperature between 170 ºC and 175 ºC, under low–dose imaging conditions. Images were recorded with a CCD Eagle camera (FEI, Eindhoven, The Netherlands) and processed with Xplore3D software (FEI Eindhoven, The Netherlands).

2.4. In vitro digestion of liposomes

4.3.4.1 Stability of liposomes under gastric and intestinal digestion

The simulated gastric fluid was prepared by dissolving NaCl (2 g) and HCl (7 mL) in 1 L of deionized water. Composition of the simulated intestinal fluid was K_2HPO_4 6.8 g/L, NaOH 190 mL of 0.2 M solution/L, NaCl 150 mM, $CaCl_2$ 30 mM, and bile extract 0.1 g/L in deionized water.

RP+ST^{LC} liposomes were incubated separately in gastric fluid, intestinal fluid, gastric fluid + pepsin (defined as, *gastric digestion*), and intestinal fluid + pancreatin (defined as, *intestinal digestion*), according to the methodology described by Liu et al. (2013). Pepsin 57 ng/mL, and pancreatin 0.015 mg/mL at a 2:1 v/v ratio (3 mL total) were used. The pH of the samples in the simulated gastric and intestinal fluids were adjusted to 1.5 and 7.4 respectively; 0.05 M NaOH or 1 M HCl were used as needed. The mixtures were incubated with agitation (30 rpm) (Unitronic 320 P–Selecta, Barcelona, Spain) during 120 min, at 37 °C (Minekus et al., 2014); 200 µL of the sample were taken for analysis after 1, 30, and 120 min. Particle size, polydispersity index (PDI), and ζ–potential of RP+ST^{LC} liposomes in the gastric and intestinal fluid, and during gastric and intestinal digestion were followed in

time, using a Zetasizer Nano ZS (series HT, Malvern Instrument, U.K.) at 25 °C; measurement conditions were defined according to Zhang et al. (2019b).

4.3.4.2 Enzymatic digestion of LF–loaded into different liposome formulations

The different formulations subjected to *in vitro* gastrointestinal digestion (Table 4.1) were: (1) RP+ST^{LC}; (2) liposomes in which RP and ST concentrations were 2.5–fold higher (named as RP+ST), (3) liposomes in which ST was replaced by hydrogenated phosphatidylcholine (HPC) (named as RP+HPC), and (4) liposomes in which the mass ratio of RP: HPC: ST was 70:20:10 (named as RP+HPC+ST). The digestion of free LF and LF–loaded into RP+ST^{LC}, RP+ST, RP+HPC, and RP+HPC+ST liposomes was carried as described in section 2.4.1. Digested samples were placed in vials, where the enzymes were inactivated with SDS–PAGE loading buffer (62.5 mM Tris–HCl pH 6.8, 20% glycerol, 2% SDS, 0.1% bromophenol blue and 5% β–mercaptoethanol) added in a volume ratio of 2:1 v/v. The mixtures were stored at –20 ºC until loading onto the SDS–PAGE gel.

4.3.4.3. Protein hydrolysis kinetics by SDS–PAGE

To determine the hydrolysis degree of the encapsulated LF incubated with the gastric and intestinal fluid, and after gastric and intestinal digestion, the quantity of not hydrolyzed LF was determined by SDS–PAGE using a 15% w/w polyacrylamide gel as described by Laemmli (1970). The gels were run in a Mini–Protean Tetra System (BioRad, USA) at 130 V using a Bio–Rad power supply unit PowerPac™ (BioRad, USA). Gels were stained (1.25 g/L Coomassie Blue R–250 in ethanol: glacial acetic acid: water at 52: 10: 38 v/v/v) for 120 min and then distained (ethanol: glacial acetic acid: water at 26: 0.8: 73.2 v/v/v). PageRuler™ Unstained Protein Ladder (Thermo Scientific; 10 to 250 kDa) was used as

molecular weight marker. Gel images were acquired using a RICOH MP–C3003 Photo Scanner. The relative percentages of LF in the samples (compared with the LF standard) was quantified using ImageJ 1.50i (NIH, USA) software.

4.3.4.4 Lipolysis of LF–loaded liposomes

In vitro lipid digestion was monitored as described by De Figueiredo et al. (2018). RP+ST^{LC}, RP+ST, RP+HPC, and RP+HPC+ST liposomes all of them loaded with LF, and liposomes without LF (2 mL) were mixed with 5 mL of intestinal fluid and the pH was adjusted to 7.4. Lipolysis of phospholipids was determined by the pH–stat titration technique after the addition of pancreatin (0.015 mg/mL). Briefly, the pH was maintained at 7.4 (Orion Star^{TM} A211, Thermo–Scientific) through the addition of 0.05 M NaOH, under continuous magnetic stirring (100 rpm at 37 ºC). The volume of NaOH added was used to calculate the concentration of free fatty acids (FFAs) released using:

$$\boldsymbol{FFA}\ (\boldsymbol{mM}) = (V_{NaOH\ t} - V_{NaOH\ to})\ x\ M_{NaOH}\ x\ 1000 \qquad \text{(Eq. 4)}$$

Where: $V_{NaOH\ t}$ is the volume (L) of NaOH required to titrate the FFAs produced after 30 min, $V_{NaOH\ t0}$ is the volume (L) of NaOH added at the beginning of the reaction, and M_{NaOH} is the molarity (M) of the NaOH solution.

4.3.5 Data analysis

All measurements were repeated at least three times. The results were evaluated statistically for significance ($P<0.05$) using ANOVA and the Tukey means comparison test Minitab® software version 18 (State College, PA, USA) was used. All data were expressed as means ± standard deviations.

4.4 Results and discussion

4.4.1 Characterization of the RP+ST^{LC} liposomes

4.4.1.1 X–ray scattering

SAXS method was applied to gain insight into the structural organization of RP+ST^{LC} liposomes. SAXS provides information on the larger structural units of a given sample. In our case, the lamellar repeat distance (*d–spacing*) was estimated from analysis of the peaks using Bragg's law and was attributed to the thickness of the liposomes bilayer. Results are shown in Fig. 4.1a. One broad reflection was observed, at a *q* around 0.10 Å^{-1}, corresponding to a *d* value around 63 nm, which was attributed to the thickness of the lipid bilayer. In addition, SAXS may also be used to provide an indication of the lamellarity of a liposome population (Kiselev & Lombardo, 2017). Shape of the SAXS patterns, was very broad and with only one symmetric peak which does not show other reflections, this can be associated with unilamellar liposomes (Rodríguez et al., 2012). In general, SAXS from multilamellar liposomes exhibit first and second order diffraction peaks at regular intervals that is 1/*d*; 2/*d*, etc. (Andrade et al., 2018).

Wide angle X–ray scattering (WAXS) provides information about the scattered intensity at angles wider than SAXS. Thus, information on smaller structural units in the sample, such as lateral packing in the lamellar phase can be acquired. Fig. 4.1b shows WAXS profile for RP+ST^{LC} liposomes. Two possible reflections were observed at 1.50 Å^{-1} and 1.70 Å^{-1}. This reflection could correspond to Bragg distances at approximately 4.2 and 3.7 nm, respectively. It is known that lipids are able to exhibit different lateral symmetry that give rise to determine *d*–spacing in WAXS profile. This lateral packing can be orthorhombic (*d*–spacing at 41 and 37 nm), hexagonal (41 nm), or liquid–disordered (46 nm) (Rodríguez et al., 2012). WAXS pattern on Fig. 4.1b shows *d*–spacing that could be

ascribed to an orthorhombic organization. In our case, the complex composition of the phospholipids (RP) (Vergara & Shene, 2019) used for liposomes preparation, related to extension of the alkyl chain and presence of unsaturations, could alter both the tendency for monolayer curvature, and the packing stresses within the system (Gupta et al., 2019).

4.4.1.2 Differential scanning calorimetry (DSC)

DSC analysis was performed to determine the liquid–crystalline phase transition temperature (T_m) of the lipid phase in RP+ST^{LC} liposomes. Phospholipids forming bilayers have a specific T_m depending on the length and saturation degree of the alkyl chain. When temperature exceeds T_m, the gel to liquid–crystalline phase transition occurs, and lipid membranes experience some physicochemical changes (Romero–Arrieta et al., 2019). In the calorimetric study, both cooling and heating curves were determined for the RP+ST^{LC} liposomes (Fig. 4.1c). No peaks associated with a main lipid transition were observed in the temperature range studied (–60 to +60 °C); the peak at approximately 5 °C corresponded to ice melting. Thus, we assumed that the main transition was suppressed in the system studied. This suppression could be related with the inclusion of ST (and other sterols) in phospholipid membranes. Rodríguez et al. (2012) working with membranes elaborated with 2–dimyristoyl–sn–glycero–3–phosphocholine (DMPC) and cholesterol sulphate (SCHOL) reported the formation of an extra lamellar phase, "the liquid–ordered phase", with characteristics between solid ordered (gel) and liquid disordered phases. A similar phenomenon was described by Neunert et al. (2018) that incorporated α–tocopherol in 1,2–dipalmitoyl–sn–glycero–3–phosphocholine (DPPC) liposomes. To evaluate the possible effect of ST, and for comparison purposes, DSC analysis of RP liposomes without the inclusion of ST was determined. Heating thermogram, shown in Fig. 4.1d did not show

peaks related with T_m it could not be discarded the effect of endogenous α– γ– and δ–tocopherols content of RP (77.67 mg/100 g) (Vergara & Shene, 2019), on the order–disorder of the bilayer and decreasing the enthalpy of the main transition. Therefore the presence of this phase would not imply significant conformational changes; these results were as expected on the basis of the origin of the phospholipid fractions used.

4.4.1.3 Cryogenic transmission electron microscopy (cryo–TEM)

The microstructure of the RP+ST^{LC} liposomes was observed using cryo–TEM; images are shown in Fig. 4.1e–f. In general, images showed unilamellar vesicles, which is highly consistent with the SAXS results. The cryo–TEM analysis revealed nano–sized vesicles with diameters lower than 200 nm. In addition, vesicular shaped structures as well as, irregulars, cochleates, or elongated lipid assemblies were observed (Fig. 4.1e); these are usually made of negatively charged phospholipids and cations. The formation of these structures would be due to the different distribution of the RP in the different aggregates (Rahnfeld et al., 2018). Fig. 4.1f shows liposomes in close contact (see arrow) that are deformed at the contact area. This could indicate a "flaccid" membrane character with domains of low rigidity given by lipid irregular distribution in the liposomal structure. In addition, according to the WAXS and DSC results that suggest an orthorhombic structure and a liquid–ordered phase respectively, the distribution of phospholipids and sterols in domains of different stiffness is also evidenced. One important result of the morphological analysis is the absence of irregularities such as perforations and/or breakages, in the bilayer membranes of the vesicles.

4.4.2 Physicochemical stability of RP+ST^{LC} liposomes during in vitro digestion

RP+ST^{LC} liposomes were incubated separately in gastric fluid, intestinal fluid, gastric fluid + pepsin (*gastric digestion*), and intestinal fluid + pancreatin (*intestinal digestion*) respectively. Physicochemical behavior (particle size, PDI, and ζ–potential) was followed as a function of time (0–120 min). These experiments were carried out to check the effectiveness and stability of the lipid membrane of liposomes not loaded with LF under gastrointestinal conditions. Results showed that particle size of the liposomes increased during *in vitro* digestion (Fig. 4.2a–f); average particle size of RP+ST^{LC} liposomes (291.47 ± 4.63 nm) increased 1.4–fold after the incubation with the gastric fluid, and 1.7–fold after gastric digestion. For the intestinal conditions, the average particle size of RP+ST^{LC} liposomes (initially equal to 312.03 ± 2.29 nm) increased 1.3–fold after the incubation with the intestinal fluid, and 1.4–fold after intestinal digestion. The changes in particle size of liposomes correlated with changes in PDI values. ζ–potential of RP+ST^{LC} liposomes increased from –8.07 ± 2.02 mV to –1.96 ± 0.98 mV after the incubation in the gastric fluid; and to –2.50 ± 0.56 after gastric digestion. Non–significant differences were observed in the changes of ζ–potential of the RP+ST^{LC} liposomes exposed to intestinal conditions; average initial value was –10.70 ± 1.21 mV that decreased to –11.19 ± 1.99 mV after the incubation in the intestinal fluid and to –11.48 ± 0.18 mV after intestinal digestion.

The observed increase in the average particle size of RP+ST^{LC} liposomes during digestive conditions suggests possible vesicle aggregation or fusion. This fact could be due to the important decrease in pH from neutral (pH 7.4 liposomal formulation) to strongly acid (pH 1.5) during gastric phase; changes in the pH modify the strength and range of colloidal interaction between particles, allowing liposome coalescence. Additionally, an osmotic effect due to the pH gradient (inside – outside the vesicles) could promote

destabilization and fusion. The increase in the average particle size of RP+ST^{LC} liposomes is in accordance with the results reported by Machado et al. (2019) for liposomes elaborated with rice and soybean phospholipids for the encapsulation of phenolic extracts. However, Liu et al. (2013) reported that during *in vitro* gastrointestinal digestion of LF–loaded liposomes, prepared with milk fat globule membrane phospholipids, particle size decreased. So, the structure of different liposomal systems would present a different behavior due to the different conditions (pH and temperature) of digestion process. Studies carried out to solubilize liposomes with bile salts and other surfactants, reported an initial increase in size followed by a decrease (López et al., 1998). Then, foreseeable variations in size are certainly expected.

The electronegative ζ–potential value registered in the initial formulations is due to phosphate groups (PO_4^{3-}) in phospholipids (Liu et al., 2013). In addition, the presence of impurities in RP, such as FFA and amino acids, might also contribute to the electronegative ζ–potential of liposomal formulations (McClements, 2016). A high absolute value (higher +/– 30 mV) of ζ–potential indicates that liposomes are more electrically and physically stable. In our case, the low absolute values obtained suggest low stability of the liposomal formulation. In addition, the ζ–potential value under intestinal digestion could be attributed to the presence of the different anionic particles in the intestinal fluids (such as bile salts) or due to lipid digestion products, such as FFAs. Additionally, lysophospholipids in RP or those originated in phospholipid lipolysis, have a charge more negative than the parent lipids, which would also increase the negative charge of the liposomes (Zhang et al., 2019a). Overall, physicochemical results indicated that the integrity and stability of RP+ST^{LC} liposomes was more affected by gastric digestion than by intestinal digestion, however in both digestions vesicular structures persisted.

4.4.3 Stability of encapsulated LF during in vitro digestion of LF–loaded in different liposomal formulations

The SDS–PAGE was used to evaluate the hydrolysis of LF, free and encapsulated into RP+ST^{LC}, RP+ST, RP+HPC, and RP+HPC+ST liposomes during *in vitro* gastrointestinal digestion. LF–loaded into RP+ST^{LC} liposomes was almost completely degraded under gastric digestion; only 20.48 ± 3.57% of the initial LF remained after 120 min of digestion (Table 4.2). Taking into account the "liquid–ordered phase" of the of RP+ST^{LC} liposomes membrane, a saturated phospholipid (HPC) was used in the liposome formulation to increase the rigidity and stability of the liposomal membrane.

Fig. 4.3a–b shows compares the intensity of the protein bands of LF standard and liposome samples after gastric and intestinal digestion (0–120 min) separated by SDS–PAGE. LF standard showed one strong band near 78–80 kDa, and some minor bands visible around 55, 35, and 15 kDa, which might be residual proteins remaining from the protein purification. The relative percentages of LF in the samples (compared with the standard LF) are summarized in Table 4.2. Free LF was totally hydrolyzed after 120 min of gastric digestion. LF in RP+ST^{LC}, RP+ST, RP+HPC, and RP+HPC+ST liposomes decreased gradually under gastric digestion as time increases (0 to 120 min) (Fig. 4.3a). After 120 min of gastric digestion the percentage of residual LF in RP+ST (67.49 ± 1.79%), RP+HPC (79.98 ± 1.82%), and RP+HPC+ST (69.99 ± 0.99%) liposomes was significantly ($P<0.05$) higher than in RP+ST^{LC} liposomes (20.48 ± 3.57%). During intestinal digestion of free LF, hydrolysis occurred mainly during the first seconds (Table 4.2). Pancreatin and bile salts were responsible of the significant solubilization of the liposomal membrane and reduced amounts of LF remained in RP+ST^{LC} (10.88 ± 0.60%), RP+ST (34.80 ± 0.65%), RP+HPC (32.19 ± 1.87%), and RP+HPC+ST (15.85 ± 1.56%) liposomes, after 120 min of

digestion. Nevertheless, LF encapsulated in RP+ST and RP+HPC liposomes resisted the hydrolysis better than free LF (10.18 ± 1.10%).

The improved performance exhibited by the new liposomal formulations, especially RP+HPC liposomes, under gastric digestion could be related to the encapsulation and the load capacity of the vesicles. Under gastric conditions LF would be positively charged whereas the liposomes would be negatively charged, suggesting that unloaded LF could cover the liposomes surface by electrostatic interactions (Liu et al., 2017). The comparison of results obtained with RP+ST^{LC} and RP+ST suggests that increasing the concentration of phospholipids in liposomal formulations increases the percentage of LF effectively encapsulated, delaying the protein hydrolysis by pepsin. During the intestinal digestion, the presence of bile salts, phospholipids free or hydrolyzed, and fatty acids may form mixed micelles or different complexes protecting LF from hydrolysis. The composition of the liposomal wall is another factor that can significantly influence the behavior of liposomes during digestion. Liu et al. (2017) determined that the addition of cholesterol in phospholipid bilayers improves the stability of liposomal membranes under *in vitro* gastrointestinal conditions. However, our results using ST (a plant cholesterol) are not superior to those obtained incorporating HPC into the liposome formulation. Maherani et al. (2013) established that liposomes prepared with lipids having low T_m values exhibited a greater permeability. Therefore, lipids with higher T_m such as HPC (T_m ~55 °C) used in our formulations can form more stable and less permeable liposomes, preventing the hydrolysis of LF. One characteristic of RP is the high percentage of unsaturated fatty acids; percentages of oleic (C18:1), linoleic (C18:2), and α–linolenic (C18:3) acid are 55.02 ± 0.06%, 27.97 ± 0.07%, and 6.26 ± 0.01%, respectively (Vergara & Shene, 2019). Maherani et al. (2013) reported that the increase of unsaturation in the lipids of the liposomal bilayer

increases the fluidity of the liposomal membrane. However, unsaturated fatty acids would make artificial membrane more permeable. This would explain the better results obtained with liposomes formulations containing HPC (mixture that has 85% of 1,2–distearoyl–sn–glycero–3–phosphocholine (18:0 DSPC) and 15% of 1–palmitoyl–2–stearoyl–3–phosphocholine (16:0 PSPC).

LF free and loaded into RP+ST^{LC}, RP+ST, RP+HPC, or RP+HPC+ST liposomes incubated in gastric or intestinal fluid showed a lower initial percentage of LF compared with LF standard (which corresponds to 100%). This loss could be due to two factors, (1) the action of non–enzymatic components of the gastric or intestinal fluid (pH 1.5 and 7.4, respectively) on the protein and/or (2) the conditions used in the elaboration of LF–loaded liposomes such as, temperature and sonication. In the case of RP+ST^{LC} liposomes incubated in the intestinal fluid, LF percentage was lower than in free LF. This could be due to the molar relation between bile extract and phospholipids used. By increasing the bile salt concentration, the vesicles become saturated with bile salt molecules and bile salt partitioning to phospholipid membrane occurred. Kokkona et al. (2000) observed that at a higher molar ratio of bile extract: phospholipids liposomes were more unstable releasing 100% of the encapsulated compound. In our study, the non–encapsulated LF could surround the liposomal membrane affecting the digestion rate of the liposomes by pancreatin through competitive absorption process (Meshulam & Lesmes, 2014).

During the *in vivo* digestion, hydrolysis and absorption of nutrients in the small intestine occurs simultaneously. Destabilization of the liposomal membrane is necessary for that the released LF can reach the intestinal mucosa and be taken up by enterocytes. In addition, it is well known that the mean residence time of a formulation administered orally is well over 120 min in the small intestine (Boland, 2016). Therefore, it is important to obtain

percentages of intact LF higher than 30% after 120 min under intestinal digestion. The non–gradual reduction of the percentage of LF remaining under intestinal digestion in RP+ST and RP+HPC liposomes is attributable to the condition of the digestion assay. The presence of diffuse bands as well as, the interference caused by the intestinal fluid, which generates precipitates could affect the homogeneous sampling. After 120 min under intestinal digestion, the system was found to be more homogenous due to the agitation and temperature (100 rpm, 37 °C) therefore, the generated band is sharper.

Our results shows that RP+HPC liposomes can be very useful systems for the oral delivery of LF, because nearly 80% of the LF remained intact after 120 min of gastric digestion. This result is compared with the less than 1% absolute oral bioavailability of free LF reported by Troost et al. (2002).

4.4.4 In vitro lipid digestion under intestinal digestion

Pancreatin lipolysis of phospholipids in RP+ST^{LC}, RP+ST, RP+HPC, and RP+HPC+ST liposomes under intestinal digestion was quantified indirectly measuring the concentration of released FFAs (Fig. 4.4). Loaded LF had a significant effect on the amount of FFAs released from RP+ST and RP+HPC+ST liposomes ($P<0.05$). On the contrary, the effect of loaded LF on the FFAs released from RP+ST^{LC} and RP+HPC liposomes was not significant ($P>0.05$). The release of FFAs confirmed the destruction of phospholipids that compose the liposome structure. The concentration of FFAs released increased rapidly in all formulations during the first 30 min of intestinal digestion, without reaching the maximum value in this time interval.

Our results indicate that LF facilitated the release of FFAs in RP+ST and RP+HPC+ST liposomes (Fig. 4.4b–d). Similar results were observed by Liu et al. (2017) who found that

in liposomes composed of L–α–phosphatidylcholine and cholesterol LF facilitated the release of FFAs and increased the microfluidity of the bilayers, reducing the structural integrity. These findings concurred with the observation made by Sarkar et al. (2010) who showed that LF–stabilized in oil–in–water emulsions (soy oil) was more susceptible than other emulsions to lipolysis by pancreatic lipase. This effect can be attributed to polymers such as LF that could form a broad network allowing the localization of bile salts at the phospholipid bilayers interface increasing the fluidity of the membrane (Wilde & Chu, 2011). Bile salts at the interface would increase lipase adsorption damaging the structural organization of liposomes. It is noted that pancreatin is not only source of intestinal lipase but it also contains protease, trypsin, ribonuclease, and amylase activity. Therefore, while lipase would be responsible of phospholipids hydrolysis, proteases would hydrolyze LF. At pH close to 7, protons are released during protein hydrolysis by proteases decreasing the pH. On the other hand, in RP+ST and RP+HPC+ST liposomes without LF (Fig. 4.4b–d), the FFAs release was slower and lower after 30 min of digestion. The increase of the concentrations of RP, HPC, and ST would increase the viscosity of the medium decreasing the movement of the lipase molecules towards the surface of the liposomes. An increase in the number of total liposomal particles could lead to a higher lipid surface available for the enzyme adsorption will decrease the rate of lipolysis in the bilayer, since the amount of enzyme is the same for the liposomal formulation with low (RP+ST^{LC}) and high (RP+ST, RP+HPC, and RP+HPC+ST) lipid concentration. For RP+ST^{LC} liposomes (Fig. 4.4a) the results obtained (0.05 ± 0.01 mM with LF and 0.04 ± 0.01 mM without LF) presented non–significant differences; this was explained by the low lipid concentration.

The high percentage of unsaturated fatty acids in RP could also be responsible for the fast hydrolysis rate of liposomes during the first 30 min of intestinal digestion. In general,

the fatty acid composition and the type of phospholipids play an important role in lipid hydrolysis. For instance, phosphatidylserine and phosphatidylinositol are more susceptible to lipase hydrolysis than phosphatidylcholine and phosphatidylethanolamine (Liu et al., 2019). This could explain the behavior exhibited by RP+HPC liposomes (Fig. 4.4c) in both the SDS–PAGE patterns and the amount of FFAs released. Membranes of RP+HPC liposomes would be more compacted given by the presence of 18: 0 DSPC and 16: 0 PSPC, in HPC, compared with those in RP+ST^{LC}, RP+ST, and RP+HPC+ST liposomes.

Finally, it is essential to consider that an optimum relation between liposome stability and destabilization is necessary for the LF release during digestion. Liposomal particles elaborated with RP may be useful to modulate LF stability and offer a platform to deliver intact LF in the intestine.

4.5 Conclusions

This work provides a characterization of lipid bilayer membrane in terms of structural organization and contributes to increase the knowledge about the protection offered to LF by different liposomal formulations against gastrointestinal digestion. Analysis of the lipid organization in terms of chain conformational order, lateral packing, and lipid phase transitions explains the stability performance of RP+ST^{LC} liposomes on LF encapsulation. RP+ST, RP+HPC, and RP+HPC+ST liposomes can be used to encapsulate LF, to improve its stability delaying its hydrolysis during gastric and intestinal digestion. The release of FFAs during *in vitro* intestinal digestion, indicated that the phospholipids in the liposomes were hydrolyzed and LF accelerated lipolysis from RP+ST and RP+HPC+ST liposomes. On the whole, these results allowed envisaging these liposome formulations as a potential system for the oral delivery of LF and possibly to other functional proteins. Future work

should be aimed to check antimicrobial bioactivity of digested LF–loaded into RP+ST, RP+HPC, and RP+HPC+ST liposomes, and to evaluate the effect of these formulations on the intestinal bacterial population, i.e. the prebiotic effect of the protein.

4.6 Acknowledgements

This research was supported by funds from CONICYT through CONICYT Doctoral Scholarship 21161448; the Centre of Biotechnology and Bioengineering (CeBiB) FB–0001 and MINECO RTC–2016–4957–1 project. In addition, we would like to acknowledge the Department of Chemical and Surfactant Technology at Institute of Advanced Chemistry of Catalonia (IQAC–CSIC), Barcelona, Spain; the Department of Chemical Engineering, and the Scientific and Technological Bioresource Nucleus (BIOREN) at Universidad de La Frontera, Temuco, to Jaume Caelles, Sonia Pérez, and Lidia Delgado for the expert technical assistance. Authors are also grateful to Lipoid GmbH for kindly providing Phospholipon® 90H.

Table 4.1. Composition of RP liposomes submitted to *in vitro* gastrointestinal digestion.

	mg/mL		
Formulation	**RP**	**ST**	**HPC**
RP+ST^{LC}	10.20	2.20	—
RP+ST	25.50	5.50	—
RP+HPC	25.50	—	5.50
RP+ST+HPC	21.70	3.10	6.20

RP, rapeseed phospholipids; ST, stigmasterol; ^{LC,} low concentration; and HPC, hydrogenated phosphatidylcholine.

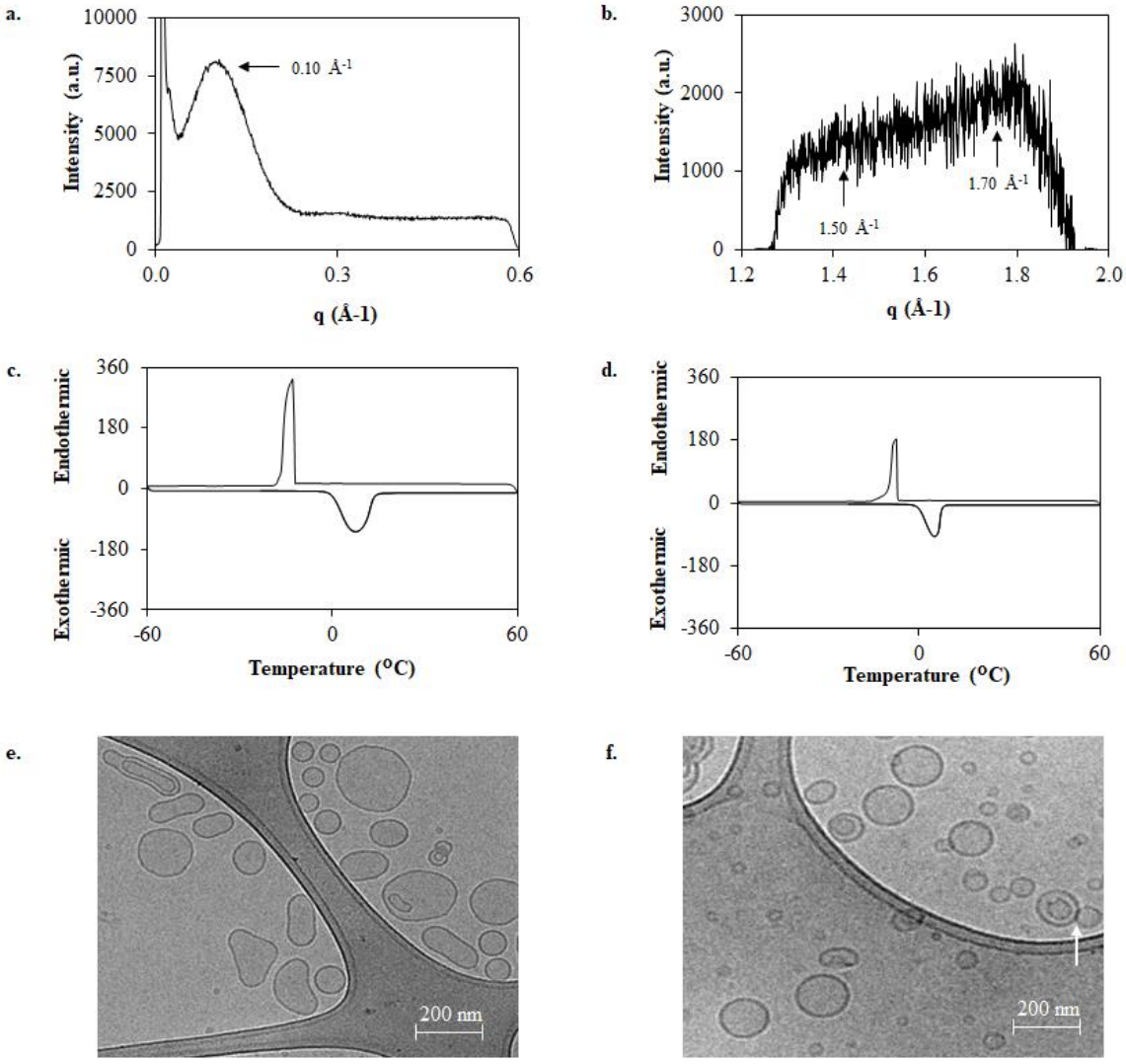

Fig. 4.1. Characterization of RP+ST*LC* liposomes. X–ray scattering profile of. (a) Small angle X–ray scattering (SAXS); (b) Wide angle X–ray scattering (WAXS); (c–d) Differential scanning calorimetry (DSC) thermograms; (e–f) Cryo–TEM micrographs.

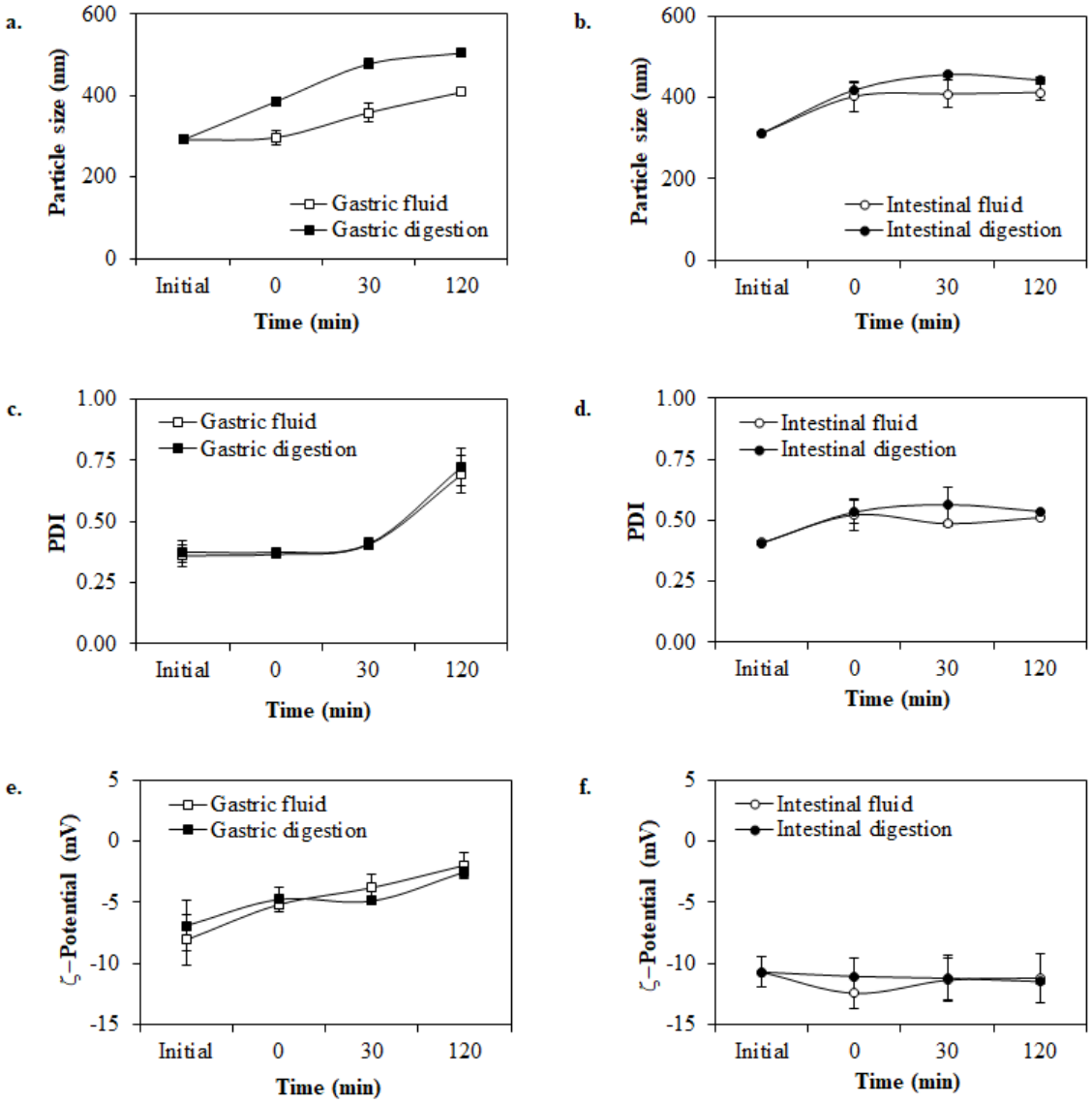

Fig. 4.2. Physicochemical stability of RP+ST*LC* liposomes in gastric (□) and intestinal (○) fluid; gastric (pepsin) digestion (■) and intestinal (pancreatin) digestion (●), (a–b) particle size, (c–d) polydispersity index (PDI), and (e–f) ζ–potential.

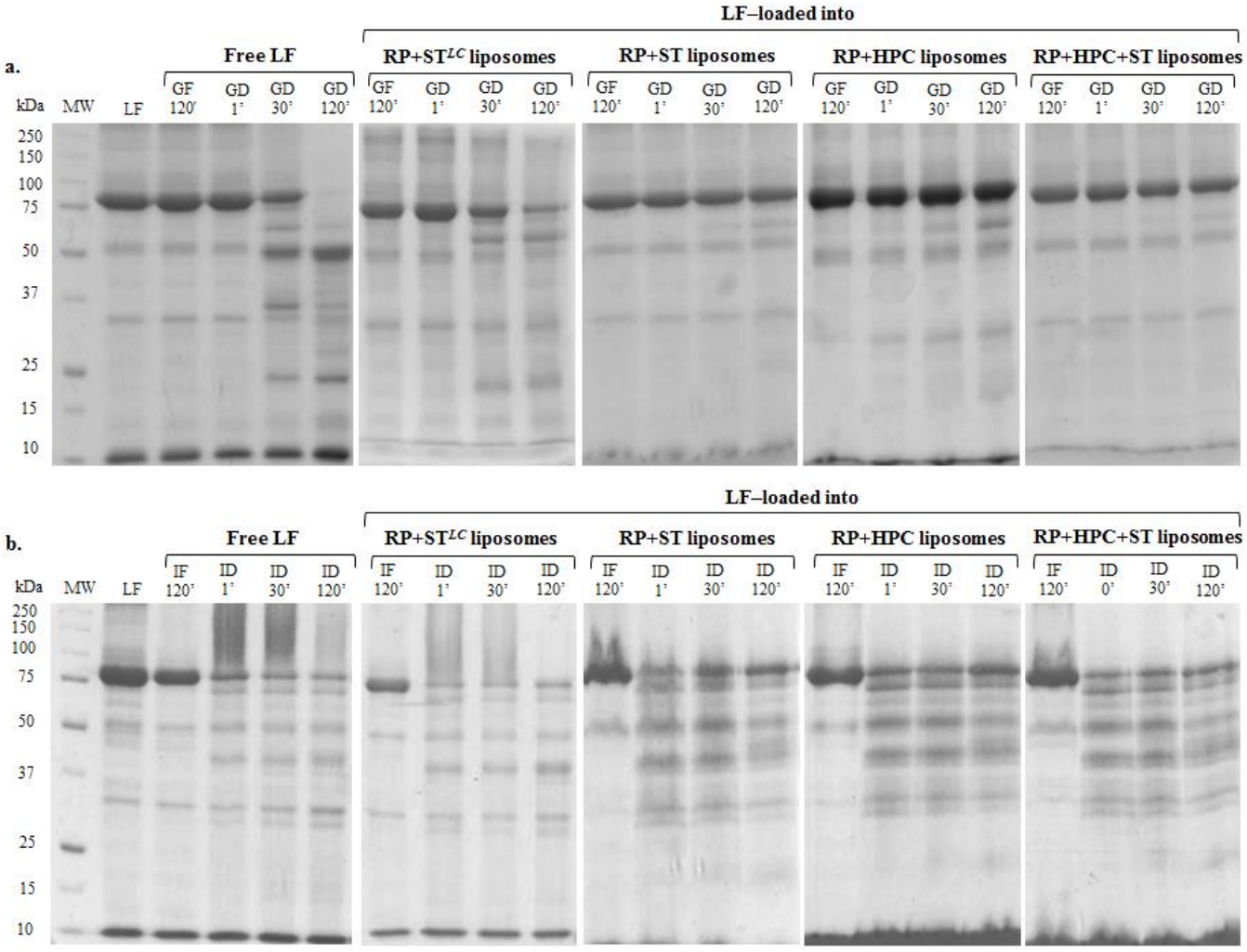

Fig. 4.3. SDS–PAGE patterns of free LF and LF–loaded into RP+ST^{LC}, RP+ST, RP+HPC, and RP+HPC+ST liposomes under (a) gastric and (b) intestinal conditions. Lanes: MW, molecular weight standard; LF, free lactoferrin (standard); GF, gastric fluid (without pepsin); GD, gastric digestion (with pepsin); IF, intestinal fluid (without pancreatin); ID, intestinal digestion (with pancreatin). The numbers 1, 30, and 120 represent the sampling time (min).

Table 4.2. Residual LF after the incubation of RP+ST^{LC}, RP+ST, RP+HPC, and RP+HPC+ST–liposomes, with the gastric and intestinal fluid (GF and IF) and after gastric and intestinal digestion (GD and ID), based on relative measurements from the SDS–PAGE. Values are means ± standard deviations (n≥3). The numbers 1', 30', and 120' represent the sampling time (min). Different superscript letters indicate significant differences (P<0.05) for LF in the different liposomes in the column (n=3).

	LF (%)			
Sample	**GF**	**GD**		
	120'	**1'**	**30'**	**120'**
Free LF	92.16 ± 1.80^{a}	89.43 ± 3.30^{a}	34.98 ± 3.85^{c}	0.00 ± 0.00^{d}
LF–loaded RP+ST^{LC}	81.08 ± 1.22^{ab}	89.22 ± 3.18^{a}	46.43 ± 0.08^{c}	20.48 ± 3.57^{c}
LF–loaded RP+ST	74.71 ± 0.72^{a}	69.51 ± 3.07^{a}	67.92 ± 1.90^{b}	67.49 ± 1.79^{b}
LF–loaded RP+HPC	74.94 ± 6.66^{a}	88.83 ± 9.03^{a}	85.42 ± 5.76^{a}	79.98 ± 1.82^{a}
LF–loaded RP+ST+HPC	83.05 ± 6.55^{a}	69.93 ± 0.71^{a}	69.66 ± 0.99^{b}	67.51 ± 0.24^{b}
Sample	**IF**	**ID**		
	120'	**1'**	**30'**	**120'**
Free LF	81.38 ± 0.08^{a}	14.89 ± 0.88^{b}	12.65 ± 0.19^{c}	10.18 ± 1.10^{c}
LF–loaded RP+ST^{LC}	83.25 ± 1.69^{a}	21.95 ± 0.47^{a}	13.29 ± 0.64^{c}	10.88 ± 0.60^{bc}
LF–loaded RP+ST	89.66 ± 4.18^{a}	16.16 ± 1.66^{b}	20.34 ± 0.32^{a}	34.80 ± 0.65^{a}
LF–loaded RP+HPC	94.44 ± 1.19^{a}	19.07 ± 1.96^{ab}	17.36 ± 1.36^{b}	32.19 ± 1.87^{a}
LF–loaded RP+HPC+ST	81.53 ± 7.13^{a}	16.52 ± 0.76^{b}	16.17 ± 0.02^{b}	15.85 ± 1.56^{b}

LF, lactoferrin; RP, rapeseed phospholipids; ST, stigmasterol; ^{LC}, low concentration; HPC, hydrogenated phosphatidylcholine; GF, gastric fluid (without pepsin); GD, gastric digestion (with pepsin); IF, intestinal fluid (without pancreatin); ID, intestinal digestion (with pancreatin).

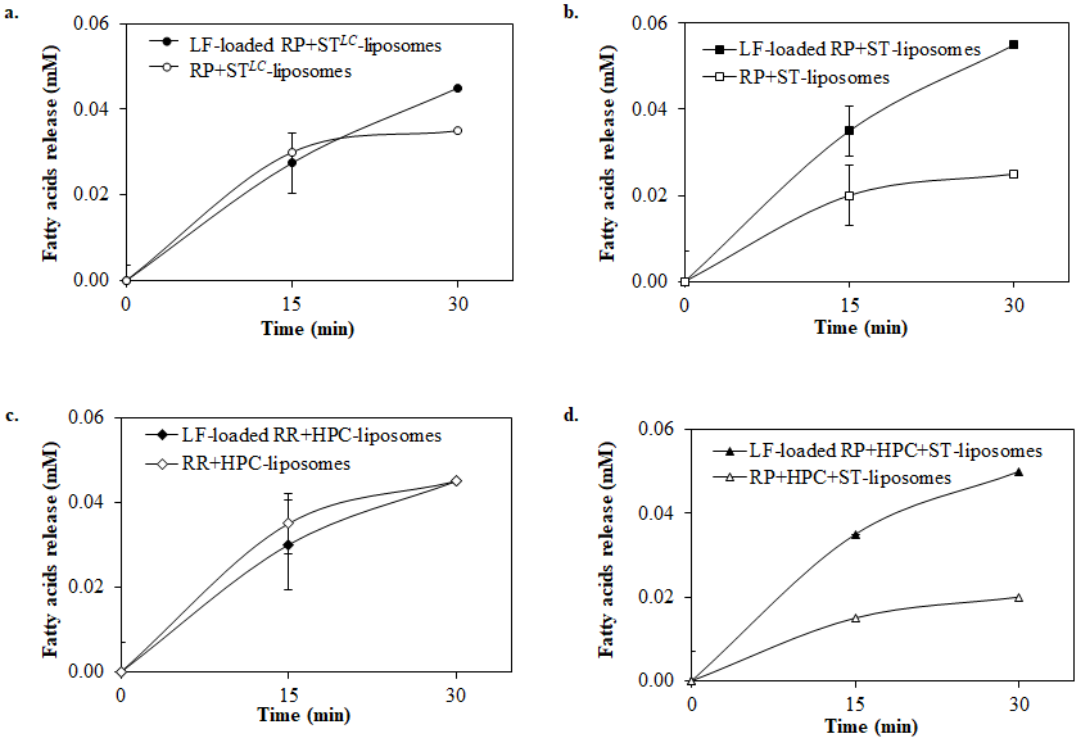

Fig. 4.4. Concentration profile of the free fatty acids (FFAs) released during *in vitro* intestinal digestion of (a) RP+ST^{LC}, (b) RP+ST, (c) RP+HPC, and (d) RP+HPC+ST liposomes with (•) or without (○) LF.

CHAPTER V

"Lactoferrin loaded in liposomes prepared from rapeseed phospholipids and hydrogenated phosphatidylcholine: Behaviour under gastrointestinal digestion in vitro and antibacterial and prebiotic bioactivity".

Daniela Vergara[a,b*], Olga López[d], Mariela Bustamante[b], Carolina Shene[b,c]

[a] Doctoral Program in Sciences of Natural Resources, Universidad de La Frontera, Ave. Francisco Salazar 01145, Box 54–D, Temuco, Chile.

[b] Center of Food Biotechnology and Bioseparations, Scientific and Technological Bioresource Nucleus (BIOREN), Centre for Biotechnology and Bioengineering (CeBiB). Universidad de La Frontera, Ave. Francisco Salazar 01145, Box 54–D, Temuco, Chile.

[c] Department of Chemical Engineering, Universidad de La Frontera, Ave. Francisco Salazar 01145, Box 54–D, Temuco, Chile.

[d] Department of Chemical and Surfactant Technology, Institute of Advanced Chemistry of Catalonia (IQAC–CSIC), C/Jordi Girona 18–26, 08034, Barcelona, Spain.

Associated to specific objective 2 and 3.

Lactoferrin loaded in liposomes prepared from rapeseed phospholipids and hydrogenated phosphatidylcholine: Behaviour under gastrointestinal digestion *in vitro* and antibacterial and prebiotic bioactivity

5.1 Abstract

Lactoferrin (LF), a protein considered as a prebiotic, has to be protected against proteolysis inside the gastrointestinal tract to preserve its activity. In this work the effectiveness of liposomes elaborated with rapeseed phospholipid (RP), and hydrogenated phosphatidylcholine (HPC) for the encapsulation LF was studied. The hydrolysis of the encapsulated LF was studied during sequential gastrointestinal *in vitro* digestion and antibacterial and prebiotic activity of LF–loaded RP+HPC–liposomes against pathogenic and probiotic bacteria was determined. Behavior of the physicochemical parameters (particle size, polydispersity index, and ζ–potential) indicated that the structure of the RP+HPC liposomes was stable under gastric digestion; nevertheless, the structure was destabilized during intestinal digestion. A high percentage of residual LF was detected in LF–loaded RP+HPC liposomes submitted to gastric (73.87 ± 0.99%) whereas this decreased after 120 h of intestinal (20.49 ± 1.18%) digestion. The encapsulation of LF into RP+HPC liposomes did not compromise its antimicrobial bioactivity on *Staphylococcus aureus*, and the prebiotic bioactivity on *Bifidobacterium infantis*, *Bifidobacterium longum*, and *Lactobacillus plantarum*. Our results suggest that liposomes elaborated with RP+HPC, can be a useful oral delivery system of molecules sensitive to digestive enzymes.

***Keywords*:** Rapeseed phospholipids, Liposomes, Lactoferrin, Sequential digestion, Antibacterial, Prebiotic.

5.2 Introduction

Lactoferrin (LF) is an 80 kDa iron–binding glycoprotein distributed in the body fluids (milk, saliva, tears, mucus, and bronchial secretions) which are synthesized by exocrine glands and neutrophils (Kanwar et al., 2015). LF is considered an important host defense molecule with a diverse range of physiological functions such as antimicrobial, anti–inflammatory and immunomodulatory activities (Moreno–Expósito et al., 2018). The presence of LF in human gastrointestinal tract may contribute to re–structure the composition of the intestinal microflora such as pathogens and probiotics bacteria (Latuga et al., 2014). Tian et al. (2010) used *in vitro* tests to investigate the effects of LF on the growth of different groups of bacteria. LF showed a significant inhibitory effect on the growth of pathogens (*Listeria monocytogenes, Staphylococcus aureus, Salmonella typhimurium and Escherichia coli*) but not on probiotics (*Lactobacillus acidophilus, plantarum, reuteri, rhamnosus, Pediococcus acidilactici* and *Bifidobacterium lactis*). Chen et al. (2017) provided strong evidence that LF stimulate the growth of specific probiotics, such as *Bifidobacterium* (*breve, angulatum, and catenulatum*) and *Lactobacillus* (*coryniformis, delbrueckii, acidophilus, paraplantarum, rhamnosus,* and *paracasei*).

Considering the physiological activity of LF in host defense the protein could be used as a functional ingredient in commercial food products. However, to preserve bioactivity it is absolutely necessary that intact LF reach and be absorbed at the intestine LF it is easily hydrolyzed by the proteolytic digestive enzymes (pepsin, pancreatin, and trypsin) (Balcão et al., 2013). Moreover, conditions such as pH, temperature, conductivity, and processing affect its functional properties (Wang et al., 2017), resulting in less than 1% absolute oral bioavailability levels (Troost et al., 2002). Several studies have suggested liposome

encapsulation of LF (Vergara & Shene, 2019; Liu et al., 2018) for enhancing the bioavailability of protein.

Liposomes are nano/micro–sized spherical vesicles, having an aqueous core enclosed by one or more phospholipid bilayers (Liu et al., 2019). Due to the presence of a lipid and an aqueous phase in the structure, liposomes can be used for the entrapment and delivery of either amphiphilic, hydrophilic, or lipophilic compound (Imran et al., 2015). Saturated phospholipids such as, hydrogenated phosphatidylcholine (HPC) are frequently used in the liposome formulations to increase the rigidity and stability of the liposomal membrane; however, liposomes can be manufactured using phospholipids extracted from plant raw materials such as, rapeseed phospholipids (RP) a by–product of the oil refining process (Vergara & Shene, 2019).

Liposomes improve the stability and prevents the degradation during *in vitro* gastrointestinal digestion of LF (Liu et al., 2013; Liu et al., 2017). It has been shown in previous work that liposomes prepared with RP+HPC can be useful systems for the oral delivery of LF, because nearly 80 and 35% of the LF remained intact after **separated** *in vitro* gastric and intestinal digestions, respectively (Vergara et al., 2020). However, the fate of LF encapsulated in RP+HPC liposomes during sequential gastrointestinal *in vitro* digestion remains to be determined. Bioactive effectiveness (antimicrobial and prebiotic) of the encapsulated LF is still unknown. Thus, to extend our previous work, the behavior of LF loaded in RP–liposomes during sequential gastrointestinal *in vitro* digestion, and the biological activity of LF post–encapsulation were studied; the objectives of this study were: (1) to evaluate protein hydrolysis during sequential gastrointestinal *in vitro* digestion of LF–loaded RP+HPC liposomes, and (2) to evaluate the antibacterial and prebiotic activity of LF–loaded RP+HPC liposomes. The results obtained from this research may contribute

to the knowledge and provide information that can be useful for the development of an effective system for the oral delivery of LF.

5.3 Materials and methods

5.3.1 Materials

Rapeseed oil was obtained from the residue left after cold pressing process carried out by OleoTop S.A. (Freire, Araucania Region, Chile). Rapeseed phospholipids (RP) were extracted following the methodology described in our previous study (Vergara & Shene 2019). Hydrogenated soy phosphatidylcholine (HPC) (Phospholipon® 90H) was supplied from Lipoid GmbH (Ludwigshafen, Germany). Lactoferrin (LF) was purchased from Jarrow Formulas, (Los Angeles, California, USA). Pepsin from porcine gastric mucosa (enzymatic activity of 3,200–4,500 U/mg protein) pancreatin from porcine pancreas (4 × United States Pharmacopeial (USP) specifications) and bile bovine were purchased from Sigma–Aldrich (St. Louis, MO, USA). All chemicals and solvents used were of analytical or HPLC grade.

5.3.2 Preparation of LF–loaded into RP+HPC liposomes

RP+HPC liposomes were prepared by the thin–layer dispersion method described by Liu et al. (2012). Briefly, RP and HPC dissolved in chloroform (2 mL) were placed into a round–bottom flask. The solvent was removed in a rotary evaporator (Buchi R–100, Flawil, Switzerland) at 40 °C; a thin lipid film was formed on the flask walls. To ensure the complete removal of the dissolvent from the film, the round–bottom flask was left overnight inside a vacuum desiccator. Then, the dried lipid film was rehydrated with phosphate buffer (pH 7.4, 0.01 M), containing LF at 1 mg/mL and subjected to sonication

using a bath sonicator Ultrasons H–D (P–Selecta, Barcelona, Spain) during 4 min. Finally, liposomal formulations were maintained 24 h at room temperature to ensure hydration.

5.3.3 Preparation of simulated gastric and intestinal fluids

The simulated gastric fluid was prepared dissolving NaCl 2 g, and concentrated HCl 7 mL in 1 L of deionized water. The simulated intestinal fluid was prepared dissolving K_2HPO_4 6.8 g/L, NaOH 0.038, NaCl 8.77 g, $CaCl_2$ 3.33 g, and bile extract 0.01 g (Sigma–Aldrich, St. Louis, MO) in 1 L of deionized water.

5.3.4 Physicochemical characterization of RP+HPC liposomes during in vitro enzymatic digestion

RP+HPC liposomes were incubated separately in gastric fluid, intestinal fluid, gastric fluid + pepsin (defined as, gastric digestion), and intestinal fluid + pancreatin (defined as, intestinal digestion), according to the methodology described by Liu et al. (2013). Solutions of pepsin (57 ng/mL), and pancreatin (0.015 mg/mL) at a 2:1 v/v ratio (RP–HPC liposomes: fluid, 3 mL total) were used. The pH of the samples in the simulated gastric and intestinal fluids were adjusted to 1.5 and 7.4, respectively; 0.05 M NaOH or 1 M HCl were used as needed. The mixtures were incubated with agitation (100 rpm) (Unitronic 320 P–Selecta, Barcelona, Spain) during 120 min at 37 °C (Minekus et al., 2014); 200 µL of sample were taken for analysis after 1, 60, and 120 min. Particle size, polydispersity index (PDI), and ζ–potential of RP+HPC liposomes in the gastric and intestinal fluid, and during gastric and intestinal digestion were followed in time, using a Zetasizer Nano ZS (series HT, Malvern Instrument, U.K.) at 25 °C; measurement conditions were defined according to Yao et al. (2014).

5.3.5 In vitro enzymatic digestion of LF–loaded RP+HPC liposome

According to the results of gastric, and intestinal digestion, and the lipid digestion presented in the IV Charpter, the RP+HPC liposome formulation was chosen to perform the sequential in vitro digestion assays. The sequential digestion of free LF, and LF–loaded into RP+HPC liposome was carried out as described in section 5.3.4. The pepsin inactivation was carried out by pH change (from pH 1.5 to 7.4). Digested samples were placed in Eppendorf vials, solubilization of liposomes and inactivation of pancreatin were performed with SDS–PAGE loading buffer (62.5 mM Tris–HCl pH 6.8, 20% glycerol, 2% SDS, 0.1% bromophenol blue and 5% β–mercaptoethanol) added in a volume ratio of 2:1 v/v (sample: loading buffer). The mixtures were stored at –20 ºC for further analysis.

5.3.6 Protein degradation kinetics by SDS–PAGE

To determine the hydrolysis degree of the encapsulated LF in the gastric and intestinal fluid, and under gastric and intestinal digestion, the quantity of not hydrolyzed LF was determined by SDS–PAGE using a 15% w/w polyacrylamide gel as described by Laemmli (1970). The gels were run in a Mini–Protean Tetra System (BioRad, USA) at 130 V using a Bio–Rad power supply unit PowerPacTM (BioRad, USA). Gels were stained (1.25 g/L Coomassie Blue R–250 in ethanol: glacial acetic acid: water at 52: 10: 38 v/v/v) for 120 min and then distained (ethanol: glacial acetic acid: water at 26: 0.8: 73.2 v/v/v). PageRuler™ Unstained Protein Ladder (Thermo Scientific; 10 to 250 kDa) was used as molecular weight marker. Gel images were acquired using a RICOH MP–C3003 Photo Scanner. The relative percentages of LF in the samples (compared with the LF standard) was quantified using ImageJ 1.50i (NIH, USA) software.

5.3.7 Evaluation the antibacterial and prebiotic activity of RP+HPC liposomes on the growth of pathogenic and probiotic bacteria

5.3.7.1 Bacterial culture preparation

The selected probiotic strains were: *Bifidobacterium infantis* ATCC 15679, *Bifidobacterium longum* ATCC 15707, and *Lactobacillus plantarum* ATCC 8014. The following pathogenic strains were selected: *Escherichia coli* ATCC 25922 and *Staphylococcus aureus* ATCC 25923. Briefly, pathogens and probiotics microorganisms were sub–cultured with 5% (v/v) inoculum in 5 mL of the respective broth. *B. infantis* and *B. longum* were cultured in de Man, Rogosa and Sharpe (MRS) broth (Difco^{TM}, USA) with 0.05% cysteine under anaerobic conditions (GasPak generator, Becton Dickinson, Sparks, MD, USA) at 37 °C for 12 h. *L plantarum* was incubated in MRS broth at 37 °C for 12 h. *E. coli* and *S. aureus* were cultured in tryptic soy broth (TSB) (Bacto^{TM}, USA) at 37 °C for 12 h. Microorganisms were collected at their logarithmic phase and re–suspended in their respective broths to obtain a final microbial density of about 1×10^{6} CFU mL^{-1}. Each microorganism was incubated separately, under the conditions described above in the broth supplemented with LF–loaded RP+HPC liposomes in a volume ratio of 1:2 v/v (microorganism: LF–loaded RP+HPC liposomes) at 37 °C for 24 h. Controls were incubated without LF.

5.3.7.2 Viability of pathogenic and probiotic bacteria

Survival and viability after the incubation of the microorganisms were determined by the standard plate count method. Briefly, the culture sample (0.5 mL) was diluted in 4.5 mL of sterile buffered peptone water (0.1 g peptone in 100 mL distilled water). The appropriate

dilution of the suspension was seeded on tryptic soy or MRS agar; incubation was made at 37 °C for 48 h under anaerobiosis when needed. Viability of microorganisms was expressed as colony forming units per mL (CFU mL^{-1}).

5.3.7.3 Morphology

The morphology of *E. coli* and *S. aureus* incubated with LF–loaded RP+HPC liposomes was observed using scanning transmission electron microscopy (STEM) (Hitachi SU–3500 microscope, Tokyo, Japan) at 5.00 Kv of accelerating voltage and 2.5–5.4 mm of working distance.

5.3.8 Data analysis

All measurements were repeated at least three times. The results were evaluated statistically for significance ($P<0.05$) using ANOVA and Tukey means comparison test with Minitab® software version 18 (State College, PA, USA). All data were expressed as means ± standard deviations.

5.4 Results and discussion

5.4.1 Physicochemical stability of RP+HPC liposomes during in vitro digestion

RP+HPC liposomes were submitted to gastric and intestinal digestion, respectively. Behavior of physicochemical parameters (particle size, PDI, and ζ–potential) was followed as a function of the incubation time (initial, 1, 60, and 120 min). These experiments were carried out to check the behavior, effectiveness, and stability of the lipid membrane of liposomes loaded with LF under gastrointestinal conditions. Results showed that particle size of the liposomes increased during *in vitro* digestion (Fig. 5.1); initial average particle

size of RP+HPC liposomes (212.10 ± 5.23 nm) increased 1.2–fold after gastric digestion and 111–fold after intestinal digestion. The changes in particle size of liposomes correlated with changes in PDI values. Due to the drastic increase of the particle size during intestinal digestion, the PDI value obtained is around 1.00. ζ–potential of RP+HPC liposomes increased from –28.08 ± 2.94 mV to –7.34 ± 1.48 mV after gastric digestion; and decreased to –29.97 ± 3.00 mV after intestinal digestion.

The particle size of LF–loaded RP+HPC did not present significant variation during gastrc digestion (Fig. 5.1a). However, an increase in particle size was observed at the beginning of intestinal digestion, but it decreased as incubation time increased. Similar results were reported by Nacka et al. (2001); the authors stated that the liposomal particle size decreased gradually to reach about 50% of the initial diameter after storage at pH 1.5 for 30 min. During gastric digestion, membrane shrinkage probably causes the decrease in the particle size of the RP+HPC liposomes, because of water leaking from the inside of the RP+HPC liposomes (pH 7.4, low osmolarity) to the outside (pH 1.2, high osmolarity). However, the slight change in the particle size during gastric digestion suggested that the liposomes could retain their integrity, and that pepsin did not further hydrolyze the phospholipid membrane of the RP+HPC liposomes keeping the LF encapsulated.

The effects of intestinal digestion (pancreatin + bile salts), on the RP+HPC liposomes were more severe; the particle size of the LF–loaded RP+HPC liposomes increased 111–fold during the first 2 h of digestion (Fig. 5.1a). The ζ–potential became slightly more negative during the intestinal digestion (Fig. 5.1c). These changes may be attributed to the hydrolysis of the liposome phospholipids by pancreatin; pancreatin is a mixture of digestive enzymes including protease, lipase, phospholipase A2, and cholesterol esterase. Pancreatic

lipase has been found to catalyze the hydrolysis of 1–linked fatty acids of phospholipids, releasing fatty acids and 1–acyl lysophospholipids (de Haas et al. 1965).

The release of free fatty acids (FFA) from the liposomes during intestinal digestion in our previous study (Vergara et al., 2020) confirmed the phospholipids lipolysis. Another source of phospholipid bilayers hydrolysis is phospholipase A2 in pancreatin. Furthermore, cholesterol esterase, stimulated by bile salts, can hydrolyze phospholipids (Liu et al. 2013; Liu et al. 2017). Therefore, the organized structure of the liposomal bilayers could be modified by the three above mentioned enzymes, resulting in aggregation of the liposomes, as indicated by the increase in the particle size. Additionaly, ions in the medium can form insoluble saponified compounds with the FFA, increasing the average particle size (Beltrán et al. 2019).

The high PDI value (~1.00) of the LF–loaded RP+HPC liposomes under intestinal digestion (Fig. 5.1b) can be attributed to the hydrolysis of phospholipids, and LF released form the particles or small molecules, such as FFAs, monoacylglycerols, and peptides, which are susceptible to coalescence to different sized particles (Li et al. 2012), causing broad distribution of particle sizes.

5.4.2 Stability of encapsulated LF into RP+HPC liposomes during sequential in vitro digestion

RP+HPC liposomes were used to evaluate the hydrolysis of the encapsulated LF during sequential *in vitro* digestion by SDS–PAGE. Fig. 5.2 shows the intensity of the LF bands generated after 120 min of gastric digestion followed by intestinal (120 min) digestions (sequential digestion). The strong band near 78–80 kDa corresponds to LF (Fig. 5.2, lane LF, standard); some minor bands visible around 55, 35, and 15 kDa, might be residual

proteins from purification. The relative percentages of LF in the samples quantified using ImageJ 1.50i software are summarized in Table 5.1. Residual LF after the incubation of free LF and LF–loaded RP+HPC liposomes with gastric and intestinal fluids (without digestive enzymes) were not significantly different ($p<0.05$). However, free LF was completely hydrolyzed after 120 min under gastric digestion. LF encapsulated into RP+HPC liposomes decreased to 73.87 ± 0.99% after 120 min of gastric digestion. The amounts of LF remaining after 120 min of intestinal digestion of RP+HPC liposomes containing the protein decreased to 20.49 ± 1.18% and is ascribed to the major destruction of the liposomal membrane.

Results obtained with the samples incubated with the gastric and intestinal fluids showed a reduction in the percentage of LF encapsulated compared with LF standard, (Fig. 5.2), line LF, which comprises 100% of LF in the gel). This loss could be due to two factors, (1) the action of gastric or intestinal fluid (pH 1.5 and 7.4, respectively) and/or (2) the conditions (temperature and sonication) used for the elaboration of LF–loaded RP+HPC liposomes. LF–loaded RP+HPC liposomes demonstrated excellent behavior under gastric digestion: nearly 75% of the LF remained intact after 120 min; this result is consistent with the physicochemical stability of the liposomes reported above (Fig. 5.1). LF hydrolyzed during *in vitro* gastric digestion (~25%) could correspond to LF that was covering the liposome surface. Lipid–LF electrostatic interactions between the phospholipid head groups (PO_4^{-3}) and the specific functional groups (NH_3^+) of alkaline proteins can take place (Chen et al., 2020). Liu et al., 2017 have reported that the LF deposited on the surface of the liposomes facilitates lipid digestion decreasing the system stability. However, in our previous study conducted with LF–loaded RP+HPC liposomes the influence of LF on the release of FFAs from liposomes during *in vitro* digestion was not observed (Vergara et al.,

2020). On the contrary, the non–encapsulated LF could form a barrier to digestive lipolysis, and/or bile salts, decreasing the lipolysis rate, and protecting the effectively encapsulated LF.

On the other hand, because of the hydrolysis of phospholipids and protein by lipase and protease in pancreatin, it is reasonable to expect a gradual degradation of the LF released from the damaged liposomes. In addition to the effect of the enzymes, the low pH, and high ionic force, could favor protein denaturation during the digestion (Furlund et al., 2013). However, some LF still remained in the liposome suspension intestinal digestion (Fig. 5.2); this was not the case of free LF that was completely hydrolyzed. This indicated that some of entrapped LF in liposomes could survive under sequential gastrointestinal *in vitro* digestion. It is well known that the mean residence time in the small intestine of an orally administered formulation is well over 120 min (Kokkona et al., 2000). Although the results are encourage, conditions to obtain percentages of intact LF higher than 20% after *vitro* digestion need to be determined.

5.4.3 Antibacterial and prebiotic activity of LF encapsulated into RP+HPC liposomes on the growth of pathogenic and probiotics bacteria

The antibacterial and prebiotic activity of LF encapsulated in RP+HPC liposome was evaluated. Table 5.2 shows the effect of the RP+HPC liposomes loaded with LF on the growth of pathogenic and probiotic bacteria. The encapsulated LF increased 1.49, 2.98, 2.54, and 1.50–fold the growth of *B. infantis*, *B. longum*, *L. plantarum,* and *E. coli* (4.10×10^{10} ± 2.12×10^{9}, 5.85×10^{10} ± 2.47×10^{9}, 1.20×10^{10} ± 3.18×10^{8}, and 3.34×10^{9} ± 3.54×10^{7} CFU mL^{-1}) and inhibited 3.21–fold the growth of *S. aureus* (1.97×10^{10} ± 3.04×10^{9} CFU mL^{-1}) compared to control assays conducted without LF (2.75×10^{10} ±

7.07×10^{8}, $1.96\times10^{10} \pm 4.24\times10^{8}$, $4.40\times10^{9} \pm 2.83\times10^{8}$, and $6.34\times10^{10} \pm 2.55\times10^{9}$ CFU mL^{-1}).

In our study we did not observe antibacterial activity of LF against the *E. coli* strain ATCC 25922. Atef Yekta et al. (2010) registered reduced growth of *E. coli* O157:H7 after 6 h incubation with LF. However, after 8 h the LF treated bacterium recovered, and started to growth reaching the same optic density values as in the assay with the non–treated bacterium. Fig. 5.3a–d show SEM images of *E. coli* and *S. aureus*, cultured without LF and with LF–loaded RP+HPC liposomes. Evident differences in the morphology of bacterial surfaces were revealed. *E. coli* presented sign of cell wall damage (Fig. 5.3b, see arrows) which could indicate the antibacterial activity of LF loaded into the liposomes; however, this effect was not reflected in the growth density (Table 5.3). On the other hand, cells of *S. aureus* in control the culture (Fig. 5.3c) were uniform in size, with the typical grape globular shape; in contrast Fig. 5.3d shows that cell surface of *S. aureus* are covered with a film (not observed in cells from the control assay Fig. 5.3c) probably composed of the LF–loaded RP+HPC liposomes. This film could prevent the exchange of nutrients and cell wastes, and offer a possible explanation to the reduced cell density observed (Table 5.2). Although the mechanism of action of LF has not been clearly elucidated LF could be limiting iron availability to *S. aureus*, essential element for bacterial growth (bacteriostatic capacity). In adittion, LF also could adhere to the celular membrane destabilizing the cytoplasmic membrane, increasing its permeability (Ortíz–Estrada et al., 2012).

Prebiotic activity of LF–loaded RP+HPC liposomes agreed with those reported by Chen et al. (2017b). These authors provided strong evidence that bovine LF stimulates the growth of differentprobiotic species, such as *Bifidobacterium* (*breve, angulatum, and catenulatum*), and *Lactobacillus* (*coryniformis, delbrueckii, acidophilus*, *paraplantarum*, *rhamnosus*, and

paracasei). The mechanism through which LF acts a prebiotic is unknown; Tian et al. (2010) established that the special cell structures or metabolic substances synthesized by probiotics may protect the cells from the activities of cationic proteins such as LF. Beside, LF may serve as iron donor, and in this manner stimulate the growth of some bacteria with lower iron demands such as *Lactobacillus* spp. or *Bifidobacterium* spp. (Sherman et al., 2014).

Although the intact form of LF has maximal bioactivity, during the *in vitro* gastric and intestinal digestion different peptides were formed (Fig. 5.2). Moscovici et al. (2014) established that LF peptides with antibacterial, antiviral, or immuno–modulating functions can be generated by gastrointestinal proteolysis. According to Hamosh, (1998) the action of digestive enzymes on LF generates peptides with even greater bactericidal activity than the intact protein. In particular, the 2.92 kDa (LFcin) and 2.04 kDa (LFampin) peptide fragments found as a digestion products (Haney et al., 2012) exerted strong antimicrobial activity against a variety of $Gram^{+}$ and $Gram^{-}$ bacteria as well as candidacidal activity (Bellamy et al., 1992; Van der Kraan et al., 2004). Therefore, the most suitable way to deliver LF will depend on its therapeutic or nutritional purpose.

Finally, microbial resistance to antibiotics raises the need to develop novel compounds and approaches for microbial control. Antimicrobial proteins offer a promising opportunity to combat microbial pathogens. LF encapsulated into RP+HPC liposome could be used to inhibit the growth of pathogenic bacteria such as *S. aureus* and maintain specific probiotics in the intestinal tract such as, *B. infantis*, *B. longum*, and *L. plantarum*. Encapsulation does not affect the bioactive properties of LF on these bacteria studied.

5.5 Conclusion

This Chapter contributes to the knowledge about the effects of *in vitro* gastrointestinal digestion of LF encapsulated into RP+HPC liposomes on bioactive properties of the protein. FFAs were released during intestinal digestion, indicating that the phospholipids in the liposomes were hydrolyzed. The presence of LF accelerates the release of FFAs from RP+ST and RP+HPC+ST–liposomes. The loaded RP+HPC liposomes retained physicochemical stability after *in vitro* gastric digestion; however, as expected, this is not the case of intestinal digestion where the particle size, PDI and ζ–potential increased. RP+HPC liposomes can be used to encapsulate LF and to improve the stability during gastrointestinal digestion. In addition, encapsulation of LF into RP+HPC liposomes does not compromise antimicrobial and prebiotic activity of the protein. On the whole, the results allowed envisaging these liposome formulations as a potential oral delivery form for LF, and other functional proteins. Future work should be aimed to check the effective probiotic activity of LF–loaded RP+HPC liposomes on the heterogeneous intestinal bacterial population.

5.6 Acknowledgements

This research was supported by funds from CONICYT through CONICYT Doctoral Scholarship 21161448; the Centre of Biotechnology and Bioengineering (CeBiB) FB–0001 and MINECO RTC–2016–4957–1 project. In addition, we would like to acknowledge the Department of Chemical and Surfactant Technology at Institute of Advanced Chemistry of Catalonia (IQAC–CSIC), Barcelona, Spain; the Department of Chemical Engineering, and the Scientific and Technological Bioresource Nucleus (BIOREN) at Universidad de La

Frontera, Chile. Authors are also grateful to Lipoid GmbH for kindly providing Phospholipon® 90H.

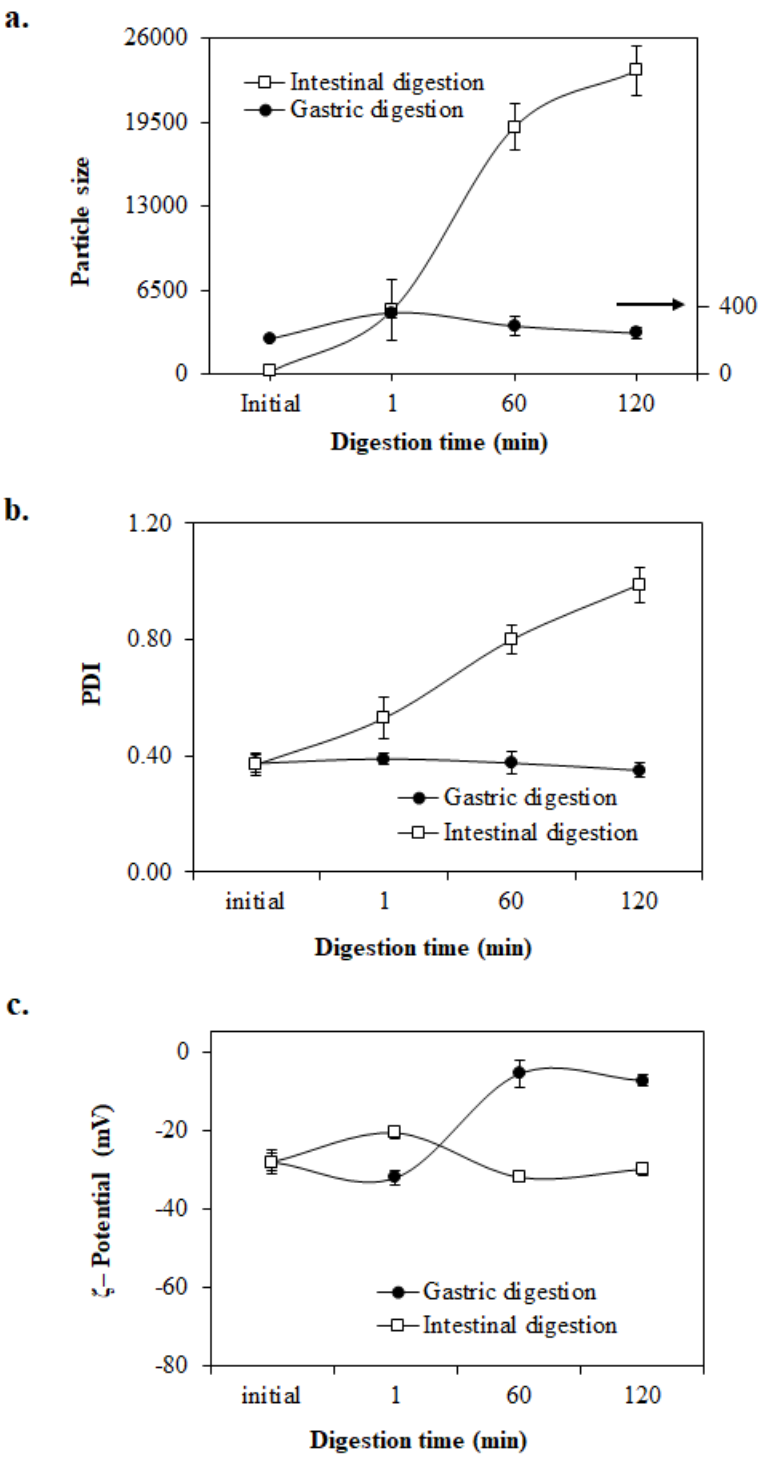

Fig. 5.1. Physicochemical stability of LF–loaded RP+HPC liposomes in gastric (with pepsin) (□) and intestinal (with pancreatin) (●) digestion. (a) Particle size, (b) polydispersity index (PDI), and (c) ζ–potential.

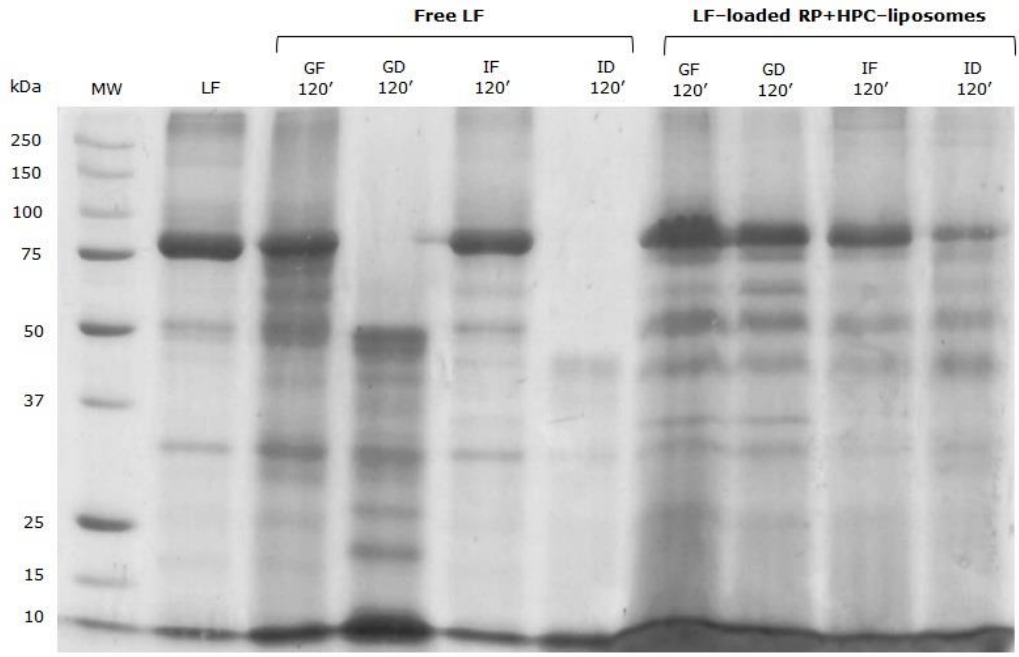

Fig. 5.2. SDS–PAGE patterns of free LF and LF–loaded into RP+HPC liposomes under sequential gastrointestinal *in vitro* digestion. Lanes: MW, molecular weight standard; LF, free lactoferrin (standard); GF, gastric fluid (without pepsin); GD, gastric digestion (with pepsin); IF, intestinal fluid (without pancreatin); ID, intestinal digestion (with pancreatin). The number 120 represent the sampling time (min).

Table 5.1. Residual lactoferrin (LF) after the incubation of free LF and LF–loaded RP+HPC liposomes, in gastric and intestinal fluids (GF and IF), and during gastric and intestinal digestion (GD and ID), based on relative measurements from the SDS–PAGE (Fig 3). Values are means ± standard deviations (n≥3). Samples were collected after 120' min incubation. Different superscript letters indicate significant differences ($P<0.05$) for each form of LF in the same column (n=3).

	LF (%)			
Sample	**GF**	**IF**	**GD**	**ID**
Free LF	91.94 ± 2.41^{a}	76.88 ± 0.29^{a}	0.00 ± 0.00^{a}	0.00 ± 0.00^{a}
LF–loaded RP+HPC liposomes	94.34 ± 3.96^{a}	72.03 ± 5.51^{a}	73.87 ± 0.99^{b}	20.49 ± 1.18^{b}

RP, rapeseed phospholipids; HPC, hydrogenated phosphatidylcholine; GF, gastric fluid (without pepsin); GD, gastric digestion (with pepsin); IF, intestinal fluid (without pancreatin); ID, intestinal digestion (with pancreatin).

Table 5.2. Effect of the LF–loaded RP+HPC liposomes on the growth of pathogens (*E. coli*, and *S. aureus*) and probiotic (*L. plantarum, B. infantis*, and *B. longum*) strains incubated at 37 °C during 48 h.

	CFU mL^{-1}	
Microorganism pathogen	**Control without LF**	**LF–Loaded RP+HPC liposomes**
E. coli	$2.23\times10^{9} \pm 4.95\times10^{7}$	$3.34\times10^{9} \pm 3.54\times10^{7}$
S. aureus	$6.34\times10^{10} \pm 2.55\times10^{9}$	$1.97\times10^{10} \pm 3.04\times10^{9}$
Microorganism probiotic		
L. plantarum	$4.40\times10^{9} \pm 2.83\times10^{8}$	$1.12\times10^{10} \pm 3.18\times10^{8}$
B. infantis	$2.75\times10^{10} \pm 7.07\times10^{8}$	$4.10\times10^{10} \pm 2.12\times10^{9}$
B. longum	$1.96\times10^{10} \pm 4.24\times10^{8}$	$5.85\times10^{10} \pm 2.47\times10^{9}$

CFU, colony forming units; LF, lactoferrin; RP, rapeseed phospholipids; HPC, hydrogenated phosphatidylcholine.

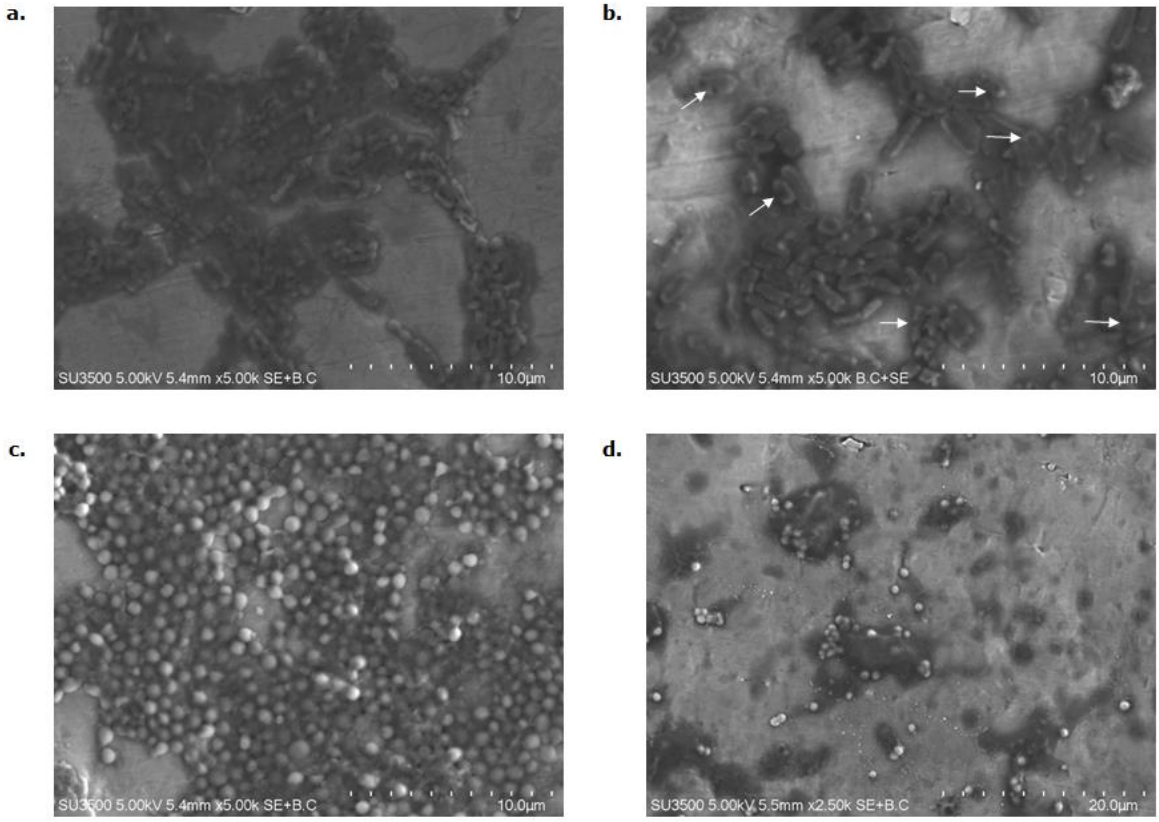

Fig. 5.3. Scanning electron microscope (SEM) images of microorganisms cultivated at 37 ºC for 24 h. (a) *E. coli* control, (b) *E. coli* incubated with LF–loaded RP+HPC liposomes, (c) *S. aureus* control, and (d) *S. aureus* incubated with LF–loaded RP+HPC liposomes.

CHAPTER VI

General discussion, concluding remarks, and future directions

6.1 GENERAL DISCUSSION

Lipid based delivery systems have attracted increasing scientific and commercial attention during the last few years as alternative materials to protect peptides and proteins during food processing, storage, and digestion in the gastrointestinal tract (Sagis, 2015). In this context, the use of novel raw renewable materials has emerged for the replacement of traditional sources of phospholipids. Therefore, during this Doctoral Thesis, RP extracted from residues of the processing of rapeseed oil allowed the elaboration of liposomes that preserve biological properties of a protein, LF, for possible applications in food products.

According to Chapter III, for the optimization of the conditions for liposomes preparation using RSM, different RP concentrations (3–12 mg/mL), ST concentrations (0–3 mg/mL), and sonication times (0–20 min) were selected as independent variables. The same experimental design was applied using SP as a control, in replacement of those extracted from RP. Based on the results obtained in this chapter, factors affecting EE in liposomes can be broadly divided in two categories, the process and formulation variables (Curic et al., 2013). Phospholipid concentration, ST concentration, and phospholipid type affected the EE of LF in liposomes. It is known that phospholipid concentration affects liposomal EE of most hydrophilic bioactive compounds (independent of the size of the molecule). Generally, a higher phospholipid concentration leads to higher EE. This is attributed to its positive impact on the total internal volume of liposomes (Xu et al., 2011). The total internal volume is determined by two factors: the volume entrapped in individual vesicles (which is a function of vesicle size and size distribution, as well as vesicle lamellarity) and the total vesicle number. The increase in EE of LF, as a result of the increased phospholipid concentration is primarily attributed to the increase in the total vesicle number. On the other hand, the sonication process plays an important role in reducing particle size of liposomes.

The purpose of implementing the model with RP and SP is based on the need to compare our extracted material (RP) with other having proven encapsulation capacity. Our results showed that RP achieves better EE, and smaller particle sizes than commercial SP. The differences found between one material and the another are mainly due to their composition (phospholipids and fatty acids) as has been reported by Tehrany et al. (2012).

According to Chapter IV, the physicochemical behavior of optimized formulation named as, RP+ST^{LC} liposomes was observed under **separated** gastric and intestinal digestion *in vitro*; an increase in particle size was observed, attributed to the aggregation of the vesicles given by the different pH of the gastric phase and liposomal vesicles (internal outside). On the other hand, the electronegativity (ζ–potential) registered in the RP+ST^{LC} liposomes would be given by the phosphate group (PO_4^{3-}) in the phospholipids extracted from the rapeseed oil residue. The low liposomal electrostability could be due to ions in the intestinal fluid or digestion products such as lysophospholipids. Because of the hydrolysis of phospholipids and protein by lipase and protease in pancreatin, it was reasonable to expect a gradual degradation of the LF released from the damaged liposomes. The characterization of the membrane of the RP+ST^{LC} liposomes proved to be an "ordered–liquid" phase, which would explain the low stability of the liposomes under gastrointestinal digestion *in vitro* (Vergara et al., 2020). Therefore, to increase the percentage of not hydrolyzed LF, and the physicochemical stability in liposomes loaded with LF under simulated gastric and intestinal digestion, four different formulations were developed. HPC was tested to replace ST; the following formulations were defined: RP+ST^{LC}, RP+ST, RP+HPC and RP+HPC+ST liposomes.

Among the new formulations, LF–loaded RP+HPC liposomes showed excellent performance, under *in vitro* gastrointestinal digestion which could be related to the

encapsulation capacity of the vesicles. Because LF exhibits a positive charge under the conditions of gastric digestion, and the liposomes are negatively charged, LF might cover the surface of the liposomes by electrostatic interaction (Liu et al. 2017). Increasing the concentration of phospholipids in the new liposomal formulations increases the percentage of LF effectively encapsulated, delaying hydrolysis by pepsin. Furthermore, the non–encapsulated LF layer surrounding the liposomal membrane could affect the speed and digestion of liposomes by pancreatin through competitive absorption moreover, accumulated digestion products (peptides) could delay enzymatic action (Robbins, 1977). However, LF facilitated the release of FFAs in RP+ST and RP+HPC+ST liposomes. Similar results were observed by Liu et al. (2017) who found that in liposomes composed of L–α–phosphatidylcholine and cholesterol, LF facilitated the release of FFAs, and increased the microfluidity of the bilayers, reducing the structural integrity. This effect can be attributed to the fact that polymers such as LF could form a broad network allowing the localization of bile salts at the phospholipid bilayers interface increasing the fluidity of the membrane (Wilde & Chu, 2011).

Based on the results obtained by RP+HPC liposomes (Chapter V), this formulation was chosen to evaluate protein hydrolysis during *in vitro* sequential digestion. LF–loaded RP+HPC liposomes demonstrated excellent behavior. Nearly 75% of the protein was not hydrolyzed during gastric digestion while nearly 20% of the LF remained intact after gastric + intestinal digestion. This results was consistent with the physicochemical stability reported for this formulation. On the other hand, because of the hydrolysis of phospholipids and protein by lipase and protease in pancreatin, it was reasonable to expect a gradual degradation of the LF released from the damaged liposomes. Additionally, low pH values, gastrointestinal juices, and high ionic strength parameters have a high impact in protein

denaturation during the digestion (Furlund et al., 2013). However, the results of our study are promising based on the percentage of unhydrolyzed protein (20%) that remains bioavailable to be assimilated, compared with previous studies that demonstrate approximately 1% of absolute levels of oral bioavailability of LF (Troost et al. 2002).

Bioactivity of LF–loaded RP+HPC liposomes on the viability of pathogenic (*S. aureus*) and probiotic (*B. infantis*, *B. longum*, and *L. plantarum*) bacteria indicated that the encapsulation does not affect LF activity. LF–loaded RP+HPC liposomes, could limit iron availability to *S. aureus* and/or interact with cell surface causing destabilization of the cytoplasmic membrane, increasing its permeability (Ortíz–Estrada et al., 2012). In the case of the probiotic strains LF may serve as iron donor stimulating the growth of some probiotic bacteria (Sheman et al., 2014).

For the assays performed with *E. coli*, the length of the incubation time (48 h) would interfere with antimicrobial response of the LF–loaded RP+HPC liposomes (discussed in section 5.4.3). The foregoing could be resolved through a colorimetric assay using 3–(4,5–dimethylthiazol–2–yl) –2,5–diphenyltetrazolium bromide (MTT) used to evaluate cell viability. On the other hand, for a correct evaluation of the factors in the LF bioactivity tests, it is necessary to perform analyzes that consider both the antibacterial and prebiotic activity of: (1) free LF, (2) LF–loaded RP+HPC digested liposomes, and (3) RP+HPC liposomes without LF.

Finally, the results obtained in this Doctoral Thesis have confirmed the hypothesis raised and have contributed to: (1) increase the knowledge about the use of RP for developing liposomes, as LF delivery system, (2) define the conditions for LF encapsulation into RP liposomes to improve encapsulation efficiency, (3) prove the effectiveness of protection offered by RP liposomes to the LF encapsulated during *in vitro* (*separated* and *sequential*)

gastrointestinal digestion, and (4) demonstrate that the encapsulation of LF in liposomes does not affect antibacterial and prebiotic bioactivity of the protein *in vitro* tests.

6.2 CONCLUDING REMARKS

According to our results we can conclude that:

- RP was extracted from residues of rapeseed oil for the elaboration of liposomes. In RP about 90% of total fatty acids were unsaturated. The extracted RP contained PC, PE, and PA + LPC, α–, δ–, γ–tocopherols, arginine, histidine, and proline.
- The optimization of the conditions for liposomes preparation was carry out using RSM. The effect of phospholipids concentration, ST concentration, and sonication time was significant for EE ($P<0.05$) of LF–loaded RP+ST^{LC} liposomes whereas only sonication time was the main contributing variable for particle size ($P<0.05$).
- Under optimized liposomal elaboration conditions, the EE and particle size were 91.94 ± 0.61% and 148.57 ± 2.76 nm, respectively. RP+ST^{LC} liposomes had a narrow particle size distribution, and were electrically and physically stable, according to the PDI (0.23 ± 0.01) and ζ–potential (–31.03 ± 1.83 mV), respectively.
- CLSM images demonstrated the effective encapsulation of LF in RP+ST^{LC} liposomes. STEM images clearly showed the spherical shape of LF–loaded RP liposomes.
- The storage temperature (4, 25, and 37 ºC) had a significant effect on the stability of the loaded RP+ST^{LC} liposomes; the lowest temperature (4 ºC) was the most desirable storage condition at 60 days.

- LF encapsulated in RP+ST^{LC} liposomes was significantly hydrolyzed under gastric and intestinal digestion *in vitro*. The release of FFAs from the liposomes during intestinal digestion revealed that the RP+ST^{LC} liposomes were partly hydrolyzed by pancreatin.
- Physicochemical results indicated that the RP+ST^{LC} liposomes structure was unstable and was destabilized under gastric digestion; nevertheless, the structure was maintained during intestinal digestion.
- Microstructural characterization of RP+ST^{LC} liposomes indicated the presence of unilamellar liposomes, evidencing a lipid bilayer membrane of 63 nm approximately. In addition, lamellar structure was organized in a "liquid–ordered" phase with a potential orthorhombic packing domains.
- To improve the resistance of LF under gastric and intestinal digestion, four different formulations were elaborated. HPC was tested in replacement of ST; the following formulations were defined as: RP+ST^{LC}, RP+ST, RP+HPC, and RP+HPC+ST liposomes.
- Gastric digestion affected stability and size of the liposomes more than intestinal digestion; however, about 67–80% of the LF remained intact in RP+ST, RP+HPC, and RP+HPC+ST liposomes under gastric digestion. About 16–35% of the initial LF was not hydrolyzed after intestinal digestion in the same formulations.
- LF facilitated the release of FFAs in RP+ST and RP+HPC+ST liposomes during lipolysis.
- Under sequential gastrointestinal digestion free LF was completely hydrolyzed during gastric digestion; in contrast, a high percentages of residual LF was detected in LF–

loaded in RP+HPC liposomes submitted to gastric (73.87 ± 0.99%) and intestinal (20.49 ± 1.18%) digestion after 120 min.

- LF–loaded RP+HPC liposomes remain physicochemically stable during gastric digestion; however, as expected under intestinal digestion liposomes are susceptible to pancreatin hydrolysis.
- The encapsulation of LF into RP+HPC liposomes does not compromise its antimicrobial and prebiotic properties on *S. aureus*, *B. infantis*, *B. longum*, and *L. plantarum* evaluated using the standard plate count method.
- The results obtained from liposomes elaborated under the thin-layer dispersion method can be the starting point to later be taken to industrial manufacturing systems.

6.3 FUTURE DIRECTIONS

Future work could be aimed to check antimicrobial bioactivity of LF–loaded RP+HPC liposomes on the heterogeneous intestinal bacterial population. It is necessary to evaluate the antibacterial activity of peptides generated by hydrolysis of LF after digestion. Additionally, the effectiveness of RP+HPC liposomes loaded with other bioactive compounds that undergo degradation through passage through the gastrointestinal system could be verified. On the other hand, the possibility of expanding the field of application of LF–loaded liposomes is considered, since LF has anti–inflammatory, antimicrobial, and prebiotic properties that can help patients suffering from pathologies that involve wounds or damage to the oral mucosa. RP could be able to form other encapsulation systems such as bicellar systems, which due to their size are more effective in dermatological applications. Finally, one important aspect that remain to solve is how to scale–up the

production of liposomes, surpassing the barrier presented by the sonication process used on a laboratory scale. A reliable technology for the reproducible production of liposomes for product development is needed.

References

Aceituno–Medina, M., Mendoza, S., Rodríguez, B. A., Lagaron, J. M., & López–Rubio, A. (2015). Improved antioxidant capacity of quercetin and ferulic acid during *in vitro* digestion through encapsulation within food–grade electrospun fibers. *Journal of functional foods, 12*, 332–341.

Acevedo, F., Rubilar, M., Jofré, I., Villarroel, M., Navarrete, P., Esparza, M., Romero, F., Vilches, E. A., Acevedo, V., & Shene, C. (2014). Oil bodies as a potential microencapsulation carrier for astaxanthin stabilisation and safe delivery. *Journal of Microencapsulation, 31*(5), 488–500.

Ach, D., Briançon, S., Dugas, V., Pelletier, J., Broze, G., & Chevalier, Y. (2015). Influence of main whey protein components on the mechanism of complex coacervation with Acacia gum. *Colloids and Surfaces A: Physicochemical and Engineering Aspects*, *481*, 367–374.

Aghbashlo, M., Mobli, H., Rafiee, S., & Madadlou, A. (2012). Energy and exergy analyses of the spray drying process of fish oil microencapsulation. *Biosystems Engineering, 111*(2), 229–241.

Agnihotri, N., Mishra, R., Goda, C., & Arora, M. (2012). Microencapsulation a novel approach in drug Delivery: A review. *Journal of Pharmaceutical Sciences, 2*(1), 1–20.

Akbarzadeh, A., Rezaei–Sadabady, R. R., Davaran, S., Joo, S. W., Zarghami, N., Hanifehpour, Y., Samiei, M., Kouhi M., & Nejati–Koshki, K., 2013. Liposome: classification, preparation, and applications. *Nanoscale Research Letters, 8*, 102.

Alexe, P., & Dima, C. (2014). Microencapsulation in food products. *AgroLife Scientific Journal, 3*(1), 9–14.

Anderson, J. M., & Shive, M. S. (2012). Biodegradation and biocompatibility of PLA and PLGA microspheres. *Advanced Drug Delivery Reviews, 64*, 72–82.

Andersson–Trojer, M., Nordstierna, L., Nordin, M., Nydén, M., & Holmberg, K. (2013). Encapsulation of actives for sustained release. *Physical Chemistry Chemical Physics, 15*, 17727–17741.

Andrade, M., Oseliero, P. L., Garcia, C., Sinigaglia–Coimbra, R., Pinto, C. L., & Pinho, S. C. (2018). Structural characterization of multilamellar liposomes coencapsulating curcumin and vitamin D3. *Colloids and Surfaces A, 549*, 112–121.

AOCS. (2009). Official Methods and Recommended Practices of the American Oil Chemists' Society; AOCS Press: Champaign, IL, USA. Method Ca 12–55.

Araujo–Díaz, S. B., Leyva–Porras, C., Aguirre–Bañuelos, P., Álvarez–Salas, C., & Saavedra–Leos, Z. (2017). Evaluation of the physical properties and conservation of the antioxidants content, employing inulin and maltodextrin in the spray drying of blueberry juice. *Carbohydrate Polymers, 167*(1), 317–325.

Atef Yekta, M., Verdonck, F., Van Den Broeck, W., Goddeeris, B. M., Cox, E., & Vanrompay, D. (2010). Lactoferrin inhibits *E. coli* O157:H7 growth and attachment to intestinal epithelial cells. *Veterinarni Medicina, 55*(8), 359–368.

Auriemma, G., Mencherini, T., Russo, P., Stigliani, M., Aquino, R. P., & Del Gaudio, P. (2013). Prilling for the development of multi–particulate colon drug delivery systems: Pectin vs. pectin–alginate beads. *Carbohydrate Polymers, 92*(1), 367–373.

Bakry, A. M., Abbas, S., Ali, B., Majeed, H., Abouelwafa, M. Y., Mousa, A., & Liang, L. (2016a) Microencapsulation of oils: a comprehensive review of benefits, techniques, and applications. *Comprehensive Review in Food Science and Food Safety, 15*, 143–182.

Bakry, A. M., Fang, Z., Ni, Y., Cheng, H., Chen, Y. Q., & Liang, L. (2016b). Stability of tuna oil and tuna oil/peppermint oil blend microencapsulated using whey protein isolate in combination with carboxymethyl cellulose or pullulan. *Food Hydrocolloids, 60*, 559–571.

Balcão, V. M., Costa, C. I., Matos, C. M., Moutinho, C. G., Amorim, M., Pintado, M. E., Gomes, A. P., Vila, M. M., & Teixeira, J. A. (2013). Nanoencapsulation of bovine lactoferrin for food and biopharmaceutical applications. *Food Hydrocolloids, 32*, 425–431

Bansode, S, S., Banarjee, S. K., Gaikwad, D. D., Jadhav, S. L., & Thorat, R. M. (2010). Microencapsulation: a review. *International Journal of Pharmaceutical Sciences Review and Research, 1*, 38–43.

Bellamy, W., Takase, M., Yamauchi, K., Wakabayashi, H., Kawase, K., & Tomita, M. (1992). Identification of the bactericidal domain of lactoferrin. Biochimica et Biophysica Acta, 1121, 130–136.

Beltrán, J. D., Sandoval–Cuellar C. D., Bauer, K., Quintanilla–Carvajal, M. J. (2019). In–vitro digestion of high–oleic palm oil nanoliposomes prepared with unpurified soy lecithin: Physical stability and nano–liposome digestibility. Colloids and Surfaces A: Physicochemical and Engineering Aspects, 578, 123603.

Bermúdez–Oria, A., Rodríguez–Gutiérrez, G., Rubio–Senent, F., Lama–Muñoz, A., & Fernández–Bolaños, J. (2017). Complexation of hydroxytyrosol and 3,4–dihydroxyphenylglycol with pectin and their potential use for colon targeting. *Carbohydrate Polymers, 163*, 292–300.

Bhushani, J. A., & Anandharamakrishnan, C. (2014). Electrospinning and electrospraying techniques: Potential food based applications. *Trends in Food Science and Technology*, *38*(1), 21–33.

Bilek, S. E, Yilmaz, F. M., & Özkan, G. (2017). The effects of industrial production on black carrot concentrate quality and encapsulation of anthocyanins in whey protein hydrogels. *Food and bioproducts processing, 102*, 72–80.

Boland, M. (2016). Human digestion – a processing perspective. *Journal of the Science of Food and Agriculture, 96*, 2275–2283.

Bragg, W. L. (1913). The diffraction of short electromagnetic waves by a crystal. *Proceedings of the Cambridge Philosophical Society, 17*, 43–57.

Burgos–Díaz, C., Rubilar, M., Morales, E., Medina, C., Acevedo, F., Marqués, A. M., & Shene, C. (2016). Naturally occurring protein–polysaccharide complexes from linseed (*Linum usitatissimum*) as bioemulsifiers. *European Journal of Lipid Science*, *118*(2), 165–174.

Bustamante, M., Oomah, D., Rubilar, M., & Shene, C. (2017). Effective *Lactobacillus plantarum* and *Bifidobacterium infantis* encapsulation with chia seed (*Salvia hispanica L.*) and flaxseed (*Linum usitatissimum L.*) mucilage and soluble protein by spray drying. *Food Chemistry, 216*, 97–105.

Casanova, F., Estevinho, B. N., & Santos, L. (2016). Preliminary studies of rosmarinic acid microencapsulation with chitosan and modified chitosan for topical delivery. *Powder Technology*, *297*, 44–49.

Ceci, L. N., Constenla, D. T., & Crapiste, G. H. (2008). Oil recovery and lecithin production using water degumming sludge of crude soybean oils. *Journal of the Science of Food and Agriculture, 88*, 2460–2466.

Chen, J., Wei, N., Lopez–Garcia, M., Ambrose, M., Lee, J., Annelin, C., & Peterson, T. (2017a). Development and evaluation of resveratrol, vitamin E, and epigallocatechin gallate loaded lipid nanoparticles for skin care applications. *European Journal of Pharmaceutics and Biopharmaceutics, 117*, 286–291.

Chen, L., Ren, F., Zhang, Z. P., Tong, Q. Y., & Rashed, M. M. A. (2015). Effect of pullulan on the short–term and long–term retrogradation of rice starch. *Carbohydrate Polymers, 115*, 415–421.

Chen, P. W., Liu, Z. S., Kuo, T. C., Hsieh, M. C., Li, Z. W. (2017b). Prebiotic effects of bovine lactoferrin on specific probiotic bacteria. *Biometals, 30*(2), 237–248.

Chen, Y., Xia, G., Zhao, Z., Xue, F., Gu, Y., Chen, C., & Zhang Y. (2020). 7,8–Dihydroxyflavone nano–liposomes decorated by crosslinked and glycosylated lactoferrin: storage stability, antioxidant activity, in vitro release, gastrointestinal digestion and transport in Caco–2 cell monolayers. Journal of Functional Foods, 65, 103742.

Cheng, J., Jun, Y., Qin, J., & Lee, S. H. (2017). Electrospinning versus microfluidic spinning of functional fibers for biomedical applications. *Biomaterials, 114*, 121–143.

Chiu, N., Tarrega, A., Parmenter, C., Hewson, L., Wolf, B., & Fisk, I. D. (2017). Optimisation of octinyl succinic anhydride starch stablised W1/O/W2 emulsions for oral destablisation of encapsulated salt and enhanced saltiness. *Food Hydrocolloids, 69*, 450–458.

Chivero, P., Gohtani, S., Yoshii, H., & Nakamura, A. (2016). Assessment of soy soluble polysaccharide, gum arabic and osa–starch as emulsifiers for mayonnaise–like emulsions. *LWT– Food Science and Technology, 69*, 59–66.

Cho, H. T., Salvia–Trujillo, L., Kim, J., Park, Y., Xiao, H., & McClements, D. J. (2014). Droplet size and composition of nutraceutical nanoemulsions influences bioavailability of long chain fatty acids and Coenzyme Q10. *Food Chemistry, 156*, 117–122.

Ciobanu, A., Mallard, I., Landy, D., Brabie, G., Nistor, D., & Fourmentin, S. (2013). Retention of aroma compounds from *Mentha piperita* essential oil by cyclodextrins and crosslinked cyclodextrin polymers. *Food Chemistry, 138*, 291–297.

Colletier, J. P., Chaize, B., Winterhalter, M., & Fournier, D. (2002). Protein encapsulation in liposomes: efficiency depends on interactions between protein and phospholipid bilayer. *BMC Biotechnology, 2*, 1–8.

Comunian, T. A., & Favaro–Trindade, C. S. (2016). Microencapsulation using biopolymers as an alternative to produce food enhanced with phytosterols and omega–3 fatty acids: A review. *Food Hydrocolloids, 61*, 442–457.

Comunian, T. A., Gomez–Estaca, J., Ferro–Furtado, R., Andrade, G. J., Freitas, I. C., Alves, I., & Favaro–Trindade, C. S. (2016). Effect of different polysaccharides and crosslinkers on echium oil microcapsules. *Carbohydrate Polymers, 150*, 319–329.

Cook, M. T., Tzortzis, G., Charalampopoulos, D., & Khutoryanskiy, V. V. (2014). Microencapsulation of a synbiotic into PLGA/alginate multiparticulate gels. *International Journal of Pharmaceutics, 466*, 400–408.

Cui, H., Li, W., Li, C., Vittayapadung, S., & Lin, L. (2016). Liposome containing cinnamon oil with antibacterial activity against methicillin–resistant *Staphylococcus aureus* biofilm. *Biofouling, 32*(2), 215–225.

Cui, L., & Decker, E. A. (2016). Phospholipids in foods: prooxidants or antioxidants?. *Journal of the Science of Food and Agriculture, 96*(1), 18–31.

Curic, A., Reul, R., Möschwitzer, J., & Fricker, G. (2013). Formulation optimization of itraconazole loaded PEGylated liposomes for parenteral administration by using design of experiments. *International Journal of Pharmaceutics, 448*(1), 189–197.

da Rosa–Zavareze, E., Telles, A. C., El Halal, S. L. M., da Rocha, M., Colussi, R., de Assis, L. M., & de Castro, L. A. S. (2014). Production and characterization of encapsulated antioxidative protein hydrolysates from Whitemouth croaker (*Micropogonias furnieri*) muscle and byproduct. *LWT – Food Science and Technology, 59*(2), 841–848.

Dafe, A., Etemadi, H., Dilmaghani, A., & Mahdavinia, G. R. (2017). Investigation of pectin/starch hydrogel as a carrier for oral delivery of probiotic bacteria. *International Journal of Biological Macromolecules, 97*, 536–543.

de Barros, R. V., Alvarenga, D., Keven, E., Vilela, S., Rodrigues, C., Yoshida, M. I., Pessoa de Andrade, J., & Monteiro, R. C. (2016). Cashew gum and inulin: New alternative for ginger essential oil microencapsulation. *Carbohydrate Polymer, 153*, 133–142.

De Figueiredo, G., Guedes, K., Paim, C., & Lopes, R. (2018). *In vitro* digestibility of heteroaggregated droplets coated with sodium caseinate and lactoferrin. *Journal of Food Engineering, 229*, 86–92.

de Haas, G. H., Sarda, L., & Roger, J. (1965). Positional specific hydrolysis of phospholipids by pancreatic lipase. *Biochimica et Biophysica Acta, 106*, 638–640.

Desai, S., Poddar, A., & Sawant, K. (2016). Formulation of cyclodextrin inclusion complex–based orally disintegrating tablet of eslicarbazepine acetate for improved oral bioavailability. *Materials Science and Engineering C, 58*, 826–834.

Devasari, N., Dora, C.P., Singh, C., Paidi, S. R., Kumar, V., Sobhia, M. E., & Suresh, S. (2015). Inclusion complex of erlotinib with sulfobutyl ether–β–cyclodextrin: Preparation, characterization, *in silico*, *in vitro* and *in vivo* evaluation. *Carbohydrate Polymers, 10*(134), 547–556.

Dias, M. I., Ferreira, I. C., & Barreiro, M. F. (2015). Microencapsulation of bioactives for food applications. *Food and Function, 6*(4), 1035–1052.

Dima, C., Cotârlet, M., Alexe, P., & Dima, S. (2014). Microencapsulation of essential oil of pimento [*Pimenta dioica* (L) Merr.] by chitosan/k–carrageenan complex coacervation method. *Innovative Food Science and Emerging Technologies, 22*, 203–211.

Dima, S., Dima, C., & Iordachescu, G. (2015). Encapsulation of functional lipophilic food and drug biocomponents. *Food Engineering Reviews, 7*(4), 417–438.

Drosou, C. G., Krokida, M. K., & Biliaderis, C. G. (2017). Encapsulation of bioactive compounds through electrospinning/electrospraying and spray drying: a comparative assessment of food related applications. *Drying Technology, 35*(2), 139–162.

Edison, B. (2009). Analysis of tocopherols by high performance liquid chromatography. *Journal of Chemistry, 6*(2), 395–398.

Eloy, J. O., Claro de Souza, M., Petrilli, R., Barcellos, J. P., Lee, R. J., & Marchetti, J. M. (2014). Liposomes as carriers of hydrophilic small molecule drugs: Strategies to enhance encapsulation and delivery. *Colloids Surf. B Biointerfaces, 123*, 345–363.

Elsabee, Z. M., & Abdou, S. E. (2013). Chitosan based edible films and coatings: A review Materials. *Science and Engineering: C, 33*, 1819–1841.

Espirito, I., Campardelli, R., Cabral, E., Vieira de Melo, S., Della Porta, G., & Reverchon, E. (2014). Liposomes preparation using a supercritical fluid assisted continuous process. *Chemical Engineering Journal, 249*, 153–159.

Estevinho, B. N., Rocha, F., Santos, L., & Alves, A. (2013). Microencapsulation with chitosan by spray drying for industry applications – a review. *Trends in Food Science and Technology, 31*(2), 138–155.

Fang, Z., & Bhandari, B. (2010). Encapsulation of polyphenols – a review. *Trends in Food Science and Technology, 21*(10), 510–523.

Fathi, M., Martín, A., & McClements, D. J. (2014). Nanoencapsulation of food ingredients using carbohydrate based delivery systems. *Trends in Food Science and Technology, 39*(1), 18–39.

Fathi, M., Mozafari, M. R., & Mohebbi, M. (2012). Nanoencapsulation of food ingredients using lipid based delivery systems. *Trends in Food Science & Technology, 23*, 13–27.

Flores, F. P, & Kong, F. (2017). *In vitro* release kinetics of microencapsulated materials and the effect of the food matrix. *Annual Review of Food Science and Technology, 28*(8), 237–259.

Furlund, C. B., Ulleberg, E. K., Devold, T. G., Flengsrud, R., Jacobsen, M., Sekse, C., Holm, H., & Vegarud, G. E. (2013). Identification of lactoferrin peptides generated by digestion with human gastrointestinal enzymes. *Journal of Dairy Science, 96*(1), 75–88.

Gaonkar, A. G., Vasisht, N., Khare, A. R., & Sobel, R. (2014). Microencapsulation in the food industry: a practical implementation guide. Academic Press. San Diego, USA.

Garti, N., & McClements, D. J. (2012). Encapsulation technologies and delivery systems for food ingredients and nutraceuticals. Woodhead Publishing, Philadelphia.

Gentile, P., Chiono, V., Carmagnola, I., & Hatton, P. V. (2014). An overview of poly(lactic–co–glycolic) acid (PLGA)–based biomaterials for bone tissue engineering. *International Journal of Molecular Sciences, 15*, 3640–3659.

Gharib, R., Greige–Gerges, H., Fourmentin, S., Charcosset, C., & Auezova, L. (2015). Liposomes incorporating cyclodextrin–drug inclusion complexes: Current state of knowledge. *Carbohydrate Polymers, 129*, 175–186.

Gibis, M., Ruedt, C., & Weiss, J. (2016). *In vitro* release of grape–seed polyphenols encapsulated from uncoated and chitosan–coated liposomes. *Food Research International, 88*, 105–113.

Gómez–Estaca, J., Gavara, R., & Hernández–Muñoz, P. (2015). Encapsulation of curcumin in electrosprayed gelatin microspheres enhances its bioaccessibility and widens its uses in food applications. *Innovative Food Science and Emerging Technologies, 29*, 302–307.

Gonçalves, V. S. S., Poejoab, J., Matias, A. A., Rodríguez–Rojo, S., Cocero, M. J., & Duarte, C. M. M. (2016). Using different natural origin carriers for development of epigallocatechin gallate (EGCG) solid formulations with improved antioxidant activity by PGSS–drying. *RSC advances, 6*, 67599–67609.

Grimaldi, N., Andrade, F., Segovia, N., Ferrer–Tasies, L., Sala, S., Veciana, J., & Ventosa, N. (2016). Lipid–based nanovesicles for nanomedicine. *Chemical Society Reviews, 45*(23), 6520–6545.

Gulao, E. D. S., De Souza, C. J. F., Da Silva, F. A. S., Coimbra, J. S. R., & García–Rojas, E. E. (2014). Complex coacervates obtained from lactoferrin and gum arabic: Formation and characterization. *Food Research International, 65*, 367–374.

Guner, S., & Oztop, M. H. (2017). Food grade liposome systems: Effect of solvent, homogenization types and storage conditions on oxidative and physical stability. *Colloids and Surfaces A: Physicochemical and Engineering, 513*, 468–478.

Gupta, C., Chawla, P., Arora, S., Tomar, S. K., & Singh, A. K. (2015). Iron microencapsulation with blend of gum arabic, maltodextrin and modified starch using modified solvent evaporation method – Milk fortification. *Food Hydrocolloids, 43*, 622–628.

Gupta, S., De Mel, J. U., & Schneider, G. (2019). Dynamics of liposomes in the fluid phase. *Current Opinion in Colloid & Interface Science, 42*, 121–136.

Hamosh, M. (1998). Protective function of proteins and lipids in human milk. *Biolgy of the Neonate, 74*, 163–176.

Haney, E. F., Nazmi, K., Bolscher, J. G. M., Vogel, H. J. (2012). Structural and biophysical characterization of an antimicrobial peptide chimera comprised of lactoferricin and lactoferrampin. Biochimica et Biophysica Acta, 1818, 762–775.

Hasan, M., Belhaj, N., Benachour, H., Barberi–Heyobb, M., Kahnf, C. J. F., Jabbari, E., Linder, M., & Arab–Tehrany, E. (2014). Liposome encapsulation of curcumin: Physico–chemical characterizations and effects on MCF7 cancer cell proliferation. *International Journal of Pharmaceutics, 461*, 519–528.

Henna–Lu, F. S., Nielsen, N. S., Baron, C. P., Diehl, B. W. K., & Jacobsen, C. (2012). Oxidative stability of dispersions prepared from purified marine phospholipid and the role of α–tocopherol. *Journal of Agricultural and Food Chemistry, 60*(50), 12388–12396.

Hong, Y., Liu, G., & Gu, Z. (2014). Recent advances of starch–based excipients used in extended–release tablets: a review. *Drug Delivery, 23*(1), 12–20.

Hoyos–Leyva, J. D., Bello–Pérez, L. A., Alvarez–Ramirez, J., & García, H. S. (2016). Microencapsulation using starch as wall material: A review. *Food Reviews International, 34*(2), 148–161.

Husain, O., Lau, W., Edirisinghe, M., & Parhizkar, M. (2016). Investigating the particle to fibre transition threshold during electrohydrodynamic atomization of a polymer solution. *Materials Science and Engineering C, 65*, 240–250.

Iglesias–Figueroa, B. F., Espinoza–Sánchez, E. A., Siqueiros–Cendón, T. S., & Rascón–Cruz, Q. (2019). Lactoferrin as a nutraceutical protein from milk, an overview. *International Dairy Journal 89*, 37–41.

Imran, M., Revol–Junelles, A. M., Paris, C., Guedon, E., Linder, M., Desobry, S. (2015). Liposomal nanodelivery systems using soy and marine lecithin to encapsulate food biopreservative nisin. *LWT – Food Science and Technology, 62*(1), 341–349.

Ishikado, A., Imanaka, H., Takeuchi, T., Harada, E., & Makino, T. (2005). Liposomalization of lactoferrin enhanced its anti–inflammatory effects via oral administration. *Biological and Pharmaceutical Bulletin, 28*, 1717–1721.

Ishwarya, S. P, Anandharamakrishnan, C., & Stapley, A. G. F. (2014). Spray–freeze drying: A novel process for the drying of foods and bioproducts. *Trends in Food Science and Technology, 41*(2), 161–181.

Jafari, S. M., & McClements, D. J. (2017). Chapter One – Nanotechnology Approaches for Increasing Nutrient Bioavailability. *Advances in Food and Nutrition Research, 81*, 1–30.

Jambhekar, S. S, & Breen, P. (2016). Cyclodextrins in pharmaceutical formulations I: structure and physicochemical properties, formation of complexes, and types of complex. *Drug Discovery Today, 21*(2), 356–362.

Ji, J., Zhang, J., Chen, J., Wang, Y., Dong, N., Hu, C., Chen, H., Li, G., Pan, X., & Wu, C. (2015). Preparation and stabilization of emulsions stabilized by mixed sodium caseinate and soy protein isolate. *Food Hydrocolloids, 51*, 156–165.

Jovanović, A. A., Balanč, B. D., Ota, A., Grabnar, P. A., Djordjević, V. B., Šavikin, K. P., Bugarski, B. M., Nedović, V. A., & Ulrih N. P. (2018). Comparative effects of cholesterol and β-sitosterol on the liposome membrane characteristics. *European Journal of Lipid Science and Technology, 120*(9), 1800039.

Jyothi, N. V. N., Prasanna, P. M., Sakarkar, S. N., Prabha, K. S., Ramaiah, P. S., & Srawan, G. Y. (2010). Microencapsulation techniques, factors influencing encapsulation efficiency. *Journal of Microencapsulation, 27*, 187–197.

Kaddaha, S., Khreich, N., Kaddah, F., Charcosset, C., & Greige–Gerges, H. (2018). Cholesterol modulates the liposome membrane fluidity and permeability for a hydrophilic molecule. *Food and Chemical Toxicology, 113*, 40–48

Kanwar, J. R., Roy, K., Patel, Y., Zhou, S. F., Singh, M. R., Singh, D., Nasir, M., Sehgal, R., Sehgal, A., Singh, R. S., Garg, S., & Kanwar, R. K. (2015). Multifunctional iron bound lactoferrin and nanomedicinal approaches to enhance its bioactive functions. *Molecules, 20*, 9703–9731.

Karaca, A. C., Low, N. H., & Nickerson, M. T. (2015). Potential use of plant proteins in the microencapsulation of lipophilic materials in foods: A review. *Trends in Food Science & Technology, 42*(1), 5–12.

Kastner, E., Kaur, R., Lowry, D., Moghaddam, B., Wilkinson A., & Perrie, A. (2015). High-throughput manufacturing of size-tuned liposomes by a newmicrofluidics method using enhanced statistical tools forcharacterization. *International Journal of Pharmaceutics, 477*, 361–368

Katouzian, I., & Jafari, S. M. (2016). Nano–encapsulation as a promising approach for targeted delivery and controlled release of vitamins. *Trends in Food Science and Technology, 53*, 34–48.

Khattab, A., & Zaki, N. (2017). Optimization and evaluation of gastroretentive ranitidine HCl microspheres by using factorial design with improved bioavailability and mucosal integrity in ulcer model. *AAPS PharmSciTech*, 1–17.

Kim, I. H., Lee, H., Kim, J. E., Song, K. B., Lee, Y. S., Chung, D. S., & Min, S. C. (2013). Plum coatings of lemongrass oil–incorporating carnauba wax–based nanoemulsion. *Journal of Food Sciences, 78*(10), 1551–1559.

Kiselev, M. A., & Lombardo, D. (2017). Structural characterization in mixed lipid membrane systems by neutron and X–ray scattering. *Biochimica et Biophysica Acta, 1861*, 3700–3717.

Klein, M., Aserin, A., Svitov, I., & Garti, N. (2010). Interactions between whey protein isolate and gum arabic. *Colloids Surf B Biointerfaces, 79*(2), 377–383.

Kokkona, M., Kallinteri, P., Fatouros, D., & Antimisiaris, S. G. (2000). Stability of SUV liposomes in the presence of cholate salts and pancreatic lipases: effect of lipid composition. *European Journal of Pharmaceutical Sciences, 9*, 245–252.

Koyani, R. D., & Vazquez–Duhalt, R. (2016). Laccase encapsulation in chitosan nanoparticles enhances the protein stability against microbial degradation. *Environmental Science and Pollution Research, 23*(18), 18850–18857.

Kuck, L. S., & Zapata, C. P. (2016). Microencapsulation of grape (*Vitis labrusca* var. Bordo) skin phenolic extract using gum Arabic, polydextrose, and partially hydrolyzed guar gum as encapsulating agents. *Food Chemistry, 194*, 569–576.

Kuhn, K. R., Silva, F. G. D., Netto, F. M., & da Cunha, R. L. (2014). Assessing the potential of flaxseed protein as an emulsifier combined with whey protein isolate. *Food Research International, 58*, 89–97.

Kumar, L. R. G., Chatterjee, N. S., Tejpal, C. S., Vishnu, K.V., Anas, K. K., Asha, K. K., Anandan, R, & Mathew, S. (2017). Evaluation of chitosan as a wall material for microencapsulation of squalene by spray drying: Characterization and oxidative stability studies. *International Journal of Biological Macromolecules, 134*, 1986–1995.

Laemmli, U. (1970). Cleavage of structural proteins during the assembly of the head of bacteriophage T4. *Nature, 227*, 680–685.

Lam, P. L., & Gambari, R. (2014). Advanced progress of microencapsulation technologies: *In vivo* and *in vitro* models for studying oral and transdermal drug deliveries. *Journal of Controlled Release, 178*, 25–45.

Latuga, M. S., Stuebe, A., & Seed, P. C. (2014). A review of the source and function of microbiota in breast milk. *Seminars in Reproductive Medicine, 32*, 68–73.

Leong, J. Y., Lam, W. H., Ho, K. W., Voo, W. P., Lee, M. F. X., Lim, H. P., Lim, S. L., Tey, B. T., Poncelet, D., & Chan, E. S. (2016). Advances in fabricating spherical alginate hydrogels with controlled particle designs by ionotropic gelation as encapsulation systems. *Particuology, 24*, 44–60.

Li, H., Zhu, K., Zhou, H., & Peng, W. (2012). Effects of high hydrostatic pressure treatment on allergenicity and structural properties of soybean protein isolate for infant formula. *Food Chemistry, 132*, 808–814.

Li, Q., Lan, H., & Zhao, Z. (2019). Protection effect of sodium alginate against heat–induced structural changes of lactoferrin molecules at neutral pH. *LWT – Food Science and Technology, 99*, 513–518.

Li, S. (2017). Science and principles of biodegradable and bioresorbable medical polymers. Materials and properties. Woodhead Publishing is an imprint of Elsevier. (Ed. By Xiang Cheng Zhang). Duxford, UK. 37–78pp.

Liang, H., Friedman, J. M., & Nacharaju, P. (2016). Fabrication of biodegradable PEG–PLA nanospheres for solubility, stabilization, and delivery of curcumin. *Artificial Cells, Nanomedicine and Biotechnology, 45*(2), 297–304.

Liu, J., Willfo, S., & Xun, C. (2015). A review of bioactive plant polysaccharides: Biological activities, functionalization, and biomedical applications. *Bioactive Carbohydrates and Dietary Fibre*, 5, 31–61.

Liu, L., Wu, F., Ju, X. J., Xie, R., Wang, W., Niu, C. H., & Chu, L. Y. (2013a). Preparation of monodisperse calcium alginate microcapsules via internal gelation in microfluidic generated double emulsions. *Journal of Colloid and Interface Science, 404*, 85–90.

Liu, W., Lu, J., Ye, A., Xu, Q., Tian, M., Kong, Y., Wei, F., & Han, J. (2018). Comparative performances of lactoferrin–loaded liposomes under *in vitro* adult and infant digestion models. *Food chemistry, 258*, 366–373.

Liu, W., Wei, F., Ye, A., Tian, M., & Han, J. (2017). Kinetic stability and membrane structure of liposomes during *in vitro* infant intestinal digestion: Effect of cholesterol and lactoferrin. *Food Chemistry, 230*, 6–13.

Liu, W., Ye, A., Han, F., & Han, J. (2019). Advances and challenges in liposome digestion: Surface interaction, biological fate, and GIT modeling. *Advances in Colloid and Interface Science, 263*, 52–67.

Liu, W., Ye, A., Liu, W., Liu, C., & Singh, H. (2013b). Stability during *in vitro* digestion of lactoferrin–loaded liposomes prepared from milk fat globule membrane–derived phospholipids. *Journal of Dairy Science, 96*, 2061–2070.

Llorens, E., Ibáñez, H., del Valle, L. J., & Puiggalí, J. (2016). Biocompatibility and drug release behavior of scaffolds prepared by coaxial electrospinning of poly(butylene succinate) and polyethylene glycol. *Materials Science and Engineering C, 49*, 472–484.

López, O., de la Maza, A., Coderch, L., López–Iglesias, C., Wehrli, E., & Parra, J. L. (1998). Direct formation of mixed micelles in the solubilization of phospholipid liposomes by Triton X–100. *FEBS Letters, 426*, 314–318.

Lowry, O. H., Rosebrough, N. J., Fan, A. L., & Randall, R. J. (1951). Protein measurement with Folin phenol reagent. *Journal of Biological Chemistry, 193*, 256–275.

Ma, J., Guan, R., Chen, X., Wang, Y., Hao, Y., Ye, X., & Liu, M. (2014). Response surface methodology for the optimization of beta–lactoglobulin nano–liposomes. *Food & Function*, *5*(4), 748–754.

Machado, A. R., Pinheiro, A. C., Vicente, A. A., Souza–Soares, L. A., & Cerqueira, M. A. (2019). Liposomes loaded with phenolic extracts of Spirulina LEB–18: Physicochemical characterization and behavior under simulated gastrointestinal conditions. *Food Research International*, *120*, 656–667.

Macocinschi, D., Filip, D., Vlad, S., Cernatescu, C., Tuchilus, C. G., Gafitanu, C. A., & Dumitriu, R. P. (2015). Electrospun/electrosprayed polyurethane biomembranes with ciprofloxacin and clove oil extract for urinary devices. *Journal of Bioactive and Compatible Polymers*, *30*(5), 509–523.

Mahdavi, S. A., Jafari, S.M., Ghorbani, M., & Assadpoor, E. (2014). Spray–drying microencapsulation of anthocyanins by natural biopolymers: a review. *Drying Technology*, *32*(5), 509–518.

Maherani, B., Arab–Tehrany, E., Kheirolomoom, A., Geny, D., & Linder, M. (2013). Calcein release behavior from liposomal bilayer; influence of physicochemical/mechanical/structural properties of lipids. *Biochimie*, *95*(11), 2018–2033.

Maherani, B., Arab–Tehrany, E., Kheirolomoom, A., Reshetov, V., Stebee, M. J., & Linder, M. (2012). Optimization and characterization of liposome formulation by mixture design. *Analyst*, *137*, 773–786.

Marfil, P. H. M., Vasconcelos, F. H. T., Pontieri, M. H., & Telis, V. R. N. (2015). Development and validation of analytical method for palm oil determination in microcapsules produced by complex coacervation. *Química Nova*, *39*, 94–99.

Marín, D., Alemán, A., Montero, P., & Gómez–Guillén, M. C. (2018). Encapsulation of food waste compounds in soy phosphatidylcholine liposomes: Effect of freeze–drying, storage stability and functional aptitude. *Journal of Food Engineering*, *223*, 132–143.

Marsanasco, M., Piotrkowski, B., Calabró, V., del Valle, Alonso, S., & Chiaramoni, N. S. (2015). Bioactive constituents in liposomes incorporated in orange juice as new functional food: thermal stability, rheological and organoleptic properties. *Journal of Food Science and Technology*, *52*(12), 7828–7838.

Martins, I. M. D. (2012). Microencapsulation of thyme oil by coacervation: production, characterization and release evaluation, PhD thesis, Faculdade de Engenharia da Universidade do Porto, Porto.

Martins, I., Barreiro, M., Coelho, M., & Rodrigues, A. (2014). Review Microencapsulation of essential oils with biodegradable polymeric carriers for cosmetic applications. *Chemical Engineering Journal*, *245*, 191–200.

McClements, D. J. (2015a). Reduced–fat foods: the complex science of developing diet–based strategies for tackling overweight and obesity. *Advances in Nutrition: An International Review Journal*, *6*, 338–352.

McClements, D. J. (2015b). Encapsulation, protection, and release of hydrophilic active components: potential and limitations of colloidal delivery systems. *Advances in Colloid and Interface Science*, *219*, 27–53.

McClements, D. J. (2016). Interfacial properties and their characterization. Food emulsions: Principles, practices, and techniques. (3rd ed.). Taylor & Francis Group. Boca Raton, FL: CRC Press. pp. 185–244.

McClements, D. J., & Gumus, C. E. (2016). Natural emulsifiers – Biosurfactants, phospholipids, biopolymers, and colloidal particles: Molecular and physicochemical basis of functional performance. *Advances in Colloid and Interface Science, 234*, 3–26.

Meshulam, D., & Lesmes, U. (2014). Responsiveness of emulsions stabilized by lactoferrin nano–particles to simulated intestinal conditions. *Food & Function, 5*, 65–73.

Minekus, M., Alminger, M., Alvito, P., Balance, S., Bohn, T., Bourlieu, C., Carriere, F., Boutrou, R., Corredig, M., Dupont, D., Dufour, C., Egger, L., Golding, M., Karakaya, S., Kirkhus, B., Le Feunteun S., Lesmes, U., Macierzanka, A., Mackie, A., Marze, S., McClements, D. J., Menard, O., Recio, I., Santos, C. N., Singh, R. P., Vegarud, G. E., Wickham, M. S. J., Weitschies, W., & Brodkorb, A. (2014). A standardised static *in vitro* digestion method suitable for food – an international consensus. *Food Function, 5*, 1113–1124.

Mohan, A., Rajendran, S. R. C. K., He, Q. S., Bazinetc, L., & Udenigwe, C. C. (2015). Encapsulation of food protein hydrolysates and peptides: a review. *The Royal Society of Chemistry, 5*, 79270–79278.

Moomand, K., & Lim, L. T. (2014). Oxidative stability of encapsulated fish oil in electrospun zein fibres. *Food Research International, 62*, 523–532.

Morales, E., Rubilar, M., Burgos–Díaz, C., Acevedo, F., Penning, M., & Shene, C. (2017). Alginate/Shellac beads developed by external gelation as a highly efficient model system for oil encapsulation with intestinal delivery. *Food Hydrocolloids, 70*, 321–328.

Moran–Valero, M. I., Pizones, V. M., & Pilosof, A. M. R. (2017). Synergistic performance of lecithin and glycerol monostearate in oil/water emulsions. *Colloids and Surfaces B: Biointerfaces, 151*, 68–75.

Moreira, A. G. C., Martins, I. M., Fernandes, I., Barreiro, M. F., & Rodrigues, A. E. (2016). Microencapsulation of red and white thyme oil in poly(lactic–coglycolic) acid: assessment of encapsulation efficiency and antimicrobial capacity of the produced microcapsules. *The Canadian Journal of Chemical Engineering, 94*, 469–475.

Moreno–Expósito, L., Illescas–Montes, R., Melguizo–Rodríguez, L., Ruiz, C., Ramos–Torrecillas, J., & de Luna–Bertos E. (2018). Multifunctional capacity and therapeutic potential of lactoferrin. *Life Sciences, 195*, 61–64.

Moscovici, A, M., Joubran, Y., Briard–Bion, V., Mackie A., Dupont, D., & Lesmes, U. (2014). The impact of the Maillard reaction on the in vitro proteolytic breakdown of bovine lactoferrin in adults and infants. Food & Function, 5, 1898–1908

Mosquera, M., Giménez, B., da Silva, I.M., Boelter, J.F., Montero, P., Gómez–Guillén, M.C., & Brandelli, A. (2014). Nanoencapsulation of an active peptidic fraction from sea bream scales collagen. *Food Chemistry, 156*, 144–150.

Mura, P. (2015). Analytical techniques for characterization of cyclodextrin complexes in the solid state: A review. *Journal of Pharmaceutical and Biomedical Analysis, 113*, 226–238.

Nacka, F., Cansell, M., Gouygou, J. P., Gerbeaud, C., Méléard, P., & Entressangles, B. (2001). Physical and chemical stability of marine lipid–based liposomes under acid conditions. *Colloids Surf. B Biointerfaces, 20*, 257–266.

Nesterenko, A., Alric, I., Silvestre, F., & Durrieu, V. (2013). Vegetable proteins in microencapsulation: A review of recent interventions and their effectiveness. *Industrial Crops and Products, 42*, 469–379.

Neunert, G., Tomaszewska–Gras, J., Siejak, P., Pietralik, Z., Kozak, M., & Polewski, K. (2018). Disruptive effect of tocopherol oxalate on DPPC liposome structure: DSC, SAXS, and fluorescence anisotropy studies. *Chemistry and Physics of Lipid, 216*, 104–113.

Nezarati, R. M., Eifert, M. B., & Cosgriff–Hernandez, E. (2013). Effects of humidity and solution viscosity on electrospun fiber morphology. *Tissue Engineering: Part C, 19*(10), 810–819.

Niu, Z., Loveday, S. M., Barbe, V., Thielen, I., He, Y., & Singh, H. (2019). Protection of native lactoferrin under gastric conditions through complexation with pectin and chitosan. *Food hydrocolloids, 93*, 120–130.

Oliveira, J., Claro de Souza, M., Petrilli, R., Palma, Abriata Barcellos, J., Lee, R. J., & Maldonado, J. (2014). Liposomes as carriers of hydrophilic small molecule drugs: Strategies to enhance encapsulation and delivery. *Colloids and Surfaces B: Biointerfaces, 123*, 345–363.

Onishi, H. (2011). Lactoferrin delivery systems: approaches for its more effective use. *Expert Opinion on Drug Delivery, 8*(11), 1469–1479.

Ortíz–Estrada, G., Luna–Castro, S., Piña–Vázquez, C., Samaniego–Barrón, L., León–Sicairos, N., Serrano–Luna, J., & de la Garza, M. (2012). Iron–saturated lactoferrin and pathogenic protozoa: could this protein be an iron source for their parasitic style of life? *Future Microbiology, 7*, 149–164.

Paini, M., Daly, S. R., Aliakbarian, B., Fathi, A., Tehrany, E. A., Perego, P., Dehghani, F., & Valtchev, P. (2015). An efficient liposome based method for antioxidants encapsulation. *Colloids and Surfaces B: Biointerfaces, 136*, 1067–1072.

Paulo, F., & Santos, L. (2017). Design of experiments for microencapsulation applications: A review. *Materials Science and Engineering: C, 77*, 1327–1340.

Peng, C., Zhao, S. Q., Zhang, J., Huang, G. Y., Chen, L. Y., & Zhao, F. Y. (2014). Chemical composition, antimicrobial property and microencapsulation of Mustard (*Sinapis alba*) seed essential oil by complex coacervation. *Food Chemistry, 165*, 560–568.

Peng, Z., Li, J., Guan, Y., & Zhao, G. (2013). Effect of carriers on physicochemical properties, antioxidant activities and biological components of spray–dried purple sweet potato flours. *LWT – Food Science and Technology, 51*, 348–355.

Pereira, A. C., Gurak, P. D., & Ferreira, L. D. (2016). Maltodextrin, pectin and soy protein isolate as carrier agents in the encapsulation of anthocyanins–rich extract from *jaboticaba pomace*. *Food and Bioproducts Processing, 102*, 186–194.

Piornos, J. A., Burgos–Díaz, C., Morales. E., Rubilar, M., & Acevedo, F. (2017). Highly efficient encapsulation of linseed oil into alginate/lupin protein beads: Optimization of the emulsion formulation. *Food Hydrocolloids, 63*, 139–148.

Rahnfeld, L., Thamm, J., Steiniger, F., van Hoogevest, P., & Luciani, P. (2018). Study on the in situ aggregation of liposomes with negatively charged phospholipids for use as injectable depot formulation. *Colloids and Surfaces B: Biointerfaces, 168*, 10–17.

Ranadheera, C. S., Liyanaarachchi, W. S., Chandrapala, J., Dissanayake, M., & Vasiljevic, T. (2016). Utilizing unique properties of caseins and the casein micelle for delivery of sensitive food ingredients and bioactives. *Trends in Food Science & Technology, 57*, 178–187.

Ratti, C. (2013). Handbook of food powders: processes and properties. A volume in Woodhead Publishing Series in Food Science, Technology and Nutrition. (Ed. by: B. Bhandari, N. Bansal, M. Zhang and P. Schuck). 3 – Freeze drying for food powder production. Philadelphia, USA. Pages 57–84.

Ray, S., Raychaudhuri, U., & Chakraborty, R. (2016). An overview of encapsulation of active compounds used in food products by drying technology. *Food Bioscience, 13*, 76–83.

Rhim, J. W. (2013). Preparation and characterization of vacuum sputter silver coated PLA film. *LWT – Food Science and Technology, 54*, 477–484.

Ribeiro, D., Alvarenga, D., De Barros, R. V., & Vilela, S. (2017). Encapsulation as a tool for bioprocessing of functional foods. *Current Opinion in Food Science, 13*, 31–37.

Rodríguez, G., Cócera, M., Rubio, L., Alonso, C., Pons, R., Sandt, C., Dumas, P., López–Iglesias, C., de la Maza, A., & López, O. (2012). Bicellar systems to modify the phase behaviour of skin stratum corneum lipids. *Physical Chemistry Chemical Physics, 14*, 14523–14533.

Rodríguez, J., Martín, M. J., Ruiz, M. A., & Clares, B. (2016). Current encapsulation strategies for bioactive oils: from alimentary to pharmaceutical perspectives. *Food Research International, 83*, 41–59.

Romero–Arrieta, M. R., Uria–Canseco, E., & Perez–Casas, S. (2019). Simultaneous encapsulation of hydrophilic and lipophilic molecules in liposomes of DSPC. *Thermochimica Acta, 687*, 178462.

Sabouri, S., Wright, A. J., & Corredig, M. (2017). *In vitro* digestion of sodium caseinate emulsions loaded with epigallocatechin gallate. *Food Hydrocolloids, 69*, 350–358.

Sagis, L. M. C. (2015). Microencapsulation and microspheres for food applications 1st Edition, Kindle Edition. London: Academic Press.

Salvia–Trujillo, L., Qian, C., Martín–Belloso, O., & McClements, D. J. (2013). Influence of particle size on lipid digestion and β–carotene bioaccessibility in emulsions and nanoemulsions. *Food Chemistry, 141*(2), 1472–1480.

Sánchez, F. M., García, F., Calvo, P., Bernalte, M. J., & González–Gómez, D. (2016). Optimization of broccoli microencapsulation process by complex coacervation using response surface methodology. *Innovative Food Science and Emerging Technologies, 34*, 243–249.

Sánchez, M. T., Ruiz, M. A., Lasserrot, A., Hormigo, M., & Morales, M. E. (2017). An improved ionic gelation method to encapsulate *Lactobacillus* spp. bacteria: Protection, survival and stability study. *Food Hydrocolloids, 69*, 67–75.

Sarabandi, K., Mahoonak, A. S., Hamishehkar, H., Ghorbani, M., Jafari, S. M. (2019): Protection of casein hydrolysates within nanoliposomes: Antioxidant and stability characterization. *Journal of Food Engineering, 251*, 19–28.

Sarkar, A., Horne, D. S., & Singh, H. (2010). Pancreatin–induced coalescence of oil–in–water emulsions in an *in vitro* duodenal model. *International Dairy Journal, 20*, 589–597.

Sathyabama, S., Ranjith, M., Bruntha, P., Vijayabharathi, R., & Brindha, V. (2014). Co–encapsulation of probiotics with prebiotics on alginate matrix and its effect on viability in simulated gastric environment. *LWT– Food Science and Technology, 57*(1), 419–425.

Semalty, A., Tanwar, Y. S., & Semalty, M. (2014). Preparation and characterization of cyclodextrin inclusion complex of naringenin and critical comparison with phospholipid complexation for improving solubility and dissolution. *The Journal of Thermal Analysis and Calorimetry, 115*, 2471–2478.

Shah, S., Dhawan, V., Holm, R., Nagarsenker M. S., & Perrie, Y. (2020). Liposomes: Advancements and innovation in the manufacturing process. *Advanced Drug Delivery Reviews,* In Press, Corrected Proof.

Sheikh, Z., Najeeb, S., Khurshid, Z, Verma, V., Rashid, H., & Glogauer, M. (2015). Biodegradable materials for bone repair and tissue engineering applications. *Materials, 8*, 5744–5794.

Shene, C., Monsalve, M.T., Vergara, D., Lienqueo, M.E., & Rubilar, M. (2016). High pressure homogenization of *Nannochloropsis oculata* for the extraction of intracellular components: effect of process conditions and culture age. *European Journal of Lipid Science and Technology*, *118*, 631–639.

Sherman, M. P., Bennett, S. H., Hwang, F. F., & Yu, C. (2014). Neonatal small bowel epithelia: enhancing anti–bacterial defense with lactoferrin and Lactobacillus GG. Biometals, 17, 285–289.

Silva, R., Ferreira, H., Little, C., & Cavaco–Paulo, A. (2010). Effect of ultrasound parameters for unilamellar liposome preparation. *Ultrasonics Sonochemistry*, *17*, 628–632.

Singh, H., & Thompson, A. (2012). 11–Liposomes as food ingredients and nutraceutical delivery systems. Encapsulation technologies and delivery systems for food ingredients and nutraceuticals. Pages 287–318.

Singh, R.P., Gangadharappa, H. V., & Mruthunjaya, K. (2017). Phospholipids: Unique carriers for drug delivery systems. *Journal of Drug Delivery Science and Technology*, *39*, 166–179.

Soukoulis, C., Tsevdou, M., Andre, C. M., Cambier, S., Yonekura, L., Taoukis, P. S., & Hoffmann, L. (2017). Modulation of chemical stability and *in vitro* bioaccessibility of beta–carotene loaded in kappa–carrageenan oil–in–gel emulsions. *Food Chemistry*, *220*, 208–218.

Sultana, A., Miyamoto, A., Hy, Q. L., Tanaka, Y., Fushimi, Y., & Yoshii, H. (2017). Microencapsulation of flavors by spray drying using *Saccharomyces cerevisiae*. *Journal of Food Engineering*, *199*, 36–41.

Sun, N., Chen, J., Wang, D., & Lin, S. (2018). Advance in food–derived phospholipids: Sources, molecular species and structure as well as their biological activities. *Trends in Food Science & Technology*, *80*, 199–211.

Szente, L., Szemán, J., & Sohajda, T. (2016). Analytical characterization of cyclodextrins: history, official methods and recommended new techniques. *Journal of Pharmaceutical and Biomedical Analysis*, *130*, 347–365.

Tahara, K., Nishio, M., & Takeuchi, H. (2018). Evaluation of liposomal behavior in the gastrointestinal tract after oral administration using real–time *in vivo* imaging. *Drug Development and Industrial Pharmacy*, *44*(4), 608–614.

Taladrid, D., Marín, D., Alemán, A., Álvarez–Acero, I., Montero, P., & Gómez–Guillén, M. C. (2017). Effect of chemical composition and sonication procedure on properties of food–grade soy lecithin liposomes with added glycerol. *Food Research International*, *100*(1), 541–550.

Tamjidi, F., Shahedi, M., Varshosaz, J., & Nasirpour, A. (2013). Nanostructured lipid carriers (NLC): A potential delivery system for bioactive food molecules. *Innovative Food Science and Emerging Technologies*, *19*, 29–43.

Tamnak, S., Mirhosseini, H., Tan, C. P., Amid, B. T., Kazemi, M., & Hedayatnia, S. (2016). Encapsulation properties, release behavior and physicochemical characteristics of water–in–oil–in–water (W/O/W) emulsion stabilized with pectinepea protein isolate conjugate and Tween 80. *Food Hydrocolloids*, *61*, 599–608.

Tantra, R., Philipp, S., & Paul, Q. (2010). Effect of nanoparticle concentration on zeta–potential measurement results and reproducibility. *Particuology*, *8*(3), 279–285.

Tehrany, E. A., Kahn, C. K. F., Baravian, C., Maherani, B., Belhaj, N., Wang, X., & Linder, M. (2012). Elaboration and characterization of nanoliposome made of soya; rapeseed and salmon lecithins: Application to cell culture. *Colloids Surf. B: Biointerfaces*, *95*, 75–81.

Thanonkaew, A., Benjakul, S., Visessanguan, W., & Decker E. A. (2007). Yellow discoloration of the liposome system of cuttlefish (*Sepia pharaonis*) as influenced by lipid oxidation. *Food Chemistry,* 102, 219–224.

Thong, P. Q., Nam, N. H., Phuc, N. X., Manh, D. H., & Thu, H. P. (2014). Impact of PLA/PEG ratios on Curcumin solubility and encapsulation efficiency, size and release behavior of Curcumin loaded poly(lactide)–poly(ethylenglycol) polymeric micelles. *International Journal of Drug Delivery, 6*(3), 279–285.

Tian, H., Maddox, I. S., Ferguson, L. R., & Shu, Q. (2010). Influence of bovine lactoferrin on selected probiotic bacteria and intestinal pathogens. *Biometals, 23,* 593–596.

Tonon, R. V., Grosso, C. R. F., & Hubinger, M. D. (2011). Influence of emulsion composition and inlet air temperature on the microencapsulation of flaxseed oil by spray drying. *Food Research International, 44*, 282–289.

Troost, F. J., Saris, W. H. M., & Brummer, R. J. M. (2002). Orally ingested human lactoferrin is digested and secreted in the upper gastrointestinal tract *in vivo* in women with ileostomies. *Journal of Nutrition, 132,* 2597–2600.

Van der Kraan, M I A., Nazmi, K., van't Hof, W., Amerongen, A. V. N., Veerman, E. C. I., & Bolscher, J. G. M. (2006). Distinct bactericidal activities of bovine lactoferrin peptides LFampin 268–284 and LFampin 265–284: Asp–Leu–Ile makes a difference. Biochemistry and Cell Biology, 84, 358–362.

Van Echteld, C. J. A., De Kruijff, B., Mandersloot, J. G., & De Gier, J. (1981). Effects of lysophosphatidylcholines on phosphatidylcholine and phosphatidylcholine/cholesterol liposome systems as revealed by 31p–nmr, electron microscopy and permeability studies. *Biochimica et Biophysica Acta, 649*, 211–220.

Varankovich, N. V., Khan, N. H., Nickerson, M. T., Kalmokoff, M., & Korber, D. R. (2015). Evaluation of pea protein–polysaccharide matrices for encapsulation of acid–sensitive bacteria. *Food Research International, 70*, 118–124.

Varankovich, N., Martinez, M. F., Nickerson, M. T., & Korber, D. R. (2017). Survival of probiotics in pea protein–alginate microcapsules with or without chitosan coating during storage and in a simulated gastrointestinal environment. *Food Science and Biotechnology, 26*(1), 189–194.

Vélez, M. A., Perotti, M. C., Zanel, P., Hynes, E. R., & Gennaro, A. M. (2017). Soy PC liposomes as CLA carriers for food applications: Preparation and physicochemical characterization. *Journal of Food Engineering, 212,* 174–180.

Vergara, D., & Shene, C. (2019). Encapsulation of lactoferrin into rapeseed phospholipids based liposomes: optimization and physicochemical characterization. *Journal of Food Engineering, 262,* 29–38.

Vergara, D., López, O., Bustamante, M., & Shene, C. (2020). "An *in vitro* digestion study of encapsulated lactoferrin in rapeseed phospholipid–based liposomes". *Food Chemistry, 321*, 126717.

Verma, A., & Singh, S. V. (2013). Spray drying of fruit and vegetable juices–A review. *Critical Reviews in Food Science and Nutrition, 55*(5), 701–719.

Wang, B., Adhikari, B., & Barrow, C. J. (2014). Optimisation of the microencapsulation of tuna oil in gelatin–sodium hexametaphosphate using complex coacervation. *Food Chemistry, 158*, 358–365.

Wang, B., Timilsena, Y. P., Blanch, E., & Adhikari, B. (2017). Characteristics of bovine lactoferrin powders produced through spray and freeze drying processes. *International Journal of Biological Macromolecules, 95*, 985–994

Wang, Y., Liu, B., Wen, X., Li, M., Wang, K., & Ni, Y. (2017). Quality analysis and microencapsulation of chili seed oil by spray drying with starch sodium octenylsuccinate and maltodextrin. *Powder Technology, 312*, 294–298.

Wilde, P. J., & Chu, B. S. (2011). Interfacial & colloidal aspects of lipid digestion. *Advances in Colloid and Interface Science, 165,* 14–22.

Wilson, R. F. (2008). Soybean: Market driven research needs In: Stacey G, ed., Genetics and Genomics of Soybean. Springer–Verlag GmbH, Heidelberg, Germany.

Wu, Q., Zhang, T., Xue, Y., Xue, C., & Wang, Y. (2017). Preparation of alginate core–shell beads with different M/G ratios to improve the stability of fish oil. *LWT – Food Science and Technology, 80*, 304–310.

Xiao, J. X., Huang, G. Q., Wang, S. Q., & Sun, Y. T. (2014). Microencapsulation of capsanthin by soybean protein isolate–chitosan coacervation and microcapsule stability evaluation. *Journal of Applied Polymer Science, 131*(1), 39671–39678.

Xu, X., Costa, A., & Burgess, D. J. (2012). Protein encapsulation in unilamellar liposomes: high encapsulation efficiency and a novel technique to assess lipid–protein interaction. *Pharmaceutical Research, 29,* 1919–1931.

Xu, X., Khan, M. A., & Burgess, D. J. (2011). A quality by design (QbD) case study on liposomes containing hydrophilic API: I. Formulation, processing design and risk assessment. *International Journal of Pharmaceutics, 419*, 52–59.

Yamaguchi, T., Nomura, M., Matsuoka, & T., Koda, S. (2009). Effects of frequency and power of ultrasound on the size reduction of liposome. *Chemistry and Physics of Lipids, 160*, 58–62.

Yan, C., & Zhang, W. (2014). Microencapsulation in the food industry: A practical implementation guide. Chapter 12 – Coacervation Processes. Pp 125–137.

Yang, T. S., Liu, T. T., & Lin, I. H. (2017). Functionalities of chitosan conjugated with stearic acid and gallic acid and application of the modified chitosan in stabilizing labile aroma compounds in an oil–in–water emulsion. *Food Chemistry, 228*(1), 541–549.

Yang, X., Gao, N., Hu, L., Li, J., & Sun, Y. (2015). Development and evaluation of novel microcapsules containing poppy–seed oil using complex coacervation. *Journal of Food Engineering, 161*, 87–93.

Yao, X., Bunt, C., Cornish, J., Quek, S. Y., & Wen, J. (2015). Oral delivery of bovine lactoferrin using pectin– and chitosan–modified liposomes and solid lipid particles: improvement of stability of lactoferrin. *Chemical Biology & Drug Design*, *86*(4), 466–477.

Yao, X., Bunt, C., Cornish, J., Quek, S.Y., & Wen, J. (2014). Preparation, optimization and characterization of bovine lactoferrin–loaded liposomes and solid lipid particles modified by hydrophilic polymers using factorial design. *Chemical Biology & Drug Design, 83*(5), 560–475.

Yourdkhani, M., Leme–Kraus, A. A., Aydin, B., Bedran–Russo, A. K., & White, S. R. (2017). Encapsulation of grape seed extract in polylactide microcapsules for sustained bioactivity and time–dependent release in dental material applications. *Dental Materials, 33*(6), 630–636.

Yuan, Y., Kong, Z. Y., Sun, Y. E., Zeng, Q. Z., & Yang, X. Q. (2017). Complex coacervation of soy protein with chitosan: Constructing antioxidant microcapsule for algal oil delivery. *LWT Food Science and Technology*, *75*, 171–179.

Zhang, J., Han, J., Ye, A., Liu, W., Tian, M., Lu, Y., Wu, K., Liu, J., & Lou M. P. (2019b). Influence of phospholipids structure on the physicochemical properties and *in vitro* digestibility of lactoferrin–loaded liposomes. *Food Biophysics, 14*, 287–299.

Zhang, Y., Pu, C., Tang, W., Wang, S., & Sun, Q. (2019a). Gallic acid liposomes decorated with lactoferrin: Characterization, *in vitro* digestion and antibacterial activity. *Food Chemistry, 293*(30), 315–322.

Zhu, F. (2017). Encapsulation and delivery of food ingredients using starch based systems. *Food Chemistry, 229*, 542–552.